Christina Wappl

Investigations of the curing of ROMP based duroplastic materials at lower temperatures

Master Thesis

Diplomarbeit

Zur Erlangung des akademischen Grades eines

Diplom-Ingenieurs

der Studienrichtung Technische Chemie

erreicht an der Technischen Universität Graz

2013

Betreuer: Univ.-Doz. Dipl. Ing. Dr. techn. Christian Slugovc

Institut für Chemische Technologie von Materialien

Technische Universität Graz

Eidesstatliche Erklärung

Acknowledgement

Herewith I would like to express my gratitude to all those who helped and supported me during my studies and the accomplishment of this work.

First of all, I want to thank my supervisor Christian Slugovc for his support throughout my master thesis, for many helpful advices and (at least) as many good laughs. Furthermore, I want to thank him for the opportunity to gain experience in this industry-related work and on international conferences.

My gratitude goes to Armin Pfeil from Hilti Entwicklungsgesellschaft mbH for supporting me with his excellent knowledge not only in the field of chemical anchors and for giving me the possibility to improve my scientific skills during my visit in the Hilti-laboratories in Kaufering, Germany. I want to thank Klaus Gebauer from Hilti Entwicklungsgesellschaft mbH and Helga Reischl from Institute of Chemistry at University of Graz for special rheological measurements and Petra Kaschnitz for NMR measurements.

Many thanks go to the colleagues and friends at ICTM for a pleasant working atmosphere and enjoyable discussions at the 10 o'clock coffee break. I want to thank Renate Trebizan and Liane Hochgatterer for organisational assistance and our "fairy godmother" Birgit for a helping hand in the laboratory at any time. Special thanks go to the present and prior members of the Slugi group Anita, Astrid, David, Eva, Julia, Kathi, Manuel, Seba and Simone. I want to thank you for your support in- at the great time I spent with you. Further, I want to thank the nice guys for the 4th floor, Dr. Schoko and Fradi, for many enriching discussions, e.g. about the importance of being on time. Further, I want to thank the members of the Institute of Organic Chemistry for refreshments and nice conversation after long and intensive working days.

In the end, I want to thank some people who play a major role in my life outside university. Special thanks go to my best friend Angi. Thank you for your help and advice in many parts of my life and for countless hours of laughing. Further, I want to express my deep gratitude to Marko. I thank you for your loving support and the way you make me smile at any circumstances. I am most grateful to my brother Michael and my parents, Josefa and Heinrich. Thank you for all your love and support, your faith in me and the loving home you offer me.

Abstract

This work discusses the Ring Opening Metathesis Polymerisation of several norbornene derivatives with different ruthenium based initiators under solvent-free conditions at low and moderate temperature (+4 – 40 °C).

As a first monomer, commercially available dicyclopentadiene (DCPD) was investigated. Curing of DCPD was studied with a series of different initiators at different loadings and curing temperatures. Typical parameters like gelation time or glass transition temperature and mechanical characteristics (from stress-strain tests) of the cured specimens were assessed. Results were set into relation with other hydrocarbon monomers such as norbornadiene or 1,4,4a,5,8,8a-hexahydro-1,4,5,8-*endo*-*exo*-dimethanonaphtalene and in a second step with bi- and tri-functional norbornene derivatives linked by various functional groups. It could be concluded that stiff and strong specimens could only be obtained in reasonable time (minutes to hours) at curing temperatures above 60 °C. Below that temperature soft, elastic materials are obtained typically within hours. Upon days mechanical properties slowly approach the mechanical characteristics of samples obtained from curing at higher temperature.

Kurzfassung

Diese Arbeit behandelt die Ring Öffnende Metathese Polymerisation mehrerer Norbornen-Derivate mit verschiedenen Ruthenium-basierten Initiatoren unter lösungsmittelfreien Bedingungen bei niedrigen und mittleren Temperaturen (+4 – 40 °C).

Für erste Untersuchungen wurde das kommerziell erhältliche Dicyclopentadien (DCPD) ausgewählt. Die Aushärtung von DCPD wurde mit einer Reihe verschiedener Initiatoren bei unterschiedlichen Initiatorkonzentrationen und Härtungstemperaturen untersucht. Typische Parameter wie Gelierzeit oder Glasübergangstemperatur und mechanische Eigenschaften (aus Zugfestigkeitsversuchen) der ausgehärteten Proben wurden bewertet. Die Ergebnisse wurden mit anderen Kohlenwasserstoff-Monomeren wie Norbornadien oder 1,4,4a,5,8,8a-Hexahydro-1,4,5,8-*endo*-*exo*-dimethanonaphtalen und bi- und trifunktionellen Norbornen-Derivaten, welche verschiedene funktionelle Gruppen aufweisen, in Bezug gesetzt. Steife und feste Proben waren nur bei Aushärtungstemperaturen über 60 °C in angemessener Zeit (Minuten bis Stunden) erreicht. Unterhalb dieser Temperatur wurden in der Regel weiche, elastische Materialien innerhalb weniger Stunden erhalten. Nach ein paar Tagen erreichten diese langsam die mechanischen Eigenschaften von Proben, die bei erhöhten Temperaturen ausgehärtet wurden.

List of Abbreviations

ADMET	Acyclic Diene Metathesis Polymerization
ATR-IR	Attenuated Total Reflection- Infrared Spectroscopy
CAM	Cerium (IV) Sulphate / Ammonium Molybdate
CM	Cross Metathesis
cf.	Compare (lat. *confer*)
Cp	Cyclopentadiene
Cy	Cyclohexane
DCC	Dicyclohexylcarbodiimde
DCPD	Dicyclopentadiene
DMA	Dynamic Mechanical Analysis
4-DMAP	4-(Dimethyl amino)-pyridine
DMNH-6	1,4,4a,5,8,8a-Hexahydro-1,4,5,8-*endo*-*exo*-dimethanonaphtalene
DSC	Differential Scanning Calorimetry
e.g.	for example (lat. *exempli gratia*)
et. al.	et alii
EtOAc	Ethyl Acetate
NHC	N-heterocyclic carbene
NMR	Nuclear Magnetic Resonance
PCy_3	tricyclohexylphosphine
pDCPD	poly(dicyclopentadiene)
PPh_3	triphenylphosphine
RCM	Ring Closing Metathesis
R_f	Retardation Factor
ROM	Ring Opening Metathesis
ROMP	Ring Opening Metathesis Polymerization
rt	Room temperature
SIMes	saturated imidazol mesityl
STA	Simultaneous Thermal Analysis
TLC	Thin layer chromatography

Table of Content

1. Introduction and Motivation

Olefin metathesis, a carbon-carbon double bond forming reaction, is a fundamental synthetic tool which opened up new synthetic routes to organic compounds with complex architectures. Since its discovery in the middle of the last century it has emerged to a well-established method in various sectors like pharmaceutical, biotechnological or polymer industry. Along that way, three scientists made a name for themselves. In 2005, Yves Chauvin (proposal of still valid mechanism), Robert H. Grubbs and Richard R. Schrock (development of Ru- and Mo-based catalysts) were eventually granted the Nobel Prize in Chemistry in 2005.[1]

In this contribution, Ring Opening Metathesis Polymerisation (ROMP) was applied for the development of thermosets at lower to moderate curing temperatures. These ROMP-based polymers were regarded as promising alternative to the established Hilti-HIT-HY-products based on radical polymerisation of methacrylates. However, preparation of duroplastic polymers via ROMP at lower curing temperatures is challenging.

Dicyclopentadiene (***DCPD***) was investigated as a first monomer because its cured polymer, polydicyclopentadiene (***pDCPD***), prepared via industrially used processes exhibited outstanding mechanical properties and chemical resistance.[2] Generally, latent initiators were required to facilitate processing. Grubbs 1st and 2nd generation type initiators bearing indenylidene instead of benzylidene were used as those exhibit lower initiation rates.[3] The performance of the polymerisation at low temperature as well as the polymers was reveal by a number of well-established test methods like simultaneous thermal analysis, tensile testing or dynamic mechanical analysis. Curing was investigated not only at lower but also at higher temperatures (80 °C) to determine the performance of fully cured polymers. Two other hydrocarbon-based monomer were analysed as potent alternative to ***DCPD*** due to higher reactivity. Further, novel bi- and tri-functional norbornene derivatives linked by various functional groups were designed aiming at cross-linked networks with duroplastic behaviour.

[1] The Royal Swedish Academy of Sciences, Supplementary Information to Press Release "The Nobel Prize in Chemistry", 5.Oct.2005.

[2] http://www.matweb.com/search/datasheetText.aspx?bassnum=O3190, Mat Web Entry on pDCPD (2013, Aug 30).

[3] (a) S. Monsaert, E.D. Canck, R. Drozdzak, P. van der Voort, F. Verpooort, J.C. Martins, P.M.S Hendrickx, *Eur. J. Org. Chem.* **2009**, 655-665, (b) Y. Schrodi, R.L. Pederson, *Aldrichimica Acta* **2007**, *40* (2), 45-53, (c) C.E. Diesendruck, E. Tzur, N.G. Lemcoff, *Eur. J. Inorg. Chem.* **2009**, *28*, 4185-4203.

2. General aspects

2.1. Chemical anchors

Post-installed fastening systems have been a research field of increasing interest over the past decades, facilitating the design, planning and construction of new buildings as well as restoration of old buildings. More and more, chemical anchors are used due to many benefits over conventional plastic or metal dowels. They prevent corrosion of the rod and cracking of the substrates, and can be fixed also in porous substrates maintaining an outstanding load bearing capacity. Due to their paste-like state in the beginning, the space between the surface of the hole and the threaded rod is completely filled with mortar. Their sophisticated performance is based on bonding by adhesion and cohesion and keying in micro- and macro-undercuts.[4,5]

Figure 1. Adhesive capsule and injectable mortar, products by Hilti AG (Hilti HVU, Hilti HIT), taken from reference 6.

Generally, the anchors are based on threaded rods and chemical mortar. Two types of the chemical mortar are known: Adhesive anchors and injection systems. Both are two-component systems. The resin component is a mixture of resin, reactive diluents, catalysts and inhibitors, fillers and additives. Hardener, fillers and additives are the basis of the hardener component. But they differ in the way the mortar is placed into the borehole. In case of adhesive anchors, the adhesive capsule (Figure 1 left) is placed in the cleaned hole. Subsequently, a rotating threaded rod with a blade edge on top rips the capsule open and mixes the components. Polymerisation takes place leading to an adhesive bonding between the wall of the hole and the threaded rod. In injection systems, the resin and the curing agent are stored separately in two plastic chambers (Figure 1 right). The two components are mixed in the dispenser tip (static mixer) when pressing it into the cleaned hole (Figure 2). The threaded rod is then placed in the still paste-like mortar.[4]

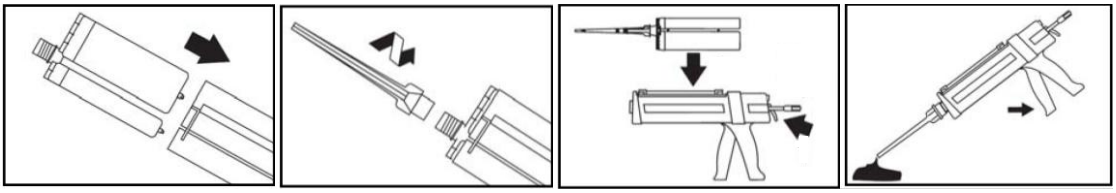

Figure 2 Preparation of injection system (injectable mortar and dispenser); taken from reference 6.

[4] (a) http://129.69.59.201/bibliothek/festschr/meszaros.pdf, J. Meszaros, B. Lehr, "Tragverhalten von Einzelbefestigungen mit chemischen Dübeln unter zentrischer Belastung" (2013, Aug 30), (b) J. Meszaros, PhD thesis " Tragverhalten von Einzelverbunddübeln unter zentrischer Kurzzeitbelastung", Stuttgart **2002**.
[5] A. Pfeil, Presentation in the series of lectures of "Doctoral School Chemistry TU Graz, "Molecules-Products-Patents; Application of Polymer Chemistry in the Field of Chemical Anchors", Graz, **2010**.
[6] Hilti information brochure "Chemical anchoring systems", **2011**.

The requirements for chemical anchors are not only restricted to their mechanical and thermal properties (*cf.* chapter 3). For the development of chemical anchors based on injection systems in concrete the setting procedure has to be considered. This procedure includes several steps, as follows: drilling, cleaning, injection and setting (Figure 3). Each step influences the performance of the chemical anchor and hence, the setting instructions have to be followed carefully.[7,8]

Figure 3. Post-installed fastening systems (drilling, cleaning, injection, setting); taken from reference 8.

In the drilling and cleaning steps, the designed borehole is prepared. The dimensions of the borehole depend on the size of the threaded rod and amount of mortar required to achieve long term bonding between rod and hole under load. Furthermore, the hole has to be cleaned manually and with compressed air to remove loose particles. Residual dust would reduce the adhesion of the mortar to surrounding concrete and negatively affect the bonding.

Then, the resin and the curing agent are pressed through the static mixer into the borehole (charge fit 2/3 of the hole). The threaded rod is placed into filled bore hole and curing takes place in an appealing time. In these last steps, gelation time also referred to as working time and curing time become important. Gelation time determines the time frame starting when resin and curing agent are mixed until gelation occurs and is synonymous with the processing window in which the rod has to be set. Curing time on the other hand refers to the time interval until the chemical anchor reaches its final strength and then, load can be applied. In terms of polymerisation, the gelation time can be regulated by polymerisation inhibitors or latent initiators. Generally, the polymerisation speed depends strongly on both the loading of the curing agent and the surrounding temperature in

[7] Hilti Product Data Sheet, "HIT-HY 150 MAX with HIT-V / HAS", **2011**.
[8] Hilti Information-Brochure, "Hilti Lösungen für nachträgliche Bewehrungsanschlüsse", **2009**.

the borehole. Apart from that, the polymerisation is influenced by the heat conducting properties of the surrounding. [4,7]

Once curing is completed, the persistence of the anchor is determined by its mechanical and thermal properties. Furthermore, chemical resistance has to be considered as concrete walls are a basic environment. Embedded steel reinforcement in concrete benefits from the high alkalinity as is preserves the steel by passivation of the surface protecting it from corrosion.[9] However, non-resistant materials would decompose from the interface onwards consequently losing contact to the surrounding wall. Additionally, the behaviour might change from thermosetting to elastic. Overall, the material would lose its ability to fixate the anchor (e.g. screw, steel bar, …) in the wall. Therefore, long term alkali resistance is a major issue in developing novel chemical anchor systems.

The commercially available chemical anchor systems Hilti HIT-HY and HIT-RE are both developed for post-installed fastenings in concrete. However, they differ in the underlying chemistry and hence, the field of application. HIT-HY systems are based on the radical polymerisation of methacrylates and are generally referred to as fast hardeners (curing time between 30 min and 12 h). Due to their high reactivity, they are also applicable at lower temperatures with good results. Typical applications are fastening of façade-substructures, railings, etc. In contrast to this, HIT-RE systems are based on the addition polymerisation of epoxy resins with amines. This system can be applied in fastening systems in the higher load range (steel beams, silos,…) due to low polymerisation shrinkage and good load application. However, the epoxy-amine system requires higher temperatures and reacts slower than the methacrylate one.[8,10]

[9] L. Li, J. Nam, W.H. Hartt, *Cement Concrete Res.* **2005**, *35*, 277-283.
[10] Hilti Information-Brochure, “Hilti HIT Injektionstechnik“, **2007**.

2.2. Ring Opening Metathesis Polymerisation (ROMP)

2.2.1. Mechanistic background

In the mid-1950s a new, transition-metal-catalysed carbon-carbon bond forming reaction, the olefin metathesis, was discovered. Since then, it attracted attention in industry and academia using this redistribution of carbon-carbon double bonds as a versatile, well-established tool in synthetic chemistry today.[11]

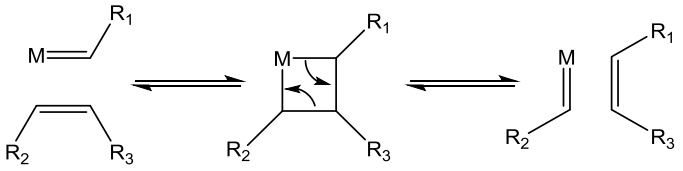

Figure 4. Mechanism of olefin metathesis, redrawn from reference 12.

In the beginning of the 1970's, Chauvin and co-workers published a mechanism based on a metallacyclobutane-intermediate (Figure 4). In particular, an interconversion of an olefin and a metal alkylidene takes place via a [2+2] cycloaddition/cycloreversion.[13] This contribution cleared the way for the development of new olefin metathesis subtypes and well-defined catalysts. Olefin metathesis can be applied in numerous varieties, namely cross metathesis (CM), Ring Closing Metathesis (RCM), Ring Opening Metathesis (ROM), Acyclic Diene Metathesis Polymerisation (ADMET) and Ring Opening Metathesis Polymerisation (ROMP).[12]

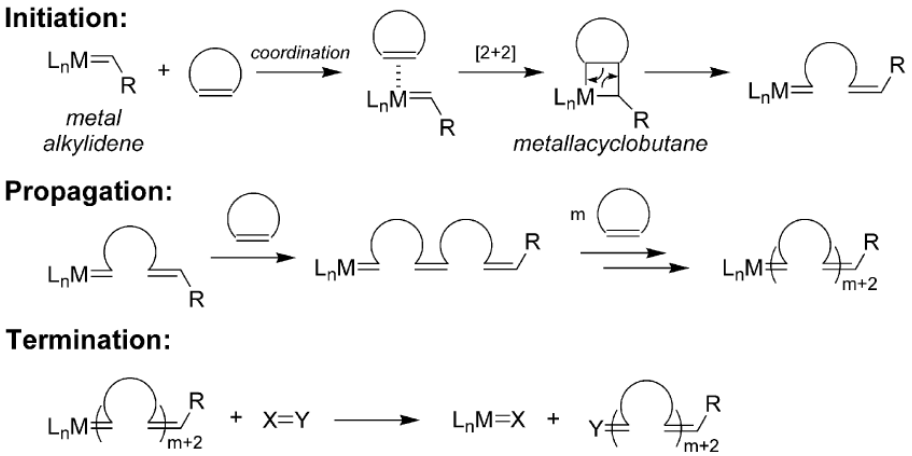

Figure 5. General mechanism of Ring Opening Metathesis Polymerisation, taken from reference 14.

The initiation and propagation steps in ROMP of cyclic olefins with metal alkylidene initiators follow the general mechanism by Chauvin (Figure 5) leading to a complex with the incorporated monomers/polymer chain as new alkylidene moiety. This complex remains active throughout the propagation resulting in a growing polymer chain in living manner.

[11] S. Monsaert, A.L. Vila, R.Drozdzack, P. Van Der Voort, F. Verpoort, *Chem. Soc. Rev.* **2009**, *38*, 3360-3372.
[12] T.M. Trnka, R.H. Grubbs, *Acc. Chem. Res.* **2001**, *34*, 18-29.
[13] J.L. Hérisson, Y. Chauvin, *Makromol. Chem.* **1971**, *141*, 161.
[14] C.W. Bielawski, R.H. Grubbs, *Prog. Polym. Sci.* **2007**, *32*, 1-29.

Termination is achieved by adding an olefinic reagent which cleaves the polymer chain and deactivates the complex. Generally, the driving force is the release of ring-strain (> 5 kcal/mol) as the cyclic olefins are opened. ROMP is a reversible, equilibrium-controlled reaction. Therefore, temperature and initiator concentration have an impact on the polymerisation progress.[14]

2.2.2. Olefin metathesis initiators

ROMP has proven a powerful tool to obtain polymeric materials with outstanding properties. This method has been employed in industry for many decades, mainly using ill-defined catalytic systems consisting of a transition metal halide and main group alkyl co-catalysts. These systems bear low control and tolerance towards functional groups and oxygen and moisture, which limits the applicability. Mentionable advancement in catalyst design was achieved with well-defined W- or Mo-based "Schrock initiators" enabling living olefin metathesis polymerisation (Figure 6, a). However, these initiators show higher reactivity towards acids, alcohols and aldehydes (and ketones) than towards olefins. Ru-based alkylidene complexes, referred to as Grubbs catalysts G1, G2 and G3 finally show the desired reactivity profile – tolerant against numerous functional groups, but very reactive with double bonds. (Figure 6, b-d).[11,14,15]

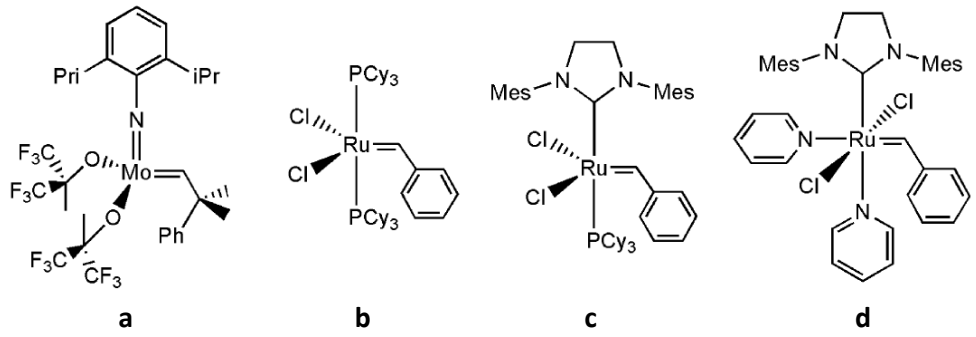

Figure 6. A Mo-based Schrock catalyst (a) and the Ru-based Grubbs 1st, 2nd and 3rd generation catalysts G1, G2 and G3 (b-d), taken from reference 11.

Grubbs 1st generation catalysts are stable in presence of air and oxygen facilitating synthesis and handling and polymerise even in protic media. Unfortunately, they don't reach the same activity as Schrock catalysts. Further, the exchange of one phosphine ligand with an N-heterocyclic carbene (NHC) ligand resulted in the 2nd generation of Grubbs catalysts. These combined the benefits of both Schrock and Grubbs 1st generation catalysts exhibiting enhanced reactivity and functional group-tolerance. Additionally, higher thermal stability was shown. However, ROMP with Grubbs 2nd generation catalysts produce uncontrollable and broad molecular weight distributions in polymers.[11,14,15] This drawback originates in the dissociation of the phosphine ligand. Mechanistic studies revealed that the propagation rate

[15] C. Slugovc, *Macromol. Rapid Commun.* **2004**, *25*, 1283-1297.

for 2nd generation is very fast, whereas the dissociation rate of the phosphine (therefore the initiation) is rather low. Furthermore, binding of an olefin to the vacant site instead of rebinding the phosphine ligand was preferred.[16] In the 3rd generation of Grubbs catalysts weakly coordinating pyridine ligands replace the phosphine ligand. Thus, complete initiation and high polymerisation rates are achieved leading to polymers with very low polydispersity indices.[14]

To date, countless olefin metathesis catalysts similar to the Grubbs catalysts have been developed differing in their activity in the different types of olefin metathesis reactions. In this contribution, we turned our attention on the 1st and 2nd generation of the Umicore® M-catalysts bearing an indenylidene ligand instead of a benzylidene (Figure 7).

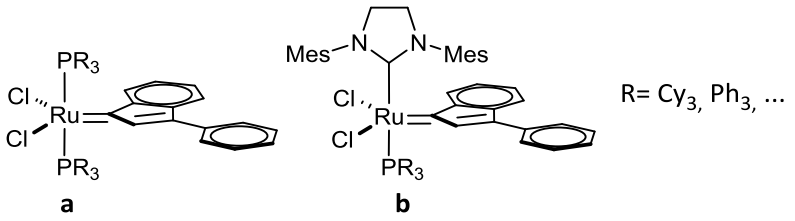

Figure 7. General chemical structure of Umicore® M 1st (a) and 2nd (b) generation catalysts.

These catalysts show pronounced latency in ROMP compared to their Grubbs analogues. Differences in initiation rates can be attributed to the respective alkylidene moiety. The reactivity of the catalysts within one generation can be tuned by the choice of phosphine ligand (tricyclohexylphosphine, triphenylphosphine,…). Generally, phosphine ligands with weak donor strength dissociate faster than stronger electron donors. This behaviour appeared beneficial in respect of the target application in which longer handling of monomer/initiator formulations before polymerisation is desired.[17]

[16] M.S. Sanford, M. Ulman, R.H. Grubbs, *J. Am. Chem. Soc.* **2001**, *123*, 749-750.

[17] (a) G.C. Vougioukalakis, R.H. Grubbs, *Chem. Rev.* **2010**, *110*, 1746-1787; (b) J.A. Love, M.S. Sanford, M.W. Day, R.H. Grubbs, *J. Am. Chem Soc.* **2003**, *125*, 10103-10109.

3. Results and Discussion

The aim of this work was the development of novel norbornene-based Ring Opening Metathesis polymerised thermosets for the application as chemical anchors in concrete walls. The reactivity of the monomer/initiator formulation should be adjusted to obtain polymers with preferable mechanical and thermal properties at lower and moderate curing temperatures within reasonable time. The Hilti HIT-HY products based on radical polymerisation of methacrylates were chosen as reference system. These systems are very reactive resulting in rather short working and curing times and an operative range between -10 and 40 °C.

The performance specifications of ROMP-based chemical anchors had to be adapted as follows:

- Working time: 15 minutes

In case of methacrylate-based systems, the working window can be adjusted by addition of inhibitor molecules to the formulation which are consumed first before the monomers are attacked. In the ROMP-based systems the working window should be regulated by the latency of the initiator. Further, both reaction temperature and initiator loading influence the polymerisation rates as ROMP is an equilibrium-controlled reaction. So, these two parameters have to be considered in the development of new formulations.
The working time determines the processing window in which the formulation has to be filled in the borehole and threaded rod has to be in its final position. In bench-scale, a homogeneous formulation has to be achieved and filled in the respective mold before gelation occurs.

- Processing duration: 24 hours

At the end of the curing time the intended load should be applicable to the chemical anchor. Preferable, 80% of the final properties of the ROMP-based chemical anchors should be reached after a curing time of 24 h., all specimen produced in this work were analysed after 24h curing time regardless of curing temperature and initiator loading.

- Curing temperatures: 4-40 °C

From a marketing perspective, chemical anchors with a rather large operative range are desired. Therefore, the polymerisations in this work were conducted at temperatures between 4 and 40 °C. Additionally, curing was performed at 80 °C to reveal the maximum performance of the cured polymers.

- Mechanical properties: Young's modulus > 1.8 GPa, $Stress_{max}$ > 20 MPa, Shore D hardness > 70

The mechanical properties of the cured polymers are of considerable significance in the application as chemical anchors. The desired Young's modulus and $Stress_{max}$, determined in tensile tests, were assessed at 1.8 GPa and 20 MPa, respectively. These values are comparable or even lower of those of polydicyclopentadiene (***pDCPD***) produced in industrial processes. To reach these values monomers with multiple polymerisation sites resulting in cross-linked networks were designed as a higher the cross-linking degree yields higher the E-modulus and $Stress_{max}$.
Shore D hardness is another classification scale for the determination of the behaviour of solid materials. With this technique, the hardness of the superficial area (depth, approx. 4 mm) can be determined. However, no information about the hardness of the bulk can be gained.

- Thermal properties: T_g > 70 °C

The glass transition temperature T_g of chemical anchors must be well above the operative temperature to ensure the determined mechanical properties. However, if the operative temperature exceeds the T_g, the properties would change from glassy to rubber-like. Then, the chemical anchor might lose the ability the bear the applied load and fails.
The glass transition temperature T_g, determined by dynamic mechanical analysis, depends mainly on the architecture of the polymers and the interactions between polymer chains and can be determined for example in dynamic mechanical analysis. Therefore, the chemical structure of the monomers and the polymerisation progress are key-parameters in this context.

- Chemical properties: long term alkali resistance

Concrete walls represent an alkaline medium. Long term alkali resistance tests were conducted with selected polymers to simulate the alkali-induced ageing processes. These were evaluated from changes in weight and Shore D hardness.

These performance specifications were considered in the selection of monomers, initiators and curing conditions as well as in the design of novel monomers.

3.1. Characterisation

This chapter describes different characterisation techniques used in this work and explains the parameters under investigation in order to enhance the understanding of the reader in the proceeding in chapters 3.2 and 1.3 concerning development of new monomers and composition of monomer/initiator formulations.

Viscosity (3.1.1.1) of the monomer proved to have an impact on both polymerisation and properties of the final polymeric material. Determination of this parameter was crucial for the interpretation of the performance of the monomer in the target application.

In a preliminary curing test (3.1.2.1), the latency of several initiators was evaluated. Therefore, monomer and initiator were mixed at several temperatures and the heat generation of the exothermic polymerisation was measured. Due to the released energy upon opening of strained rings in monomers a distinct temperature rise θ_{max} at t_{max} was observed. t_{max} served as parameter to determine latency of the initiators. Additionally, θ_{max} turned out to influence the appearance of the final polymer (e.g. foaming).

Simultaneous Thermal Analysis (STA) revealed further information about the curing behaviour of monomer/initiator systems (3.1.2.2). With this technique endo- and exothermic processes coupled with mass loss of the sample can be investigated. Onset-temperatures for polymerisation as well as the respective mass loss before polymerisation were analysed and possible side-reactions were identified.

Rheokinetics (3.1.2.3) is another technique to investigate the curing behaviour and latency of initiators. Instead of released heat, this method measures the viscosity of monomer/initiator formulations. Latency was described with the gelation time, a crucial parameter from a processing point of view.

Based on the data obtained from the tests described above, initiator loading and curing conditions were adapted to produce polymers accomplishing the required properties. The mechanical properties were determined with tensile tests and used to classify the polymers according to E-modulus and maximum strength (3.1.3.1). DMA measurements revealed glass transition temperatures, post-curing effects and thermal-mechanical properties in response to oscillatory deformation and heating program (3.1.3.2). Further, the polymeric materials were examined for their alkali resistance, necessary in the aimed application (3.1.3.3).

3.1.1. Characterisation of the monomer

3.1.1.1. Determination of viscosity

In case of bulk polymerisations, viscosity of the monomer has an immense effect on the reaction progress and hence the final mechanical properties of the polymeric material. In particular, higher viscosity reduces the polymerisation speed and hampers full conversion (degree of polymerisation and cross-links) as the ability of the monomer to diffuse through the system is hindered. Furthermore, high viscosity can cause problems concerning a homogenous distribution of the initiator in the monomer. Therefore, it was important to determine the viscosity of the monomers used in this work. Based on this data a better understanding of the observed polymerisation behaviour and obtained mechanical properties of the polymers was achieved.

For rheological measurements a cone – plate type viscometer was used (Figure 8). The undissolved monomers were placed on the plate before the cone (Θ = 2 °) was positioned 1 mm above the fixed plate. The experiments were conducted in "Controlled Shear Rate" (CSR) mode. Therefore, a shear rate between 10^{-3} and 10^{3} s^{-1} was applied on the sample while the shear stress was measured. Viscosity was then calculated using Equation 1.

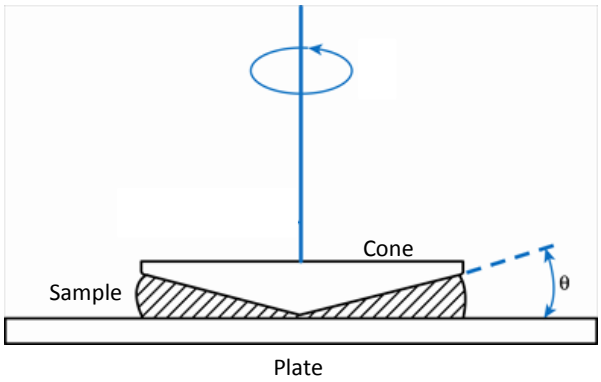

Figure 8. Apparatus of a cone-plate type viscometer.

Equation 1. Viscosity.

$$\eta = \frac{\tau}{\gamma}$$

η / mPa*s	Viscosity
τ / mPa	Shear stress
γ / s^{-1}	Shear rate

3.1.2. Characterisation of polymerisation behaviour

3.1.2.1. Preliminary Curing Tests

One of the main requirements is the latency of the initiator (low initiation rate) in order to facilitate the processing of the materials before its gel point is reached. However, polymerisation is supposed to be completed within a short period of time (high propagation rate) after the formulation is filled in the mold.

A first impression of the latency of the initiator was obtained by analysing the heat generation upon mixing monomer with various loadings of initiator. Therefore, the monomer (1 -2 g) diluted with 50 µL solvent was filled into a test tube and the required amount of initiator (dissolved in 50 µL solvent) was injected (Figure 9). A temperature sensing element covered with alumina foil was placed in the formulation and ensured homogeneity by stirring the formulation in the beginning. The starting temperature was regulated by the water bath. The temperature over time was measured. Initiator loadings between 25 and 150 ppm were used. Usually DCM was the solvent of choice. For measurements assessed at higher temperatures than 40 °C, toluene and an oil bath replaced DCM and the water bath.

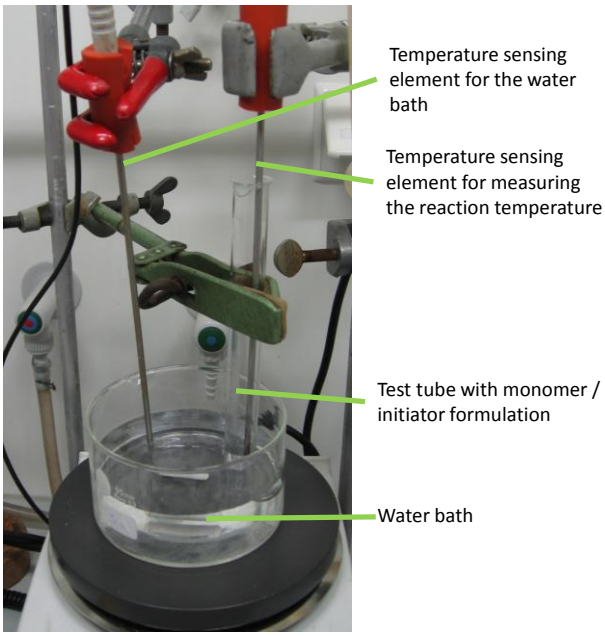

Figure 9. Measurement setup for analysing heat generation during polymerisation.

In case of a latent initiator the following curve shapes depending on the loading were expected (Figure 10). High initiator loadings (black curve) lead to a fast temperature increase after a short time, accompanied by gelation of the formulation, indicating fast initiation and propagation. The temperature decreases rather fast after overcoming a maximum (θ_{max}). The material is solid by that time. A different progress is typical for formulations with medium initiator loadings (green curve). At first, hardly any heat generation is observed as the initiation rate is rather low. After several minutes, enough energy is released to accelerate the initiation and propagation resulting in a temperature rise. Gelation is observed at the onset. The final material exhibits slightly elastic behaviour. In case of low initiator loadings (blue curve) hardly any increase in temperature is observed. However, polymerisation takes place leading to a rather elastic material. Further, post curing can be observed after a longer period of time in any case.

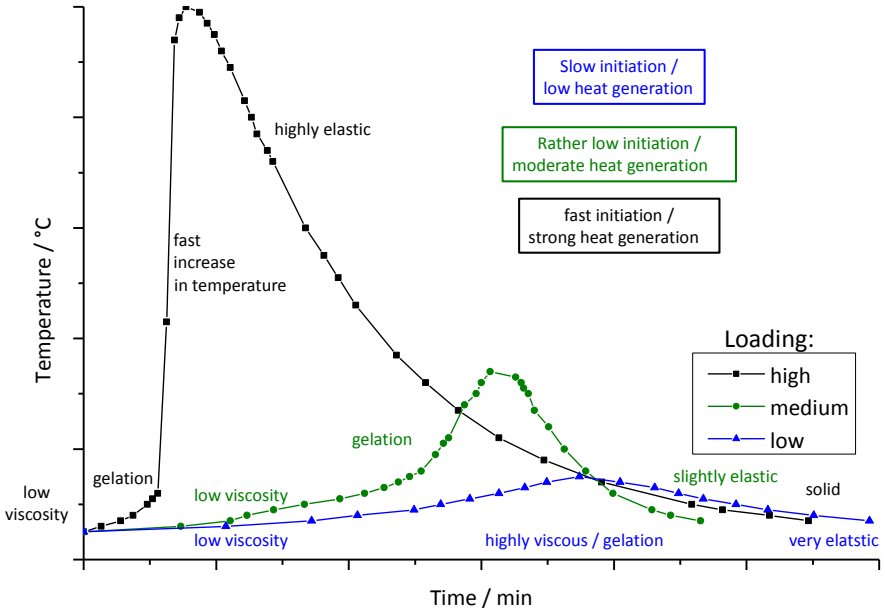

Figure 10. Heat generation during polymerisation with latent initiators.

If hardly any or no heat generation was observed characterisation of the reaction progress was achieved by a rough evaluation of the viscosity of the material. Therefore, categories were defined for graphical illustration (Table 1).

Table 1. Evaluation of curing progress.

Category	Consistency of curing formulation
0	no apparent change in viscosity
5	slightly viscous
10	viscous
15	more viscous
20	highly viscous
25	stacked, highly viscous, sticky
30	gelation, soft & sticky
35	solid, gel-like, slightly sticky
40	solid, gel-like, not sticky
50	solid, very elastic
60	solid, rather elastic
70	solid, elastic
80	solid, slightly elastic
90	solid, hardly elastic
95	solid, barely elastic
100	solid, fully cured

3.1.2.2. Simultaneous Thermal Analysis (STA)

STA is a method to reveal processes occurring in a sample (monomer, monomer-initiator-formulation, etc.) upon heating. Thereby, endothermic processes like decomposition, melting or vaporisation and exothermic processes like chemical reactions (e.g. polymerisations) or condensation are determinable. Emerging volatile substances (as a product of chemical reactions, decomposition products, etc.) are removed from the sample by a gas flow and detected as mass loss vs. temperature. Depending on the sample itself, different preparation steps have been considered (cf. chapter Experimental). Generally, the sample was placed into a closed DSC pan, and a small hole was pinched into the lid. The measurement started at 20 °C and a heating rate of 3 K*min^{-1} under constant He gas flow of 50 mL*min^{-1} was applied.

In Figure 11 a STA measurement of a polymerisation of a slightly volatile monomer is depicted. TGA measurement reveals any mass loss of the sample during heating (blue line). Exo- and endothermic processes in the sample are depicted by peaks up- and downwards in the differential scanning calorimetry (DSC) measurement (green line), respectively. Combining those two techniques, the switching temperature of an initiator at which the polymerisation starts, is easily determinable. Artefacts detected at the beginning of the measurement are typical for the machine used and negligible. The mass loss before polymerisation occurs as volatile monomers can evaporate through the small opening and is removed by the continuous gas flow. As the polymerisation starts, an exothermic peak is observed. After the exothermic polymerisation peak no mass loss occurs until decomposition as polymerisation is completed.

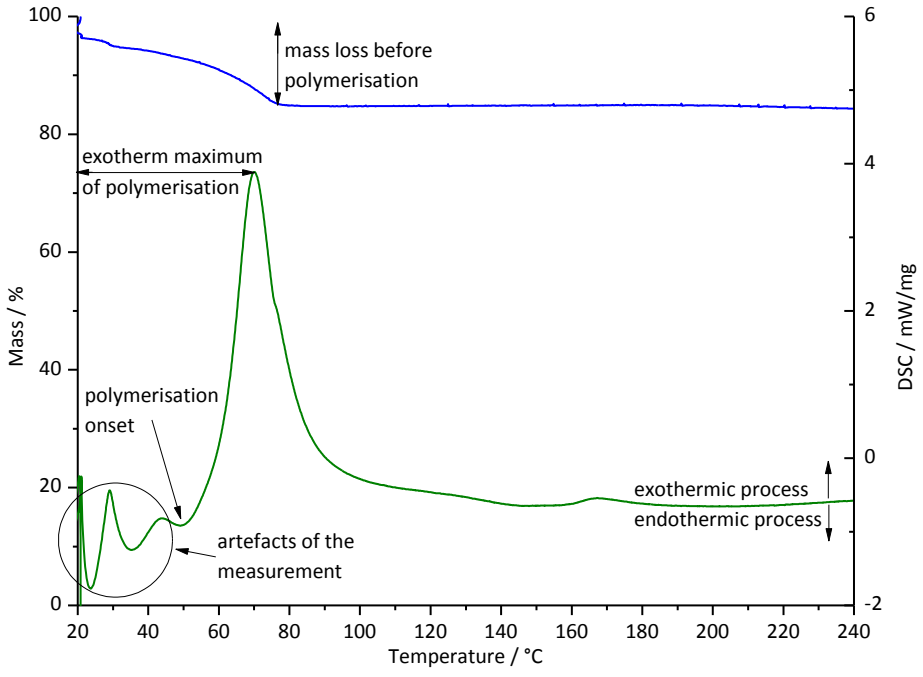

Figure 11. STA/TGA measurement of a polymerisation.

3.1.2.3. Rheokinetics

The curing progress of polymerisations without distinct temperature rise was evaluated according to Table 1 as described in chapter 3.1.2.1. With this empirical technique the gelation time was estimated. In further experiments rheokinetic measurements were conducted to determine the gelation time more accurately. Rheokinetic is a complimenting method to analyse the time- and temperature-dependent curing stages (initiator-injection, initiation, gelation, completion) during the formation of a three-dimensional polymeric network. From a processing point of view, the viscosity of the monomer-initiator formulations should not be too high in the beginning. Anyway, after the formulation is brought into the final shape, a rapid increase in viscosity resulting from fast polymerisation is favourable in order to shorten total processing time. In this context, gelation time is the critical parameter determining the time frame in processing.[18,19]

There are different ways to characterise gelation depending on the type of measurement. One way is to determine the point where viscosity increases unlimitedly (= gel point t*). After t*, the curing progress is monitored by measuring shear storage G' modulus. Curing is completed when G' reaches a plateau.[18] Another way is to analyse the evolution of viscosity by determining t_t (transition time, corresponding to initiation) and Δt (time for viscosity to increase from 1 to 15 Pa*s, corresponding to reaction progress) as shown by Kessler and co-workers.[19]

In this work, another method developed by Kessler *et al.* was used.[20] Shear storage G' and shear loss G'' modulus (representing elastic and viscous component, respectively) vs. time were measured at isothermal conditions (23 °C). In the beginning of the measurement G'' is higher than G' because the viscous character of the material dominates as long as the gelation hasn't started. Due to the progressing polymerisation the elastic component G' increases. The crossover point of G' and G'' ($\tan\delta$ = G''/G' = 1) determines the gelation time (Figure 12).

[18] A.Y. Malkin, A.I. Isayev, *Rheology. Concepts, Methods, and Applications*, ChemTec Publishing, Toronto **2012**.
[19] M.R. Kessler, G.E. Larin, N. Bernklau, *J. Therm. Anal. Cal.* **2006**, *85*, 7-12.
[20] X. Sheng, J.K. Lee, M.R. Kessler, *Polymer* **2009**, *50*, 1264 – 1269.

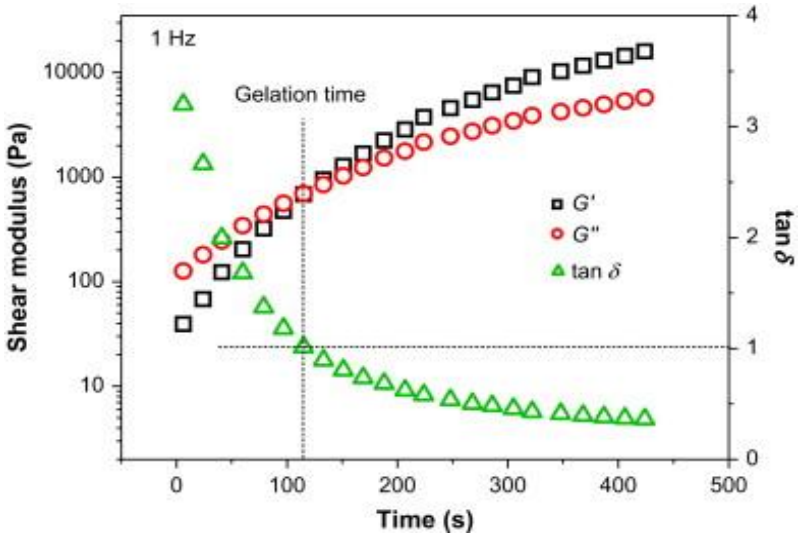

Figure 12. Shear storage and shear loss modulus G' and G'' and tanδ with progressing curing (taken from reference 20).

Sample preparation is described in details in chapter Experimental. Generally, curing measurements were performed with a plate-plate oscillatory rheometer applying a stress of 0.1% dynamic deformation at 1.0 Hz frequency and 23 °C to the monomer/initiator formulation. The curing behaviour was monitored over a longer period revealing additional information like the time until G' reaches a plateau terminating curing of the material.

3.1.3. Characterisation of polymeric material

3.1.3.1. Tensile testing

Tensile tests are usually part of testing mechanical properties of thermosets of a thermoset Thereby, the Young's modulus (also referred to as elastic modulus or E), maximum strength and maximum elongation at yield (also referred to as $Stress_{max}/\sigma_{max}$ and $Strain_{max}/\varepsilon_{max}$, respectively) are determined. Curing conditions have to be considered when comparing the mechanical properties of several polymers.

Tensile tests were performed of materials polymerised with appealingly latent initiators. Therefore, shoulder test bars were cured in open molds with dimensions depicted in Figure 13. The preparation procedure is described in chapter Experimental. Generally, each temperature required a suitable amount of initiator depending on its specific latency. For polymerizations at 4°C and 40°C, the mold was cooled or pre-warmed before it was filled with the formulation. For curing at 60 °C and 80 °C the mold was not preheated as this would lead to unwanted bubble-formation or loss of monomer.[21] Hence, the formulation was filled into the mold at room temperature and further heated up to operating temperature.

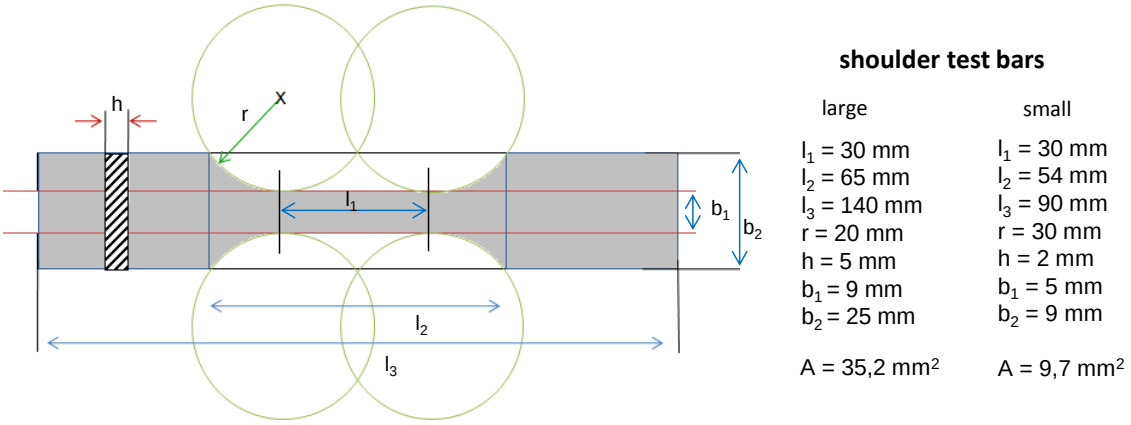

Figure 13. Dimensions of small and large shoulder test bars (adapted from reference 21)

Shrinkage occurred during curing and so it was necessary to check the dimensions of each shoulder test bar before tensile testing. Shrinkage originated from the evaporating solvent and monomer (retro-Diels-Alder) during curing. Furthermore, convex surfaces (at the mold far side) were observed when too much formulation was filled into the molds supported by surface tension. Contrariwise, too little formulation resulted in concave surfaces. Hence, the exact charge of the mold must be considered to obtain repeatable data.

[21] A. Leitgeb, PhD thesis "Contributions to the Advancement of Ruthenium Based Initiators for Olefin Metathesis", Graz **2012**.

The prepared shoulder test bars were fixated at both ends in the testing machine with two clamps as shown in Figure 14 (left). The clamp distance L_0 was 53 and 80 mm for small and large test bars, respectively. The tensile test was performed with a speed of 1 mm*min^{-1}. The applied tensile force and elongation were measured and the data plotted in a stress-strain diagram (Figure 14 right). Young's modulus was determined according to Equation 2 from the slope within the linear region at the start of the curve (Figure 14 right, blue line). Maximum strength σ_{max} and maximum elongation ε_{max} were determined at the yield (maximum stress) and rupture point corresponding to the green and red line in Figure 14 (right), respectively.

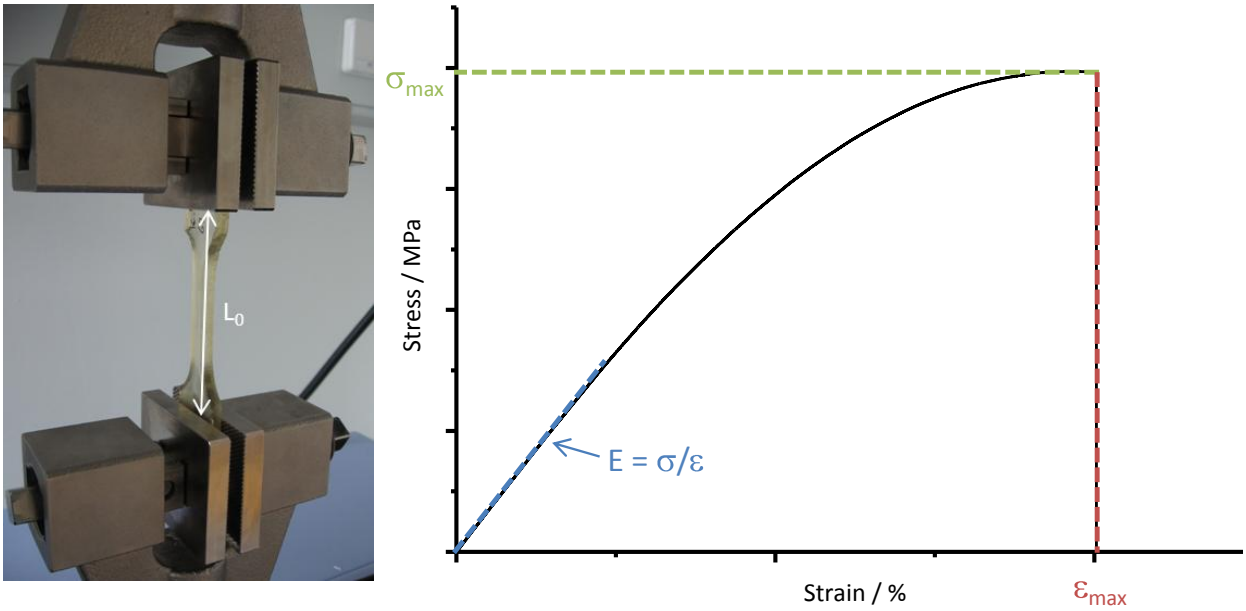

Figure 14. Shoulder test bar fixated in the machine (left); tensile strength test with Young's modulus E, max. strength σ_{max} and max. elongation at yield ε_{max} (right).

Equation 2. Young's Modulus.

$$E = \frac{\sigma}{\varepsilon} * 0.1 = \frac{F * A_0}{\Delta L * L_0} * 0.1$$

E / GPa	Young's Modulus
σ / MPa	Tensile Stress
ε / %	Tensile Strain
F / N	applied Tensile Strength
A_0 / mm^2	Cross Section Area
ΔL / mm	Elongation
L_0 / mm	Clamp distance at start

3.1.3.2. Dynamic mechanical analysis (DMA)

Dynamic mechanical analysis (DMA) is an expedient technique to investigate the thermal-mechanical properties of polymers. A sinusoidal stress is applied on the sample as a function of frequency and temperature and the sinusoidal strain and its phase lag δ is measured. Ideal solids (defined by Hooke's law) exhibit no phase difference between the amplitude of applied stress and measured strain (δ = 0 °) whereas ideal liquid behaviour (defined by Newton's law) results in δ = 90 °. Polymeric materials exhibit viscoelastic behaviour and an intermediate phase lag (0 ° < δ < 90 °, Figure 15 left). The ratio of shear stress and strain gives the complex shear modulus G* which can be transformed to the shear storage modulus G' and shear loss modulus G'' using a vectorial diagram (Figure 15 right). The dissipation factor tanδ is further calculated by using Equation 3.[22]

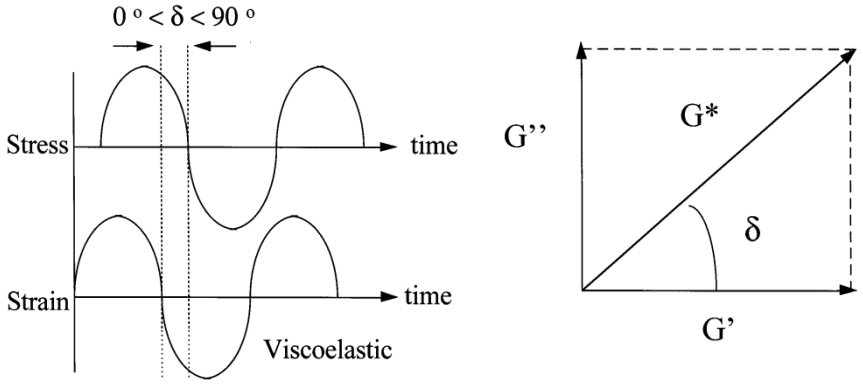

Figure 15. Phase difference between stress and strain of viscoelastic materials (left); vectorial diagram to transform the complex shear modulus G* into shear storage G' and shear loss modulus G'' (taken from reference 22).

Equation 3. Dissipation factor tanδ.

$$tan\delta = \frac{G''}{G'}$$

$tan\delta$	Dissipation Factor
G'' / Pa	Shear Loss Modulus
G' / Pa	Shear Storage Modulus

When a linear temperature rise starting from low temperatures is applied on a polymeric material, several relaxation processes can be observed. The main relaxation process, glass transition, is coupled with a change in both G' and G'' modulus (Figure 16). At glass transition temperature T_g, determined by the tanδ-maximum, the polymer changes from glass to rubber-like behaviour.[23] Thus, T_g is a crucial parameter from a user perspective as the mechanical properties change significantly above this temperature. Further, T_g was used to evaluate the cross-linking degree. The higher the amount of cross-links in the polymer the shorter the free volume of chain segments, and the less the polymer is able to move in various directions. Hence, T_g increases with an increasing degree of cross-links.[20]

[22] D.S. Jones, *Int. J. Pharm.* **1999**, *179*, 167-178.
[23] W. Stark, *Polym. Test.* **2013**, 32, 231-239.

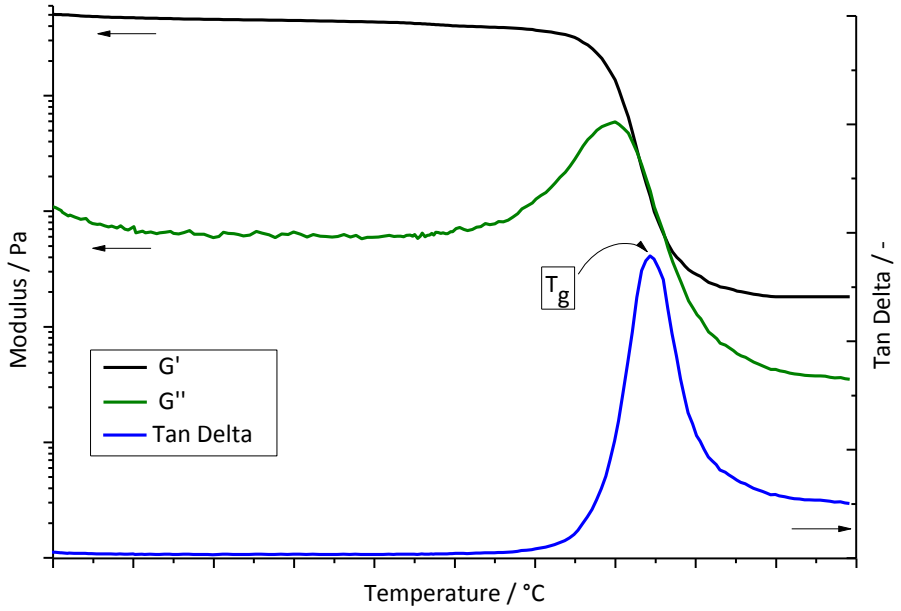

Figure 16. DMA measurement with shear storage and loss modulus (G' and G'') and dissipation factor (tanδ).

Additional information about the curing progress (e.g. possible post-curing effects) can be investigated. Therefore, the sample is heated up to elevated temperatures (180 °C) and subsequently cooled down for a re-run. The observation of a significantly higher T_g in the second run indicates incomplete curing in sample preparation, caused by too low curing temperature, initiator loading or too short curing time. Based on the DMA results the curing conditions can be adapted to tap the full potential in terms of thermo-mechanical properties of the final polymer.

DMA measurements were carried out at 1 Hz and with temperature ramp from -20 °C up to 180 °C and a heating rate of 10 $K*min^{-1}$. The cylindric samples were produced according to a general procedure (*cf.* chapter Experimental) and fixated in a furnace at both ends with clamps (Figure 17).

Figure 17. Rheometer for DMA measurement; closed furnace (left); open furnace (right).

3.1.3.3. Determination of alkali resistance

For the resistance tests, the alkaline medium was simply imitated by a strong alkaline aqueous solution (KOH-solution, pH 13.5). The tested specimens were produced comparably to shoulder test bars (3.1.3.1) though using a different mold (Figure 18), *cf.* chapter 5.2.5.5. A general procedure for the alkali resistance test was introduced consisting of conditioning and cleaning steps, measuring and adjusting of the alkaline solution.

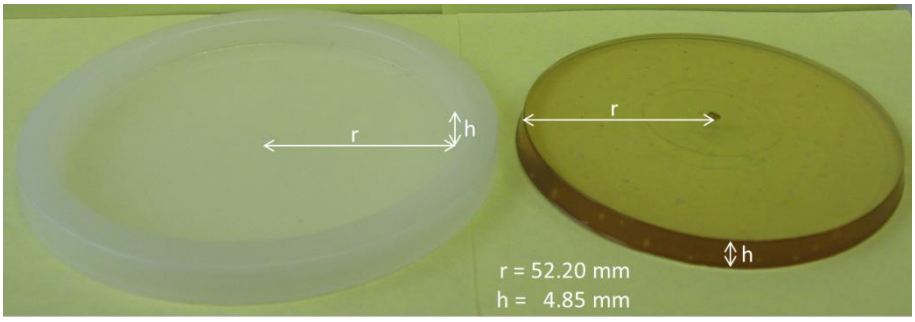

Figure 18. Dimensions of samples for alkali resistance test (left: PE – mold; right: polymerised samples).

Before applying the samples to the alkaline solution (KOH-solution, pH 13.5) weight as well as dimensions and Shore D- hardness were measured giving the reference value (O d). The appearance of the sample was determined mostly empirically and gave a hint concerning changes within the material (change of colour,…). The other parameters were then statistically evaluated and changes larger than 5% were considered critical. The samples were placed loosely in the alkaline medium in a leak-proof PE – container and stored at 40 °C. The parameters (appearance, weight, diameter, thickness and Shore D-hardness) were determined after 1 day, 3 and 7 days, 2, 4 and 12 weeks. Therefore, the samples were removed from the alkaline medium, dried and again rinsed with *iso*-propanol. Further, the samples were dried at 40 °C for 50 min (turned after the first 25 min) in the oven. Afterwards, the samples were placed in another leak-proof PE – container containing $CaCl_2$ as drying agent and stored at room temperature for 1 h. The parameters were then determined and the samples subsequently placed into the alkaline medium again. The pH-value of the solution was controlled and, if necessary, adjusted.

3.2. DCPD and other cyclic hydrocarbon-based monomers

Polymeric materials based on cyclic hydrocarbon monomers such as dicyclopentadiene (***DCPD***), norbornene, etc. have been well known for decades. One representative of this class of monomers is ***DCPD***. It is a cheap starting material for polymerisation leading to a cross-linked polymer with outstanding mechanical properties and chemical resistance.[24] Therefore it was the monomer of choice for an application as chemical anchor based on ring-opening metathesis polymerisation. The first part of this chapter will be focused on ***DCPD*** and ***pDCPD*** in combination with various Ru-based ROMP-initiators. Several experiments were conducted in order to adjust the specification of the system (latency, total reaction time, mechanical properties of polymeric material, …). Then, other cyclic hydrocarbon-based monomers as non-volatile alternatives to ***DCPD*** will be discussed.

3.2.1. Dicyclopentadiene (Mon1)

DCPD (Scheme 1) is a cheap by-product from the C5 stream in naphtha crackers. The stable dimer (Diels-Alder adduct) of cyclopentadiene (Cp) is solid at room temperature (mp. 33.9 °C, density 0.98g*cm^{-3} at 35 °C) but decomposes to Cp at elevated temperatures.[25]

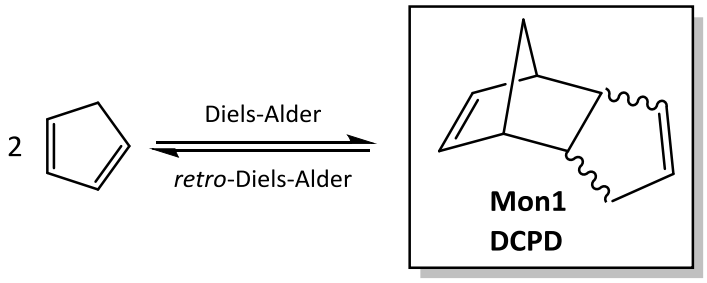

Scheme 1. Cyclopentadiene and the Diels-Alder adduct dicyclopentadiene (DCPD).

DPCD exists in both *endo* and *exo* - isomeric forms. The *endo* isomer is thermodynamically more stable and can be transformed into the *exo* form by thermal isomerisation.[26] Kinetic measurements as well as NMR studies revealed that the *exo* isomer is more reactive in ROMP initiated by Grubbs catalysts.[19,27] The two isomers can be distinguished by NMR spectroscopy as shown in Figure 19. Commercially available ***DCPD*** consists predominantly of the *endo* form (> 95%)[21].

[24] http://www.matweb.com/search/datasheetText.aspx?bassnum=O3190, Mat Web Entry on pDCPD (2013, Aug 30)
[25] (a) Ullmann's Encyclopedia of Industrial Chemistry. P*henol Derivatives/Cyclopentadiene and Cyclopentene (Online Version)* DOI: 10.1002/14356007 (2011, Nov 21); (b) T.T.P. Cheung, *Kirk-Othmer Encyclopedia of Chemical Technology*, Vol8. p. 219-235, "Cyclopentadiene and Dicyclopentadiene", *Wiley*, 1999.
[26] X. W. Zhang, K. Jiang, Q. Jiang, J.J. Zou, L. Wang, Z. T. Mi, *Chin. Chem. Lett*. **2007**, *18*, 673-676.
[27] J.D. Rule, J.S. Moore, *Macromolecules* **2002**, *35*, 7878-7882.

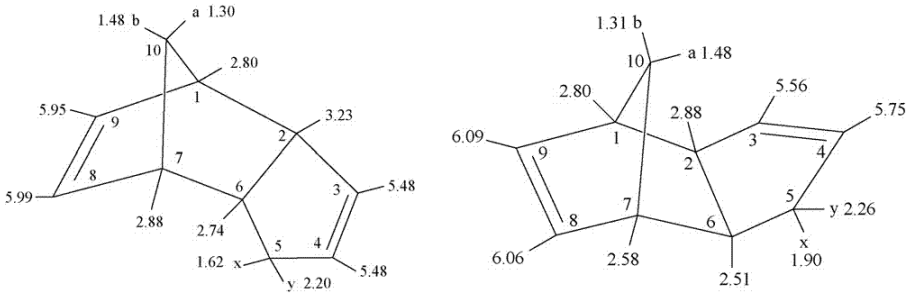

Figure 19. Chemical shifts (ppm) of *endo*- and *exo*-DCPD in ^{1}H-NMR (taken from reference 26).

The driving force of ROMP in general is the release of ring strain during polymerisation leading to a linear polymer. In case of the bicyclic ***DCPD***, the norbornene ring is more reactive in ROMP than the cyclopentene ring due to the higher ring strain. Hence, the norbornene ring is polymerised first resulting in a linear polymer chain (Scheme 2, (a)). Further, the ROMP of the less reactive cyclopentene ring (b) leads to the formation of a cross-linked network. Additional to olefin metathesis, olefin addition induced by the released heat has been reported to contribute to the formation of cross-links.[28]

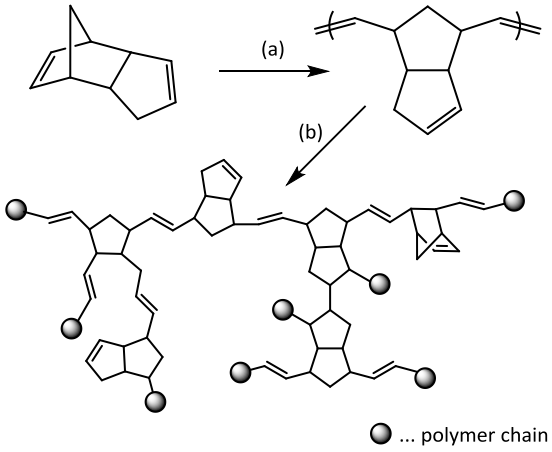

Scheme 2. ROMP of DCPD yielding a cross-linked structure (redrawn from reference 28).

Considering the profile of requirements for a chemical anchor system, ***DCPD*** (Scheme 1) seemed to be the monomer of choice due to its favourable properties. Commercially available ***pDCPD*** exhibits high toughness and rigidity (Young's modulus 1.9 GPa, tensile strength and elongation at yield 44.4 MPa and 4.5%, respectively) and excellent chemical resistance due to the high degree of cross links within the thermoset.[24] Ru-based initiators were chosen from the ***ROMP*** of ***DCPD*** due to their stability at air and moisture.[29] Several experiments were conducted in order to adjust the specification of the system (latency, total reaction time, …) to the curing at low temperatures yielding duroplastic materials.

[28] T.A. Davidson, K.B. Wagener, D.B. Priddy, *Macromolecules* **1996**, *29*, 786-788.
[29] R.H. Grubbs, *Tetrahedron* **2004**, *60*, 7117-7140.

3.2.1.1. Polymerisation with Grubbs 1st generation type catalysts

M1, a derivative of Grubbs 1st generation catalyst, was the first initiator whose latency in ROMP of ***DCPD*** was investigated in this work (Scheme 3). The Ru-based ***M1*** composed of active indenylidene ligand, two neutral ligands (tricyclohexylphosphine, PCy_3) and two anionic ligands (chloride).[30] Rather low activity (slow propagation) is expected from this initiator in ROMP bearing the advantage of latency and thereby a favourable processing window.[31]

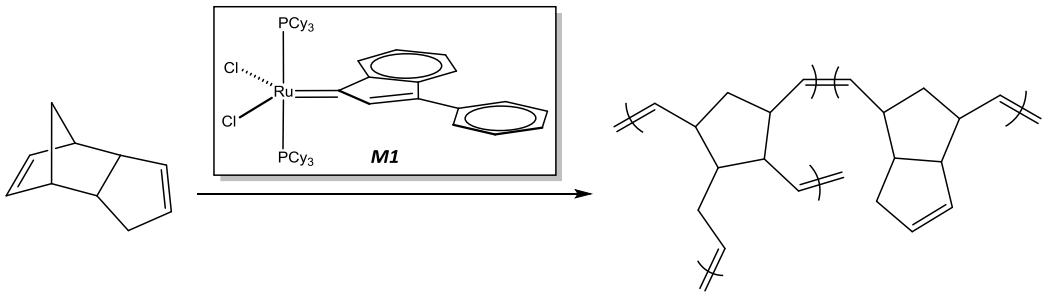

Scheme 3. ROMP of *DCPD* with *M1* as initiator.

In case of measurements assessed at 4 °C, 2 g ***DCPD*** was molten and dissolved in 80 µL DCM as 50 µL solvent appeared to be insufficient to dissolved ***DCPD*** at 4°C. The formulation was filled in a test tube and cooled down to 4 °C. ***M1*** dissolved in 20 µL DCM was added subsequently. No exothermic behaviour was observed at any initiator loading (≤ 150 ppm). Therefore, the curing progress was evaluated according to Table 1. The obtained data within 4 h is depicted in Figure 20.

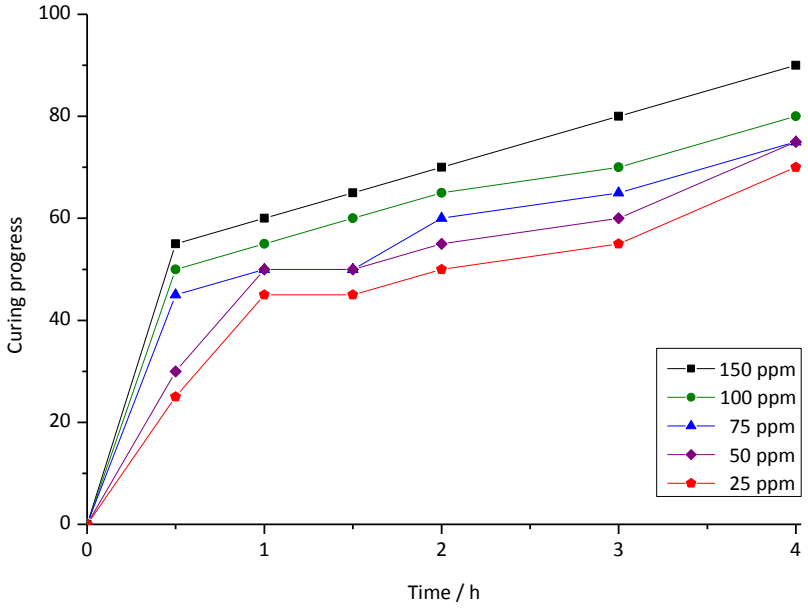

Figure 20. Curing progress according to Table 1 of *DCPD* with various *M1*-loadings at 4 °C.

[30] S. Monsaert, E.D. Canck, R. Drozdzak, P. van der Voort, F. Verpooort, J.C. Martins, P.M.S Hendrickx, *Eur. J. Org. Chem.* **2009**, 655-665.
[31] M.S. Sanford, M. Ulman, R.H. Grubbs, *J. Am. Chem. Soc*. **2001**, *123*, 749-750.

Generally, increasing viscosity and further hardening of the material was observed within the first 30 min. Within this period, gelation took place at initiator loadings higher than 50 ppm. The highest loading (150 ppm) was sufficient to obtain a solid, though and very elastic material. Afterwards the slope is less steep. The samples reached hardness of category 70 – 90 after 4 h, corresponding to elastic – hardly elastic solid materials. Curing the samples for approximately 3 days resulted in fully cured materials.

The curing of ***DCPD*** with ***M1*** at 25 °C was performed as specified in the general experiment procedure. Rather low heat generation was observed (up to 32 °C) but the materials reached elastic behaviour (category 60 – 80) in less than 15 min (=t_{end}). t_{end} was defined as time from mixing until the sample cooled down to 27 °C after overcoming θ_{max}. After 24 h all samples reached category 95 which corresponds to almost fully cured materials. The obtained data (maximal temperature θ_{max}, category at end of measurement and after 24 h, …) is summarized in Table 2 and Figure 21.

Table 2. Polymerisation of *DCPD* with various *M1*-loadings at 25°C.

$n_{Initiator}$ / ppm	θ_{max} /°C	t_{max} /min	t_{end} /min	$category_{end}$	$category_{24h}$
25	26	5.75	13.13	60	95
50	28	4.43	12.30	70	95
75	31	4.47	13.58	70	95
100	32	4.43	10.71	75	95
150	32	3.68	11.53	80	95

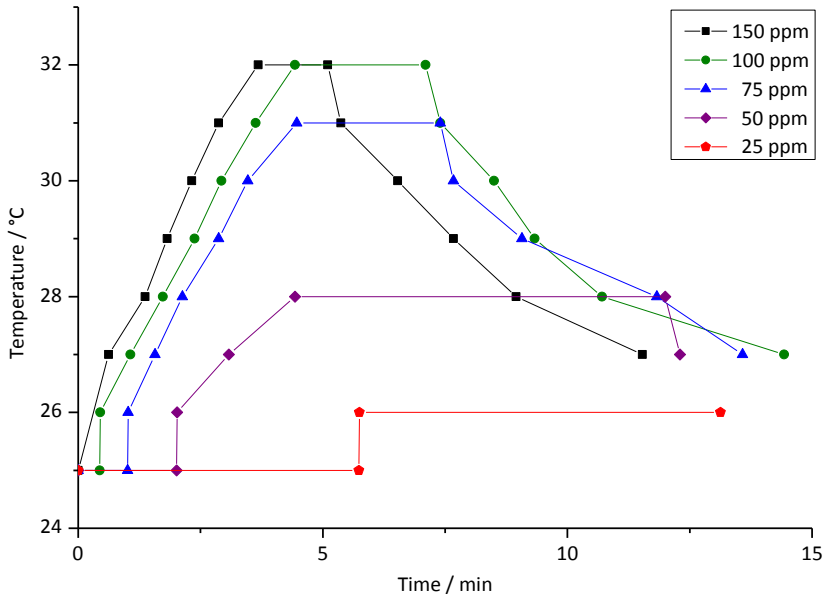

Figure 21. Heat generation upon mixing *DCPD* with various loadings of *M1* at 25 °C.

Finally, ROMP of ***DCPD*** with ***M1*** was also performed at 40 °C. In this case, **DCPD** was molten, dissolved in DCM and then heated up to 40 °C. The solvent (bp. = 39.7 °C) evaporated most probably before the experiment was started. Still the monomer remained liquid (mp. = 33.9 °C). Hence, dissolving in DCM was not required but remained one of the preparation steps in order to not alter the procedure. In later experiments, DCM was substituted by toluene (bp. = 111 °C) as specified in the respective experiments. The initiator solution was added after the monomer reached 40 °C. Heat generation was measured until t_{end} which was defined as the time until the samples reached 42 °C after overcoming θ_{max}.

At all initiator loadings, the exothermic onset was observed within the first minute and the samples reached t_{end} in less than 6.5 min. The hardness at t_{end} of the samples were similar to those cured at 25 °C (60 - 80). The samples were stored at room temperature after the measurement and reached category 95 after 6 h. The obtained data is summarized in Table 3 and Figure 22.

Table 3. Polymerisation of *DCPD* with various *M1*-loadings at 40 °C.

$n_{Initiator}$ / ppm	θ_{max} / °C	t_{max} / min	t_{end} /min	$category_{end}$	$category_{6h}$*
25	46	1.97	6.15	60	95
50	53	1.95	6.17	65	95
75	58	1.23	5.73	70	95
100	75	1.42	5.38	70	95
150	85	1.48	5.35	80	95

* samples stored at room temperature after t_{end}.

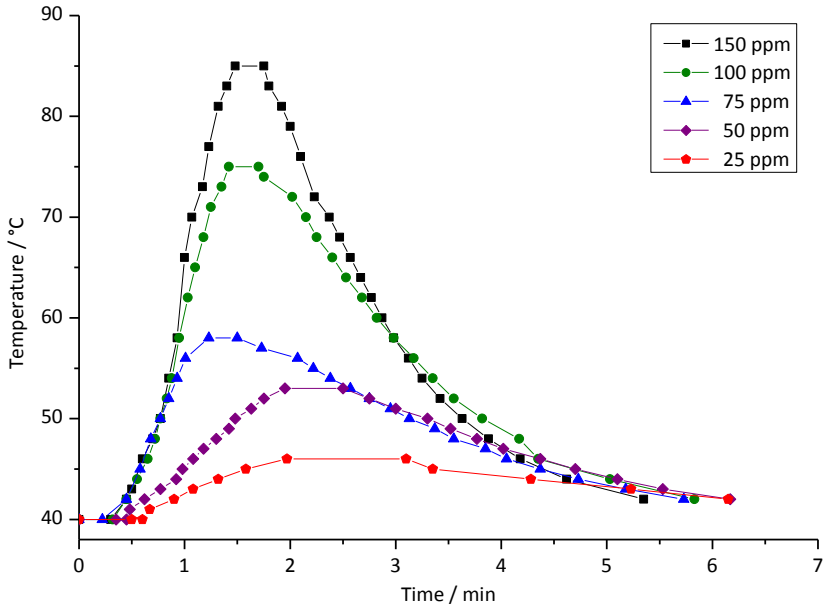

Figure 22. Heat generation upon mixing *DCPD* with various loadings of *M1* at 40 °C.

From these few measurements, some interesting conclusions could already be drawn. At low temperatures (4 °C) the energy released by opening the strained ring in the monomer is consumed to run the polymerisation. However, the latency of the system and polymerisation progress was visually observable looking at the gelation and further hardening of the material over several hours. At 25 °C, heat generation was observed at some extend with an initiator latency of few minutes. Solid material with elastic behaviour was obtained in less than 15 min. Increasing the process temperature from 25°C to 40 °C led to an earlier onset for all initiator loadings. This would give less time for processing. At both 25 and 40 °C, t_{max} increased and θ_{max} decreased with decreasing initiator loading (*cf.* Figure 21 and Figure 22). Apparently, both starting temperature and initiator loading have an influence on latency and heat generation during polymerisation. It is therefore absolutely necessary to look at those two parameters to introduce a monomer/initiator system with appealing features in processing. Although the processing window of ***M1*** in combination with ***DCPD*** might be rather short, it was no problem for the preparation of shoulder test bars for tensile testing.

First investigations of the mechanical properties aimed at the determination of the influence of the low initiator loadings. Therefore, ***DCPD*** was mixed with various ***M1***-loadings (5, 10, 20, 35 and 50 ppm) at room temperature and cured at 80 °C as described in the general procedure in chapter Experimental. At 5 and 10 ppm loading shrinkage due to mass loss occurred to a large extend, 50 and 38%, respectively (Figure 23 top). NMR spectroscopic analysis revealed uncured ***DCPD*** in the material indicating incomplete polymerisation caused probably by thermal decomposition of the initiator. So, the curing temperature was reduced to 60 °C. Nevertheless, mass loss did occur for samples with 5 and 10 ppm loading (Figure 23 bottom).

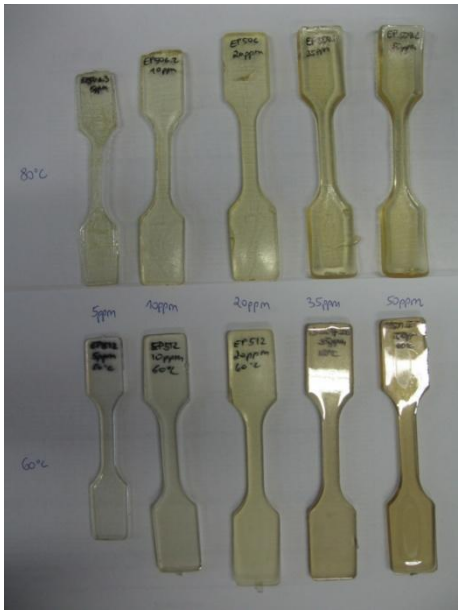

Figure 23. Shoulder test bars *pDCPD* cured at various *M1*-loadings and either 80 °C (top) or 60 °C (bottom).

The suitable shoulder test bars as named in Table 4 and Figure 24 were used in tensile testing. Decreasing the curing temperature from 80 °C to 60 °C led to an increased Young's modulus (*cf.* 50 ppm). Mechanical properties of sample cured with 35 or 50 ppm ***M1*** at 60 °C were lower in terms of both Young's modulus and $Stress_{max}$ compared with the literature.[24] However, no clear dependency of curing parameters and mechanical properties could be obtained.

Table 4. Mechanical properties of *pDCPD* cured with various amounts of *M1* compared with reference.

Curing temp. / °C	$n_{Inititator}$ / ppm	E-modulus / GPa	$Stress_{max}$ / MPa	$Strain_{max}$ / %
80°C	50	0.00402	1.52	33.7
60 °C	20	0.146	2.46	86.9
	35	1.58	31.0	x
	50	1.10	36.4	x
Reference[24]		1.87	43.0	4.00 – 5.00

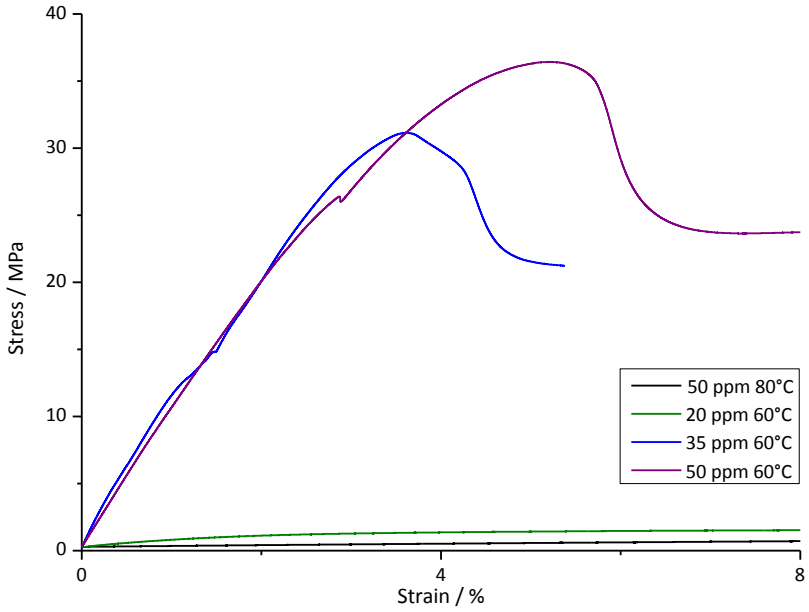

Figure 24. Tensile test of *pDCPD* cured with various amounts of *M1*.

The next experiments focused on lower curing temperatures since polymerisation of ***DCPD*** with ***M1*** takes place also at temperatures lower than 40 °C as proven before. Therefore, shoulder test bars were produced at 4, 25 and 40 °C with either 50 or 100 ppm initiator. DCM was the solvent of choice ensuring a liquid monomer also at 4 °C. At 4 °C the samples reached hardness of category 70 after 24 h possessing still the odour of the monomer, an evidence for incomplete polymerisation. The other two samples both reached category 100.

Young's modulus decreased significantly with decreasing temperature matching the observations after polymerisation concerning hardness of the material mentioned above (Table 5 and Figure 25). Unfortunately, the samples cured at 4 °C slipped from the clamps during the measurement. However, elastic behaviour was observable. Samples cured with 50 ppm initiator at 40 °C exhibited approximately the same values as sample cured 35 ppm at 60 °C (*cf.* Table 4).

Table 5. Mechanical properties of *pDCPD* cured with either 50 or 100 ppm *M1* at 4, 25, 40 °C compared with reference.

Curing temp. /°C	$n_{Initiator}$ / ppm	E-modulus / GPa	$Stress_{max}$ / MPa	$Strain_{max}$ / %
4 °C	50	0.00479	1.37*	115*
	100	0.00623*	7.15*	198.7*
25 °C	50	0.0685	3.99	246
	100	1.33	22.7	97.6
40 °C	50	1.56	37.6	12.7
	100	1.59	44.1	54.5
Reference[24]		1.87	43.0	4.00 – 5.00

*slipped from clamps before rupture.

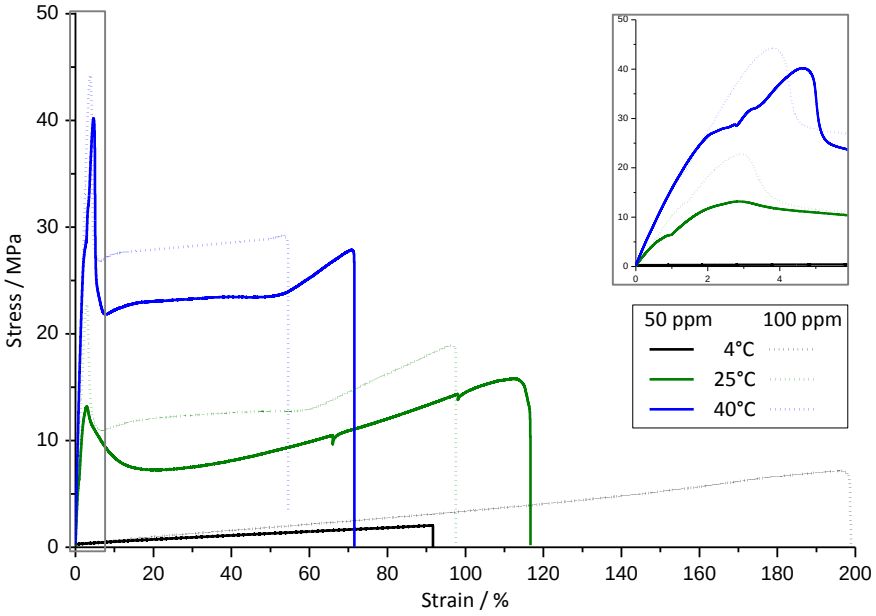

Figure 25 Tensile test of *pDCPD* cured with 50 and 100 ppm *M1* at various temperatures.

Storage of the 4 °C test bars at the same conditions for 7 days led to further polymerisation progress and enhanced mechanical properties (Table 6).

Table 6. Mechanical properties of *pDCPD* cured with either 50 or 100 ppm *M1* at 4 °C for either 1 or 7 days.

$n_{Initiator}$ / ppm	Curing time	Young's modulus / GPa	$Stress_{max}$ / MPa	$Strain_{max}$ / %
50	1 d	0.00479	1.37*	115*
	7 d	0.105	8.67	188*
100	1 d	0.00623*	7.15*	198.7*
	7 d	0.311	3.90*	92.6*

*slipped from clamps before rupture.

So far, ***DCPD***/***M1*** formulations were discussed. Next, other Ru-based initiators were investigated (Figure 26). 1st generation type initiators ***M1***, ***M11*** and ***M10*** only differ in their phosphine-ligand. Their activity decreases with increasing stability resulting from their phosphine dissociation rate as follows: ***M1*** > ***M11*** > ***M10***. Generally, small and electron-rich neutral ligands dissociate less easily, thereby slow down the initiation rate and lead to higher stability of the complex.[32,33] 2nd generation type initiators are here represented by ***M2*** and ***EP06.3***. This type of initiator contains an inert N-heterocyclic carbene (NHC) ligand (here: SIMes, 1,3-dimesityl-4,5-dihydroimidazole-2-ylidene), substituting one phosphine ligand. This ligand is not dissociating during polymerisation leaving the dissociation step in the ROMP mechanism to the remaining phosphine ligand. Generally, this initiator generation show increased metathesis activity and enhanced thermal stability compared with 1st generation initiators.[34] Furthermore, ***EPO6.3***, another latent initiator, is a *cis*-dichloro complex with a chelating benzylidene ligand.[35]

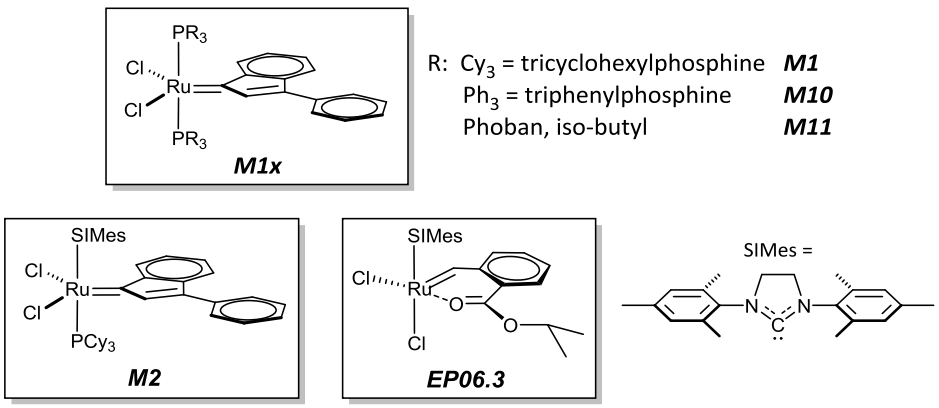

Figure 26. Ru-based initiator of 1st and 2nd generation.

Shoulder test bars were produced using ***DCPD*** and 20 ppm initiator (Figure 26) by curing for 24 h at 80 °C (except for ***M1*** formulations, see above). Apparently, ***M10*** possessed no activity under the tested conditions. The results from tensile testing are shown in Table 7 and Figure 27.

[32] G.C. Vougioukalakis, R.H. Grubbs, *Chem. Rev*. **2010**, *110*, 1771.
[33] J.L. Love, M.S. Sanford, M.W. Day, R.H. Grubbs, *J. Am. Chem. Soc.* **2003**, *125* (33), 10103-10109.
[34] Y. Schrodi, R.L. Pederson, *Aldrichimica Acta* **2007**, *40* (2), 45-53.
[35] C. Slugovc, B. Perner, F. Stelzer, K. Mereiter, *Organometallics* ***2004***, 23, 3622-3626.

Table 7. Mechanical properties of *pDCPD* cured with 20 ppm initiator at 80 °C.

Initiator	Young's modulus / GPa	$Stress_{max}$ / MPa
M1*	1.58	31.0
M10	x	x
M11	1.12	29.3
M2	1.62	32.2
EP06.3	1.71	36.4
Reference[24]	1.87	43.0

*35 ppm, 60 °C.

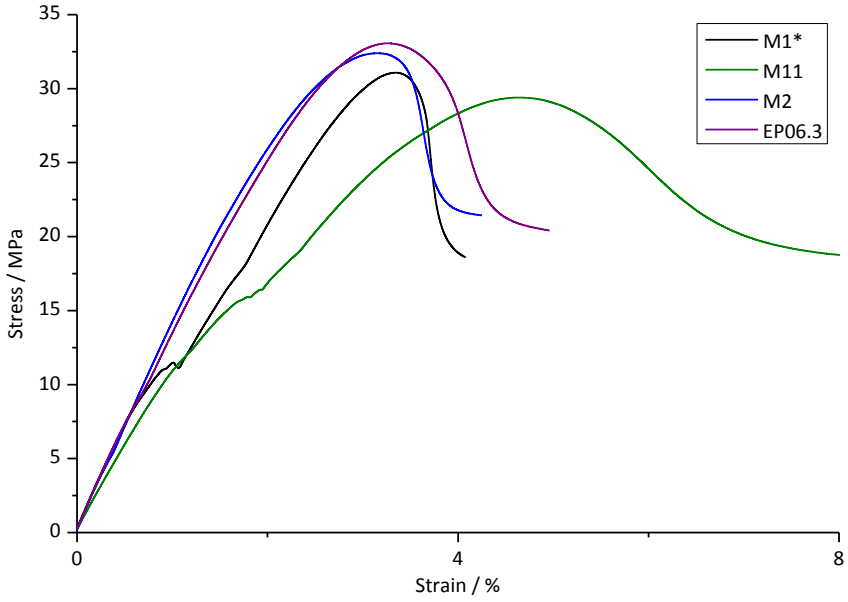

Figure 27 Tensile test of *pDCPD* cured with 20 ppm or 35 ppm* (*M1,*M11*, *M2*, *EP06.3*) at 60* or 80 °C.**

Both 2nd generation type initiators (blue and purple line) produced polymer with higher Young's modulus and maximum strength at yield compared with ***M1*** and ***M11*** (black and green line). Hence, further experiments, discussed in the following chapter 3.2.1.2, focused on the characterization of curing behaviour and polymerisation activity of initiator ***M2*** and related Grubbs 2nd generation type catalysts.

3.2.1.2. Polymerisation with Grubbs 2nd generation type catalysts

The latency of ***M2*** in ROMP of ***DCPD*** was evaluated by measuring the heat generation upon mixing monomer with various initiator loadings according to the general experiment set-up (3.1.2.1). The experiments were conducted at 4 °C (Figure 28), 25 °C (Figure 29) and 40 °C (Figure 31).

Curing at 4 °C (Figure 28) revealed no heat generation which was already observed for samples cured with ***M1*** (Figure 20). Compared with ***M1***, gelation started later and after 4 h the samples reached higher categories (for loadings ≥75 ppm). Moreover, loadings of ***M2*** differed in the curing progress. The lower the loadings the later the onset of polymerisation was detected. But once initiated, ***M2*** propagated faster compared with its first generation analogue.

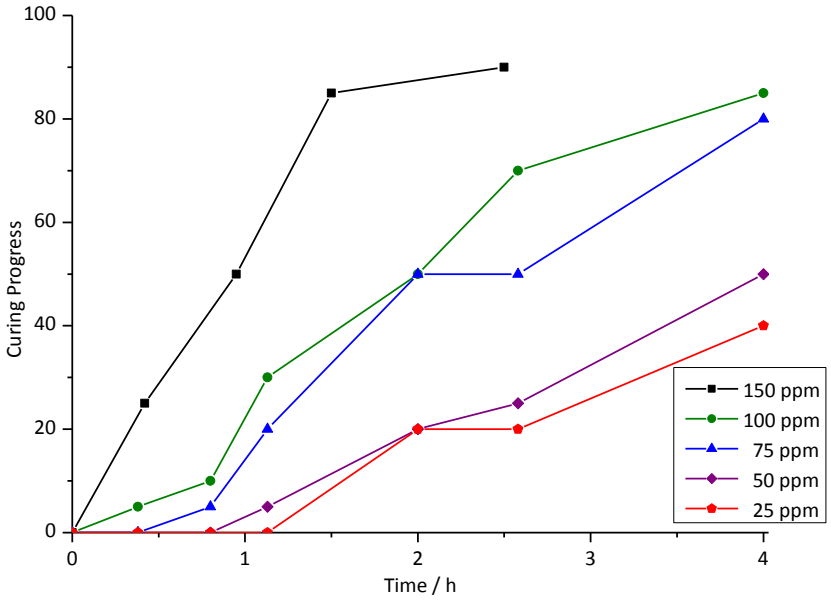

Figure 28. Curing progress according to Table 1 of *DCPD* with various *M2*-loadings at 4 °C.

Results obtained at 25 °C starting temperature revealed a dependency between initiator loading, latent behaviour and the increase in temperature (Table 8 and Figure 29). Higher loadings promoted faster initiation (reduced latency) and a distinct temperature rise compared with the measurements at 4 °C. Loadings lower than 50 ppm did not result in a detectable increase of temperature. In contrast to this, experiments performed with ***M1*** showed earlier reaction onsets (within 5 minutes) at any loading but lower temperature rise. In particular, θ_{max} of 32 °C and 113 °C at 150 ppm of ***M1*** and ***M2*** were measured, respectively. In addition, 50 ppm ***M2*** was sufficient to reached solid, though rather elastic material. Higher loadings resulted in fully cured samples (category 100).

Table 8. Polymerisation of *DCPD* with various *M2*-loadings at 25 °C.

$n_{Initiator}$ / ppm	θ_{max} /°C	t_{max} /min	t_{end} /min	$category_{end}$
25	25	x	60.00	30
50	29	30.34	43.60	80-85
75	74	16.84	21.18	100
100	69	13.36	17.17	100
150	113	6.21	10.87	100

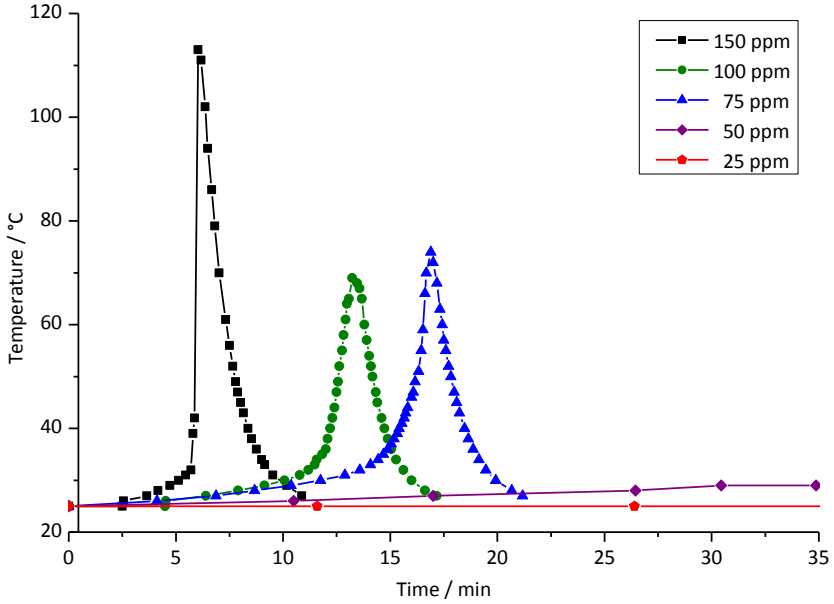

Figure 29. Heat generation upon mixing *DCPD* with various loadings of *M2* at 25 °C.

Further, polymerisation progress was monitored visually by a colour change from orange to greenish-red based on the initiation step which is enhanced at higher temperatures (Figure 30). At 25 ppm incomplete polymerisation occurred yielding category 30 and orange colour. At higher loadings and fully cured samples the colour changed to matt-red (50-100 ppm) and greenish (at 150 ppm).

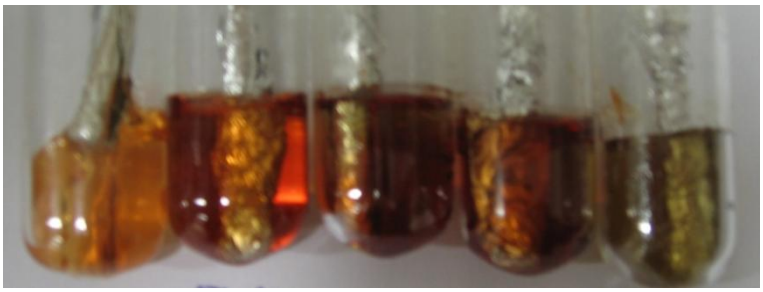

Figure 30. *pDCPD* polymerised with 25, 50, 75, 100 and 150 ppm *M2* (l.t.r.) at 25 °C.

Polymerisation at 40 °C differed from those conducted at 25 °C. At ***M2***-loadings between 150 and 50 ppm, the latency increased with decreasing loading but similar θ_{max} were observed at any loading. The samples were fully cured in less than 10 min. Polymerisation cured with 25 ppm ***M2*** did not result in a significant temperature rise and yielded a gel-like material after 14 min. In contrast, curing with ***M1*** at 40 °C led to similar onset of polymerisation at any loading (Table 3 and Figure 22).

Table 9. Polymerisation of *DCPD* with various *M2*-loadings at 40 °C.

$n_{Initiator}$ / ppm	θ_{max} /°C	t_{max} /min	t_{end} /min	$category_{end}$
25	41	11.32	14.00	40
50	132	6.63	10.62	100
75	125	3.67	8.13	100
100	134	2.10	6.27	100
150	126	0.67	5.02	100

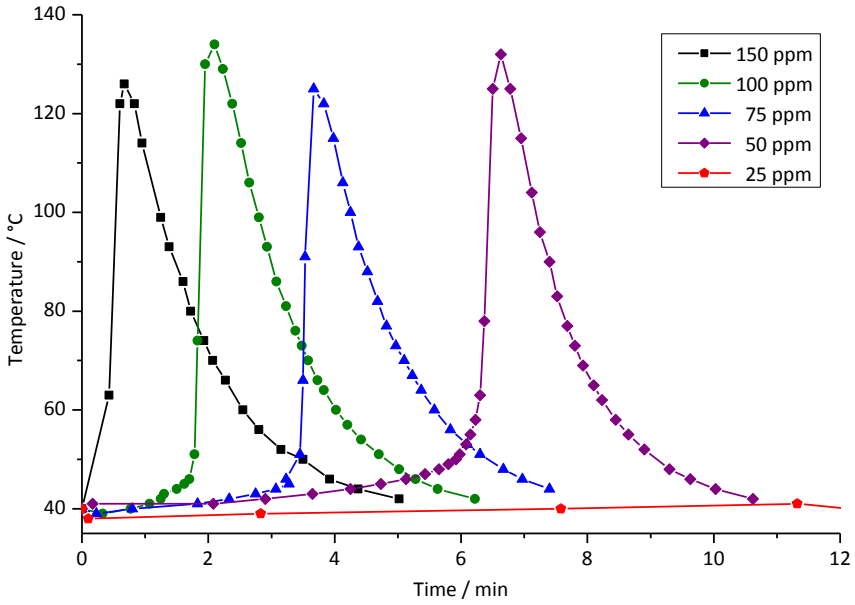

Figure 31. Heat generation upon mixing *DCPD* with various loadings of *M2* at 40 °C.

Polymers cured with different ***M2***-loadings are depicted in Figure 32. The polymerisation progress was estimated by the colour of sample as explain for those cured at 25 °C (Figure 30). Additionally, bubble generation was observed in samples with 75 ppm and higher loading as solvent or unconsumed monomer could not evaporate from the material before gelation occurred.

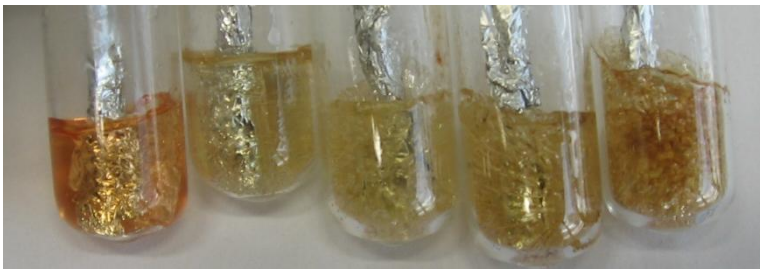

Figure 32. *pDCPD* polymerised with 25, 50, 75, 100 and 150 ppm *M2* (l.t.r.) at 40 °C.

In conclusion, latency and heat generated was controlled by the ***M2***-loading. For example, polymerisation with 75-150 ppm at 40 °C resulted in fully cured material after a short period of time (less than 10 min). Due to reduced latency and hence rather short processing windows compared with ***M2***, ***M1*** turned out to less convenient in this context.

In order to point out the capability of the ***DCPD***/***M2***-system at lower initiator loadings tensile tests were conducted. Shoulder test bars were cured at 60 °C with 5, 10 and 20 ppm initiator (Figure 33). Polymerisation of ***DCPD*** with 20 ppm was finished within few minutes yielding solid, fully cured materials containing little bubbles throughout the specimen. From the change in colour (from reddish to nearly colourless) indicated full initiation of ***M2*** at this loading. At 10 ppm ***M2***, conversion to a tough specimen was obtained after 30 min although its colour indicated incomplete initiation of ***M2***. This tendency proceeded at 5 ppm at which the reddish colour in the specimen and smell of monomer referred to incomplete initiation and polymerisation, respectively. The specimens were solid but still flexible after 2 h.[21]

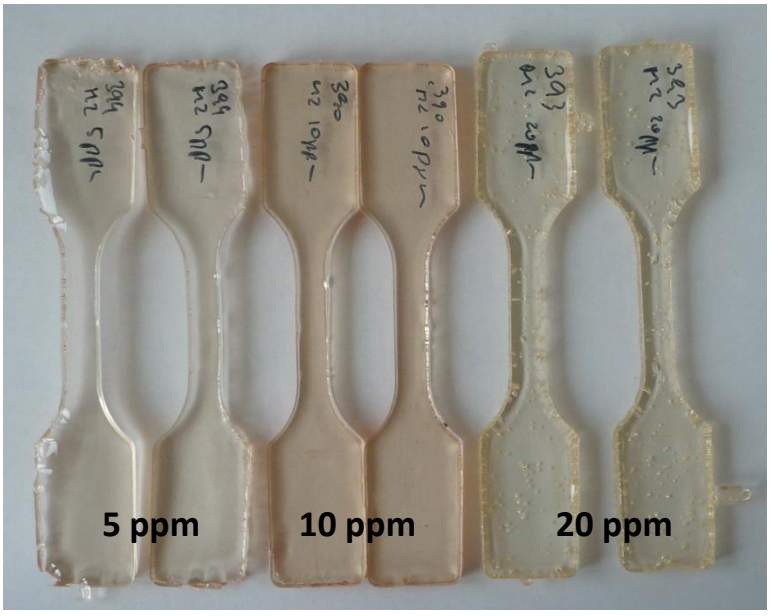

Figure 33. *pDCPD* cured with 5, 10 and 20 ppm *M2* at 60 °C (taken from reference 21).

These observations were confirmed by the data obtained in the tensile testing (Table 10 and Figure 34). Differences in mechanical properties of samples cured at 20 ppm in Table 7 and Table 10 are caused as only a small number of test bars was investigated. Such small initiator

loading was sufficient to prepare ***pDCPD*** with mechanical properties similar to those prepared via industrially used processes. At 10 ppm similar E-moduli were measured but after overcoming $Stress_{max}$ non-elastic deformation occurred in contrast to rigid behaviour at 20 ppm. This is likely caused by a rather low degree of cross-links in the polymer. As expected from previous curing tests, samples cured with 5 ppm ***M2*** reached lower E-moduli and $Stress_{max}$ followed by non-elastic deformation. Therefore, this loading is insufficient to achieve the maximum mechanical performance of this monomer/initiator system.[21]

Table 10. Mechanical properties of *pDCPD* cured with 5, 10 and 20 ppm *M2* at 60°C (taken from reference 21).

$n_{Initiator}$ / ppm	Young's modulus / GPa	$Stress_{max}$ / MPa
5	0.59	14.5
10	1.8	45
20	1.8	55
Reference[24]	1.87	43.0

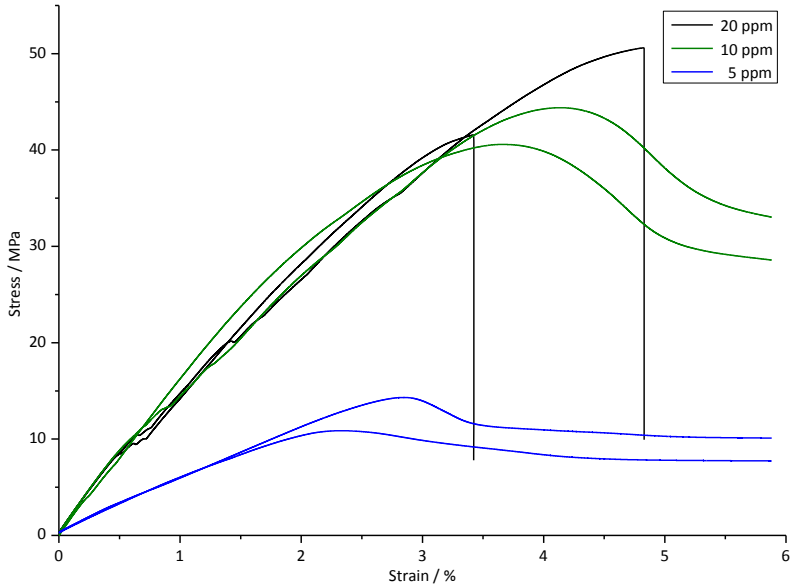

Figure 34. Tensile test of *pDCPD* cured with 5, 10 and 20 ppm *M2* at 60 °C (taken from reference 21).

STA measurements were conducted to provide further information about the curing behaviour with 20 ppm initiator loading. Both ***DCPD*** itself and a formulation of ***DCPD*** with 20 ppm ***M2*** were analysed (Figure 35). The samples were prepared as described in chapter Experimental. TGA measurement of ***DCPD*** revealed total mass loss as t and volatile components are removed by the continuous gas flow (green line). A decomposition process was observed in DSC measurements (onset temperature ≈60 °C) referring to a Retro-Diels-Alder to two equivalents Cp (green dashed line, *cf.* Scheme 1). DSC measurements of the ***DCPD***/***M2*** formulation revealed a polymerisation onset at 53 °C and the maximum of the exotherm at 75 °C (red dashed line). From a total mass loss of 16.7%, 7.4 % can be referred to solvent, resulting in 9.3% mass loss of ***DCPD*** (red line). No further mass loss was observed after the polymerisation exotherm as the volatile monomer had been consumed.

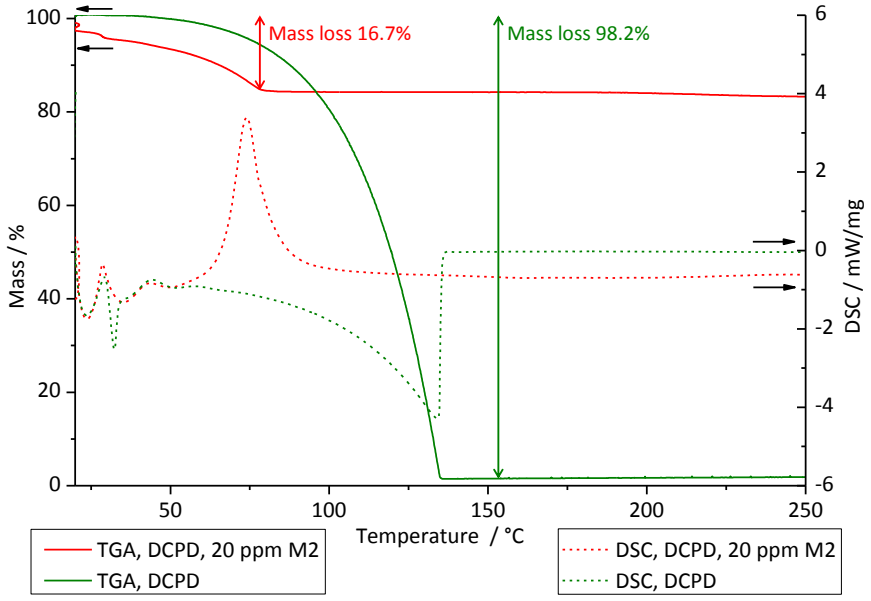

Figure 35. STA measurement of *DCPD* (green) and a formulation of *DCPD* with 20 ppm *M2* (red).

Furthermore, the performance of ***M2*** in the ROMP of ***DCPD*** at 40 °C was investigated. For the preparation of shoulder test bars a loading of 50 ppm was chosen because the preliminary curing test had revealed an appealing process window at this loading (*cf.* Figure 32). The test bars exhibited two zones coloured red and yellow (Figure 36). These zones also differed in hardness (Shore D-hardness of 68.0 and 75.5). This phenomenon was related to uneven initiation of ***M2*** inducted by uneven heating capacity of the oven.

Figure 36. *pDCPD* cured with 50 ppm *M2* at 40 °C exhibiting two zones (red and yellow).

The E-modulus and $Stress_{max}$ were lower than those of shoulder test bars cured with lower loading but higher curing temperature (Table 11 and Figure 37). In this case, it seems like the curing temperature has a larger impact on the polymerisation than the initiator loading.

Table 11. Mechanical properties of *pDCPD* cured with various *M2*-loadings at 60 °C (taken from reference 21) and 40°C.

$n_{Initiator}$ / ppm	Curing temp. / °C	Young's modulus / GPa	$Stress_{max}$ / MPa
10	60	1.8	45
20	60	1.8	55
50	40	1.56	37.6

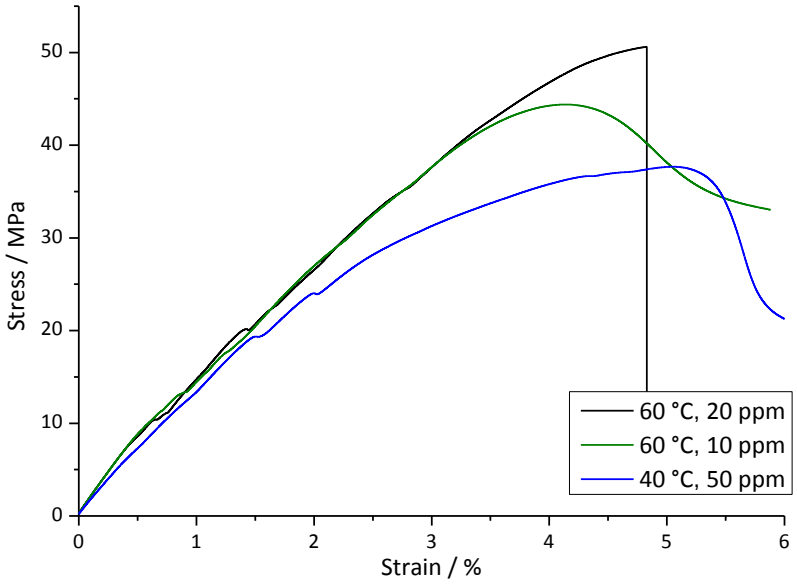

Figure 37. Tensile test of *pDCPD* cured with 10 and 20 ppm *M2* at 60 °C (taken from reference 21) and 50 ppm M2 at 40°C.

Shoulder test bars were also produced at lower temperatures exhibiting rather elastic behaviour. However, preliminary curing test conducted right afterwards with the same charge of ***DCPD*** showed different results. Reproducibility of these tests is strongly depending on constant quality of the used components. In case of ***DCPD***, the quality of the monomer changed in the melting process required each time before usage. In this process oxidation reactions take place as the monomer is exposed to air. Therefore, the results from the test bars cured at lower temperatures were not involved in the interpretation of performance of ***M2***. For the next experiments a new charge of ***DCPD*** was used and molten each time under mild conditions (water bath at 40 °C).

From the preliminary test, the low activity of ***M2*** in polymerisation of ***DCPD*** at 4 °C is known (*cf.* Figure 20). Therefore, another Grubbs 2nd generation type initiator was investigated. ***M20*** is an analogue to ***M2*** but possesses a triphenylphosphine as labile ligand instead of PCy_3 (Figure 38). This ligand is responsible for an increased initiation rate.[34]

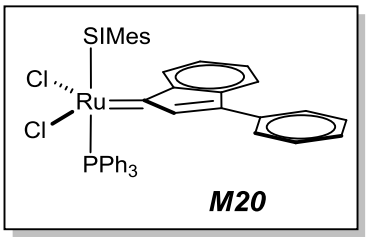

Figure 38. Grubbs 2nd generation type catalyst *M20*.

First, polymerisation of ***DCPD*** was performed at 25 °C using various initiator loadings (Table 12 and Figure 39). Clearly, initiation started faster compared to ***M2*** resulting in reduced latency at any loading. Heat generation (θ_{max} up to 110 °C) and complete curing were observed after less than 8 minutes also at low ***M20***-loadings. Reproducibility turned out to

be problematic for higher ***M20*** loadings. Inhomogeneous distribution of the initiator after injection occurred leading to further reduced t_{max}.

Table 12. Polymerisation of *DCPD* with various *M20*-loadings at 25 °C.

$n_{Initiator}$ / ppm	θ_{max} /°C	t_{max} /min	t_{end} /min	$category_{end}$
25	112	2.73	7.53	100
50	120	2.28	7.38	100
75	124	1.55	6.75	100
100	110	1.10	5.7	100
150	110	0.50	5.33	100

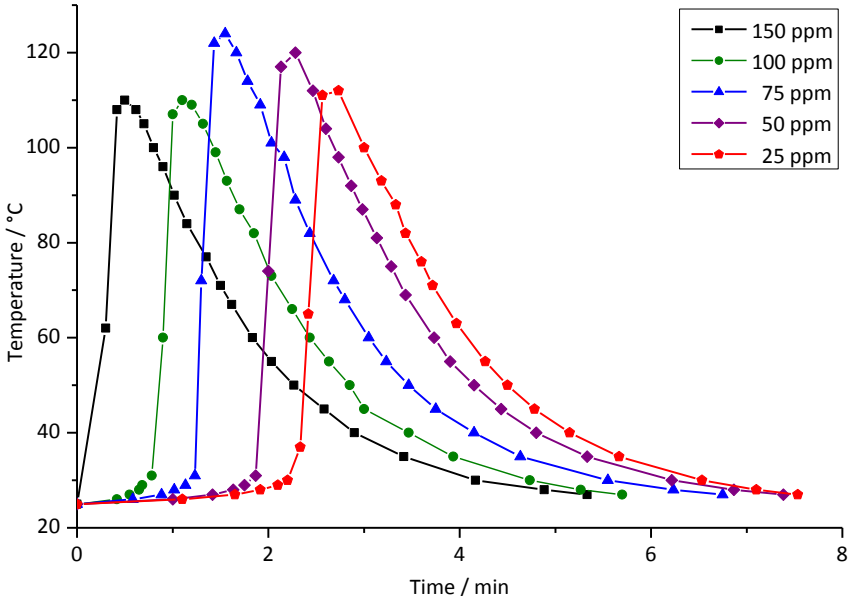

Figure 39. Heat generation upon mixing *DCPD* with various loadings of *M20* at 25 °C.

Although all loadings yielded full curing, differences in appearance were observed. The formulation's colour changed from slightly orange to yellow-brownish with increasing loading. Additionally, bubble generation was observed for both samples at 100 and 150 ppm (Figure 40).

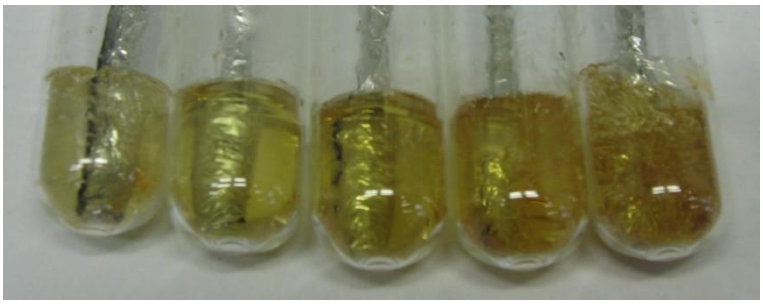

Figure 40. *pDCPD* polymerised with 25, 50, 75, 100 and 150 ppm *M20* (l.t.r.) at 25 °C.

Due to its high initiation rate/reduced latency no shoulder test bars were produced at neither ambient nor elevated temperatures as processing would be difficult. Yet reasonable mechanical properties of polymers cured at 4 °C were expected.

Shoulder test bars were cured with 50 ppm ***M20*** at 4 °C for either 1 or 7 days (Table 13 and Figure 40). After 24 h both Young's modulus and $Stress_{max}$ were significantly increased compared with ***pDCPD*** cured with ***M1*** (*cf.* Table 6). Similar to ***M1***, Young's modulus increased within 7 days as polymerisation progressed. However, the samples showed elastic behaviour and $Strain_{max}$ of about 300%.

Table 13. Mechanical properties of *pDCPD* cured with 50 ppm *M20* at 4 °C for either 1 or 7 days.

Curing time	Young's modulus / GPa	$Stress_{max}$ / MPa	$Strain_{max}$ / %
1 d	0.40	1.90	323.60
	0.63	5.86	284.10
7 d	1.30	16.35	267.25

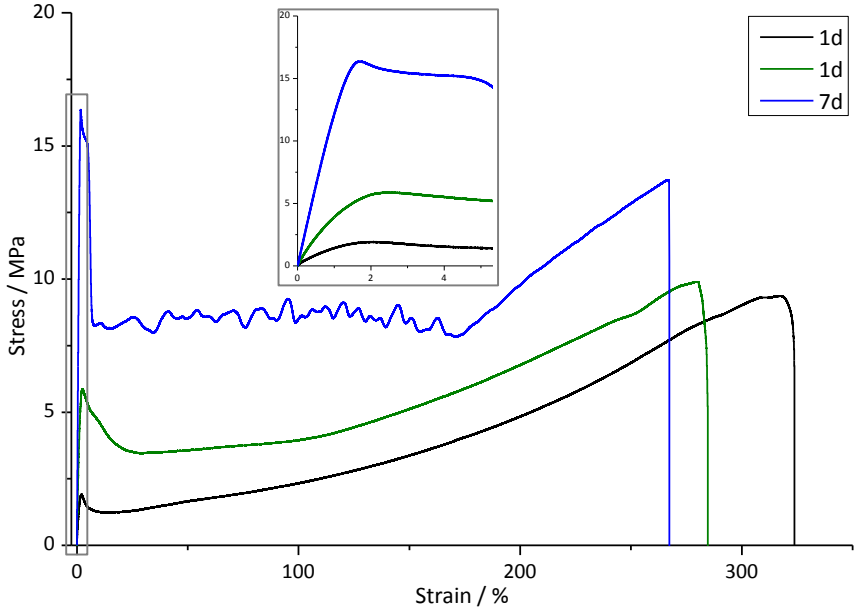

Figure 41. Tensile test of *pDCPD* cured with 50 ppm *M20* at 4 °C for either 1 or 7 days.

*3.2.1.3. Long term alkali resistance of **pDCPD***

The monomer/initiator system investigated in this work is aimed to be applied as chemical anchor in concrete walls. As discussed before (3.1.3.3), concrete is an alkaline medium. Alkali resistance is therefore a key property of polymeric materials in this context.

pDCPD specimens were produced using 50 ppm ***M2*** and curing conditions as described in the general procedure (*cf.* chapter 3.1.3.3). Four samples were produced and the respective parameters determined after 0 d, 3 d or 7 d. The changes in Shore D – hardness and weight over one week were presented in Table 14 and Figure 42. Generally, the values for Shore D-hardness and weight decreased including a recognizable change in Shore D – hardness of about 10% (values scatter from 6.7-14.6). The appearance changed and the samples turned from colourless to dark orange. The weight of the samples decreased slightly but not more than 0.20% in total. The influence of the alkaline medium over a longer period of time was not further investigated. It was assumed that the properties of ***pDCPD*** will not alter excessively over a longer period of time.

Table 14. Long term alkali resistance of pDCPD; change in Shore D – hardness and weight.

Sample	Storage Time	Shore D – hardness	Weight / g
1	0 d	82.5	8.6811
	3 d	78.3	8.6729
	7 d	77.0	8.6692
	Δ (0 d / 7 d)	*6.7%*	*0.14%*
2	0 d	79.6	8.5961
	3 d	79.7	8.5902
	7 d	70.2	8.585
	Δ (0 d / 7 d)	*11.8%*	*0.13%*
3	0 d	78.6	10.7721
	3 d	76.3	10.7634
	7 d	68.4	10.7571
	Δ (0 d / 7 d)	*13.0%*	*0.14%*
4	0 d	82.0	11.0896
	3 d	74.2	11.0785
	7 d	70.0	11.0702
	Δ (0 d / 7 d)	*14.6%*	*0.17%*

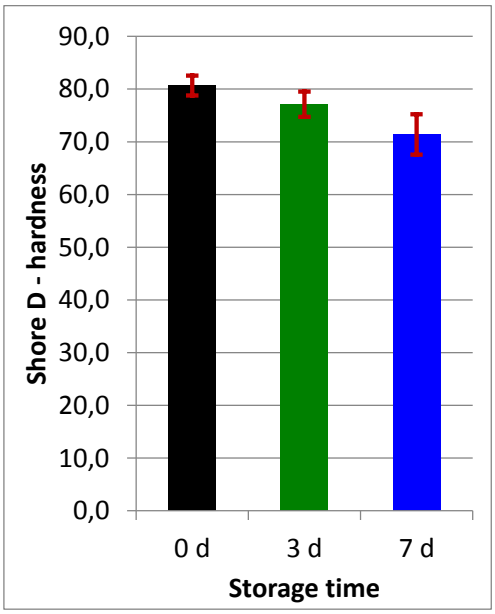

Figure 42. Alkali resistance of *pDCPD*; change in Shore D – hardness.

*3.2.1.4. Conclusion of the Ring Opening Metathesis Polymerisation of **DCPD***

So far, this work disclosed the performance of ***DCPD*** in combination with commercially available initiators (***M1***, ***M2***, ***M20***, …). The most promising results were achieved with 2nd generation type initiator ***M2***. It turned out that ***M2***-loadings lower than 50 ppm provided a suitable processing window. Shoulder test bars cured with 20 ppm ***M2*** for 24 h at 60 °C exhibited mechanical properties comparable with those of industrially produced ***pDCPD***. Recapitulating, ***pDCPD*** with appealing features for the intended application as a chemical anchor system was obtained. Nevertheless, some drawn backs were revealed. Firstly, ***DCPD*** is solid at room temperature necessitating solvent for processing. Secondly, ***DCPD*** is a volatile organic compound (VOC) which needs special declaration in future commercial products. Thirdly but most important, ***DCPD***/initiator systems investigated so far showed low reactivity at low temperature (4 °C) yielding rather elastic materials. In particular, initiation is hampered resulting in slow polymerisation progress and incomplete conversion after 24 h.

In the following, further hydrocarbon-based monomers were investigated. The obtained data concerning reactivity of the initiators at different loadings and temperatures exerted influence on the choice of initiator for the respective experiments. Monomers with higher reactivity due to their chemical nature (chapter 3.2.2 and 3.2.3) should be the key to overcome the intrinsic problem of low reactivity at low temperatures of the ***DCPD***-based system.

3.2.2. Norbornadiene (Mon2)

Norbornadiene is a bicyclic Diels-Alder adduct from cyclopentadiene and acetylene containing two equipollent double bonds (Figure 43). Compared with ***DCPD***, ***norbornadiene*** has some advantageous properties. This monomer is liquid at room temperature (mp -19 °C), which simplifies processing. Additionally, higher reactivity can be expected which is favorable for application at lower temperatures.

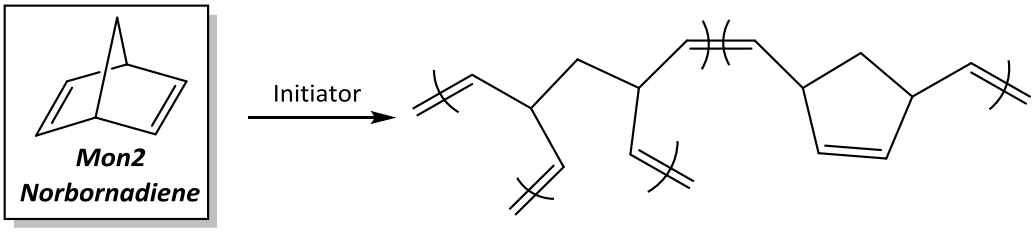

Figure 43. Polymerisation of *norbornadiene* (*Mon2*).

Firstly the heat generation upon mixing ***norbornadiene*** with various loadings of ***M2*** was investigated (Table 15 and Figure 44). Using 100 and 150 ppm ***M2*** lead to a distinct temperature rise (θ_{max} up to 130 °C) with reduced latency compared with ***DCPD***. As heat is released, foaming occurred (Figure 45) because unreacted monomer started to boil (bp. 85 °C). In case of 75 ppm ***M2***, polymerisation started after approximately 40 min. By then, the temperature level was not measured anymore. However, polymerisation progress and heat generation were observed visually as sudden foaming of the formulation occurred leading to a solid material. ***M2***-loadings of 50 ppm and lower exhibited no heat generation giving a gel-like material after 1 h.

Table 15. Polymerisation of *norbornadiene* with various *M2*-loadings at 25 °C.

$n_{Initiator}$ / ppm	θ_{max} /°C	t_{max} /min	t_{end} /min	$category_{end}$
50	-	-	60*	40
75	-	-	40*	100**
100	126	5.47	19.23	100**
150	130	3.52	16.56	100**

* approx.; ** foamed material

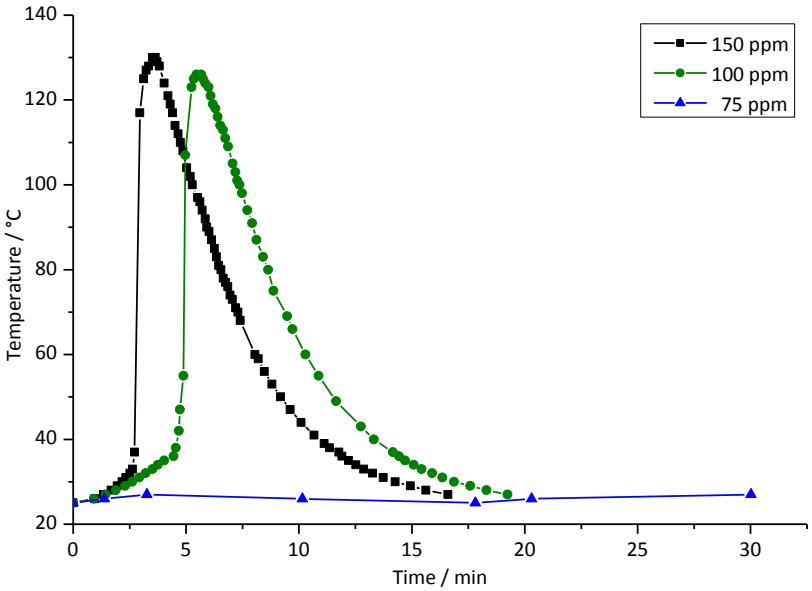

Figure 44. Heat generation upon mixing *norbornadiene* with various loadings of *M2* at 25 °C.

Figure 45. *Polynorbornadiene* polymerised with 50, 75, 100 and 150 ppm *M2* (l.t.r.) at 25 °C.

Further, the mechanical properties of ***Polynorbornadiene*** were investigated to reveal if it is a reasonable alternative to ***pDCPD***. Unfortunately, several problems occurred during processing. Due to its volatility the monomer evaporated from the mold before polymerisation started yielding irreproducible shapes (Figure 46 left). Polymerisation of ***norbornadiene*** in closed molds performed with higher initiator loadings and curing temperatures led to foaming as observed in the preliminary curing tests (Figure 46 right, *cf.* Figure 45). Polymerisation with different initiator loadings and curing conditions were conducted. However, fully cured and unfoamed samples were not obtained for this monomer/initiator system.

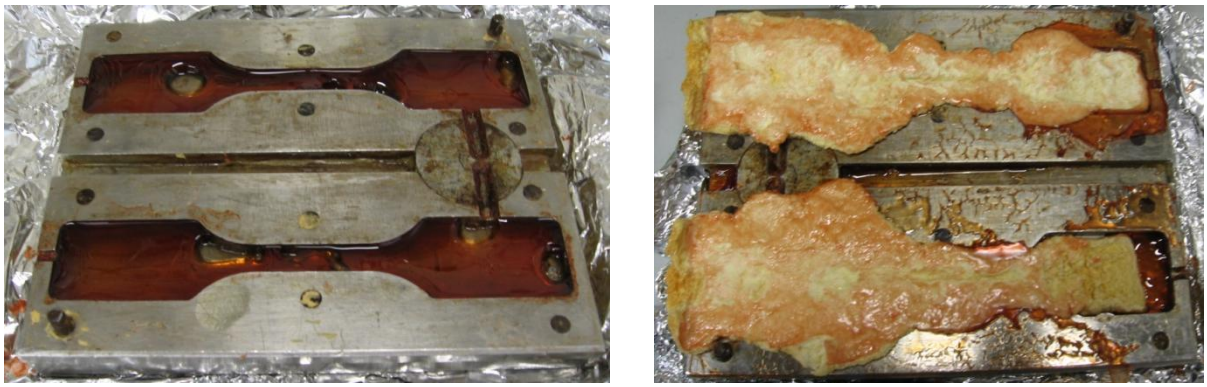

Figure 46. Curing of *norbornadiene* ; left: in open shoulder test bar mold with 100 ppm M2 at room temperature; right: in closed mold with 150 ppm at 40 °C.

Although temperature rise above the boiling point of the monomer is problematical in processing, the increased activity of ***norbornadiene*** compared with ***DCPD*** might still be a useful feature. Copolymerisation of ***norbornadiene*** in an appropriate ratio with a less reactive monomer would result in reduced reaction heat (preferably lower than the boiling point of ***norbornadiene***) but still increased polymerisation progress compared with homopolymerisation of the less reactive one. Therefore, copolymerisation of ***DCPD*** and ***norbornadiene*** at various ratios using 150 ppm ***M2*** were conducted to determine the capability of ***norbornadiene*** as reaction accelerator (Table 16 and Figure 47).

Table 16. Copolymerisation of *DCPD*:*norbornadiene* with 150 ppm *M2* at 25 °C.

Ratio	θ_{max} /°C	t_{max} /min	t_{end} /min	$category_{end}$
1:0	106	6.75	11.33	100
2:1	134	2.98	12.80	100*
1:1	133	2.80	15.33	100*
1:2	126	1.70	13.93	100*

* foamed material

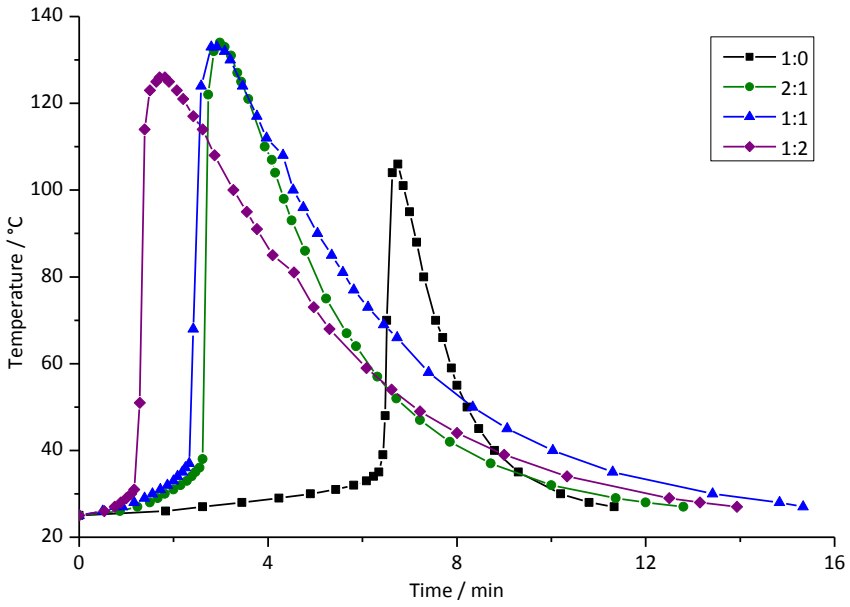

Figure 47. Heat generation upon mixing a mixture of *DCPD* and *norbornadiene* with 150 ppm *M2* at 25 °C.

The data for the homopolymerisation of ***DCPD*** was taken from chapter 3.2.1.2 (Table 8). Its θ_{max} is high above the boiling point of ***norbornadiene***In particular, θ_{max} increased with increasing amount of ***norbornadiene*** in the mixture resulting in foamed copolymers (Figure 48) while t_{max} decreased significantly already at 33wt% ***norbornadiene***.

Figure 48. Poly-*DCPD*-co-*norbornadiene* (ratios: 1:0, 2:1, 1:1, 1:2) polymerised with 150 ppm *M2* at 25 °C.

In summary, ***norbornadiene*** exhibited higher reactivity compared with ***DCPD*** due to its equipollent double bonds. However, this advantage quickly turned out to cause problems concerning processability (foaming). Using lower initiator loadings at room temperature led to imperfection in the specimens due to high volatility of the monomer. These problems could not be overcome in copolymerisation at various ratios with ***DCPD***.

3.2.3. 1,4,4a,5,8,8a-Hexahydro-1,4,5,8-endo-exo-dimethanonaphtalene (DMNH-6/Mon3)

1,4,4a,5,8,8a-Hexahydro-1,4,5,8-endo-exo-dimethanonaphtalene (***DMNH-6***) is another cyclic hydrocarbon-based monomer (Figure 49) synthesized from ***norbornadiene*** and Cp at elevated temperatures.[36] ***DMNH*-6** has already been reported as useful monomer in preparation of ROMP derived monolithic support for separation applications[37] or as polyHIPE[38]. Its two unsaturated sites exhibit equally high reactivity in ROMP. Overall, high potential can be expected in the context of chemical anchors.

A mixture of three isomers, *endo-endo*, *exo-exo*, *endo-exo*, was obtained by Diels-Alder addition (*cf.* chapter Synthesis) and used without separation of the isomers. ***DMNH-6*** is liquid at room temperature, highly reactive and beneficially less volatile than ***norbornadiene***.

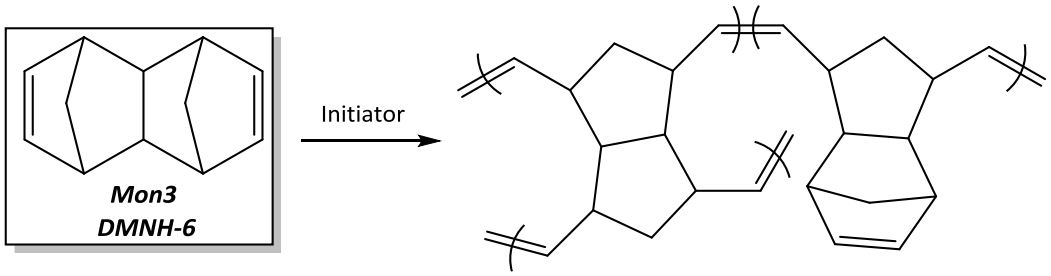

Figure 49. Polymerisation of *DMNH-6* (*Mon3*).

The heat generation was investigated with ***M2*** as initiator in order to compare ***DMNH-6*** with ***DCPD*** and ***norbornadiene***. Additionally, the initiator ***M20*** was considered to be unfavourable in this context as its higher reactivity might cause problems in processing.

Table 17. Polymerisation of *DMNH-6* with various *M2*-loadings at 25 °C.

$n_{Initiator}$ / ppm	θ_{max} /°C	t_{max} /min	t_{end} /min	$category_{end}$
25	26	5.50	17.00	60
50	130	3.92	11.70	100*
75	123	2.63	10.73	100*
100	125	1.33	9.82	100*
150	116	1.22	10.87	100*

[36] J.K. Stille, D. A. Frey, *J. Am. Chem. Soc*. **1959**, *81*, 4273-5.
[37] M.R. Buchmeiser, *Macromol. Rapid Commun.* **2001**, *22*, 1081-1094.
[38] H. Deleuze, R. Faivre, V. Herroguez, *Chem. Commun.* **2002**, 2822 - 2823.

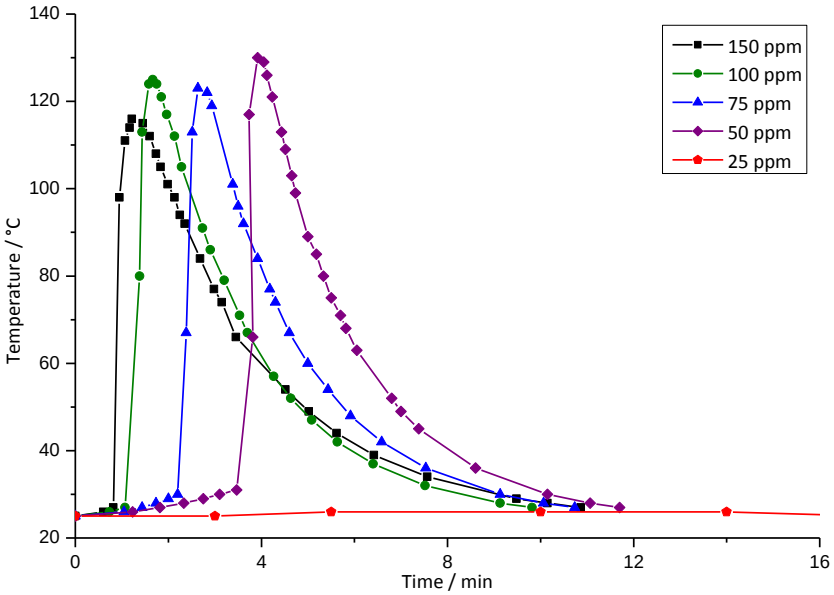

Figure 50. Heat generation upon mixing *DMNH-6* with various loadings of *M2* at 25 °C.

With 25 ppm ***M2*** no heat generation occurred (Table 17 and Figure 50). and the colour originating from the initiator did not change (Figure 51). Nevertheless, curing occurred and the polymer reached category 60 after 17 min. At loadings of 50 ppm and higher, a distinct temperature rise (θ_{max} up to 130 °C) after t_{max} (<4 min) and simultaneous foaming were observed. The foams were fully cured at t_{end} (<12 min). Similar to ***norbornadiene***, high reactivity of the monomer caused unwanted foaming.

Figure 51. *Poly3* polymerised with 25, 50, 75, 100 and 150 ppm *M2* (l.t.r.) at 25 °C.

In order to avoid foaming in production of shoulder test bars, the loading was lowered to 20 and 10 ppm ***M2***. First attempts with 80 °C as curing temperature yielded partly deformed and slightly foamed samples. Therefore, the curing temperature was reduced to room temperature. Both sample cured with 10 ppm were utilisable for tensile testing (Table 18). Curing at room temperature resulted in a rather elastic material (E-modulus $<7*10^{-4}$ GPa) whereas curing at 80 °C resulted in enhanced, but still low E-modulus (< 0.5 GPa) compared with ***DCPD*** samples.

Table 18. Mechanical properties of *Poly3* cured with 10 ppm initiator for 24 h.

Curing temp.	E- modulus / GPa	$Stress_{max}$ / MPa	$Strain_{max}$ / %	Shore D - hardness
80 °C	0.46	15.19	8.7	-
room temp.	$6.78*10^{-4}$	0.26	49.5	26.7

As discussed so far, foaming occurred at higher loadings and curing temperatures. But also at lower loadings parts of the material foamed leading to different geometries. STA/TGA measurements were conducted to identify the origin of foaming in polymerisation of ***DMNH-6***. A heating program from 20 to 500 °C at a heating rate of 3 $°C*min^{-1}$ was applied. In Figure 52 the obtained data (TG blue line, DSC green line) are depicted. At approx. 80 °C, an endothermic process started yielding complete mass loss. This decomposition process was related to a *retro*-Diels-Alder reaction to the volatile molecules ***norbornadiene*** and ***Cp*** which were removed by the gas flow from the apparatus.

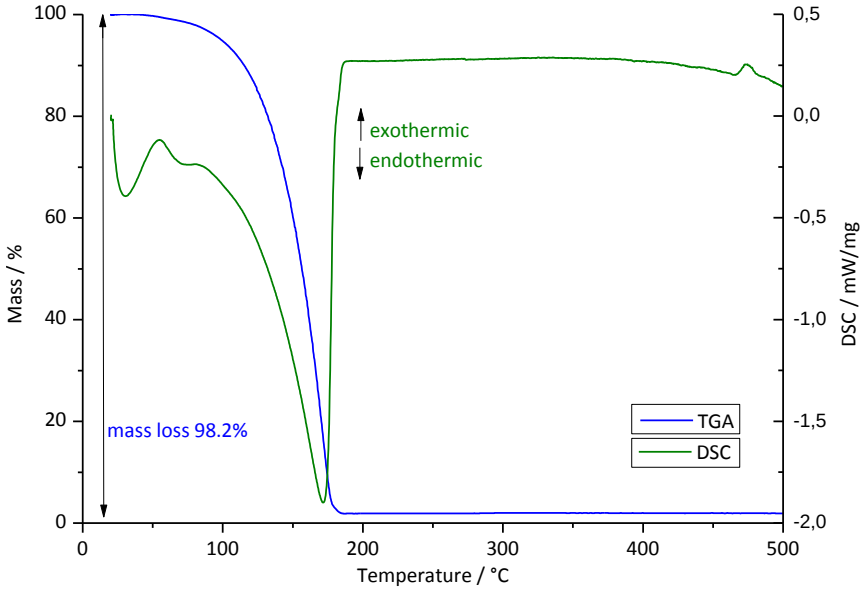

Figure 52. STA/TGA measurement of *DMNH-6*.

Clearly, this finding explains why foaming occurred at higher loadings (≥50 ppm) with θ_{max} higher than 75 °C. Both ***norbornadiene*** and Cp are in gaseous phase at that temperature.

Further experiments were conducted with ***Mon3*** purchased from Sohena GmbH. Shoulder test bars were produced to compare the monomers of different origins. During preparation a high viscosity of the monomer from Sohena hindered homogenous distribution of the initiator in the formulation. ^{1}H-NMR analysis (Figure 53) revealed that in contrast to the purchased ***DMNH-6***, the synthesized one contained ***norbornadiene*** (3%) which could not be removed by distillation from the crude product (*cf.* chapter Synthesis). This caused dilution and lower viscosity of the synthesized monomer and might have worked as reaction accelerator.

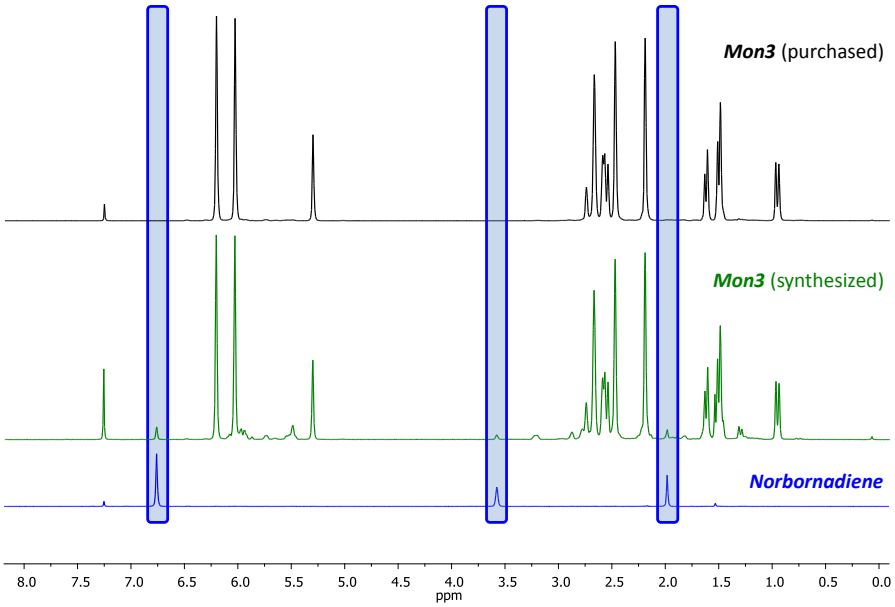

Figure 53. ^{1}H-NMR analysis (300 Hz, $CDCl_3$) of synthesized and purchased *DMNH-6* compared with n*orbornadiene*.

DCM was then exchanged by toluene as solvent in the following experiments to exclude bubbles from boiling solvent in the specimens. Shoulder test bars were produced for 24 h at 80 °C using 50 ppm ***M2*** and 100 µL solvent per test bar. Homogenous distribution of initiator was achieved by shaking the formulation. Tensile tests were conducted revealing similar mechanical properties of ***Poly3*** compared to those of ***pDCPD*** (Table 19 and Figure 54).

Table 19. Mechanical properties of *Poly3* cured with 50 ppm *M2* compared with *pDCPD* and reference.

Sample	$n_{Initiator}$ / ppm	E-modulus / GPa	$Stress_{max}$ / MPa	$Strain_{max}$ / %
Poly3 (sample 1-3)	50	1.36 – 1.72	31.77 – 37.77	2.13 – 4.01
pDCPD	20	1.8	55	4.0
Reference[24]		1.87	43.0	4.00 – 5.00

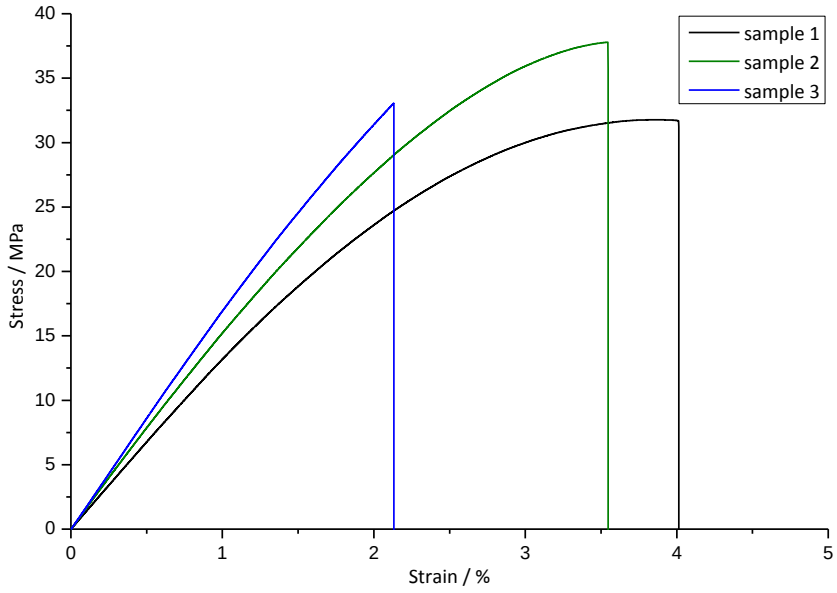

Figure 54. Tensile test of *Poly3* cured with 50 ppm *M2* at 80 °C.

Heat generation upon mixing purchased ***DMNH-6*** and ***M2*** was analysed to determine the impact of ***norbornadiene*** on the reactivity of the ***DMNH-6*** /***M2***-system when compared with the tests above (*cf.* Table 17 and Figure 50). Due to high viscosity no homogenous distribution of initiator in the monomer (here: 1 g) was achieved in the used experiment set up. The amount of solvent had to be increased to 200 µL in total. to get a homogenous distribution. However no temperature rise was detected. Although these observations did not help understanding the role of ***norbornadiene***, it did indeed provide an insight into the influence of the nature and amount of solvent on the polymerisation progress. Firstly, with increasing solvent content in the formulation, the monomers are statistically further apart. Secondly but more important, the released energy from ring opening is consumed by the solvent as it warms up. Consequently, the reactivity is reduced leading to increased latency. Nevertheless, the material was fully cured in an appropriate time.

In conclusion, ***Poly3*** yielded similar properties in terms of mechanical properties compared to ***pDCPD*** although the curing parameters had to be modified. Higher reactivity of the monomer caused some problems in processing. Above all, decomposition reactions at temperatures below θ_{max} led to unwanted foaming which was already observed in case on ***norbornadiene***.

3.2.4. Conclusion of the ROMP of hydrocarbon-based cyclic monomers

DCPD was the most potent of the investigated hydrocarbon-based cyclic monomers in respect of the target application. ***ROMP*** of ***DCPD*** with the latent 2nd generation initiator ***M2*** showed an appealing processing window and led to alkali-resistant ***pDCPD*** with an E-modulus 1.8 GPa. The disadvantages of ***DCPD*** were further sought to overcome with two other hydrocarbon-based cyclic monomers, ***norbornadiene*** and the naphthalene-derivative ***DMNH-6***. However, other problems like foaming occurred during polymerisation of these two monomers. Additionally, the mechanical properties were not as favourable as those of ***pDCPD***. Therefore, the ***DCPD***/***M2***-formulation was chosen as reference system in further discussions.

3.3. Heteroatom containing norbornene-based monomers as alternative

The main problems in ROMP of hydrocarbon-based monomers were volatility, malodour and foaming. Furthermore, the elastic behaviour of polymers cured for 24 h at low temperatures was problematic in respect of the target application. New monomers based on norbornenes were designed to overcome these problems. Introducing heteroatoms in the monomers should reduce the volatility of the monomers. Several multi-norbornene-derivatives linked by ester-, ether- or carbamate-groups were synthesized to obtain a cross-linked network and hence enhanced E-modulus and $Stress_{max}$ for the respective polymers.

3.3.1. Alkyl-linked bi- and tri- norbornene- esters Mon4, Mon6 & Mon8

In this chapter the performance of alkyl-linked norbornene-derivatives as alternative to hydrocarbon-based monomers is discussed. One advantage of this monomer-class is their easy access in one step from the commercially available Cp and the corresponding multi-acrylates. The polymerisation of these monomers was performed using either ***M2*** or ***M20***, both 2nd generation type initiators. The reactivity of these initiators has been discussed in the chapters above and was used to regulate the polymerisation speed in the following experiments.

*3.3.1.1. endo-endo-Ethane-1,4-diyl-bis-(norbornene-carboxylate) (**Mon4**) & endo-endo-Butane-1,4-diyl-bis-(norbornene-carboxylate) (**Mon6**)*

Mon4 and ***Mon6*** are both bi-norbornene-esters linked by a C_2- and C_4-alkyl chain, respectively (Scheme 4). The norbornene double bonds exhibit equipollent reactivity promoting formation of a cross-linked network. The monomers were derived by Diels-Alder addition reaction of Cp and the corresponding diacrylate. In case of ***Mon6***, the monomer was purchased from Orgentis Chemicals and contained about 10% impurities identified as unconverted acrylate. Full conversion was yielded after stirring the Orgentis-product with an excess of Cp at 40 °C (*cf.* chapter Synthesis).

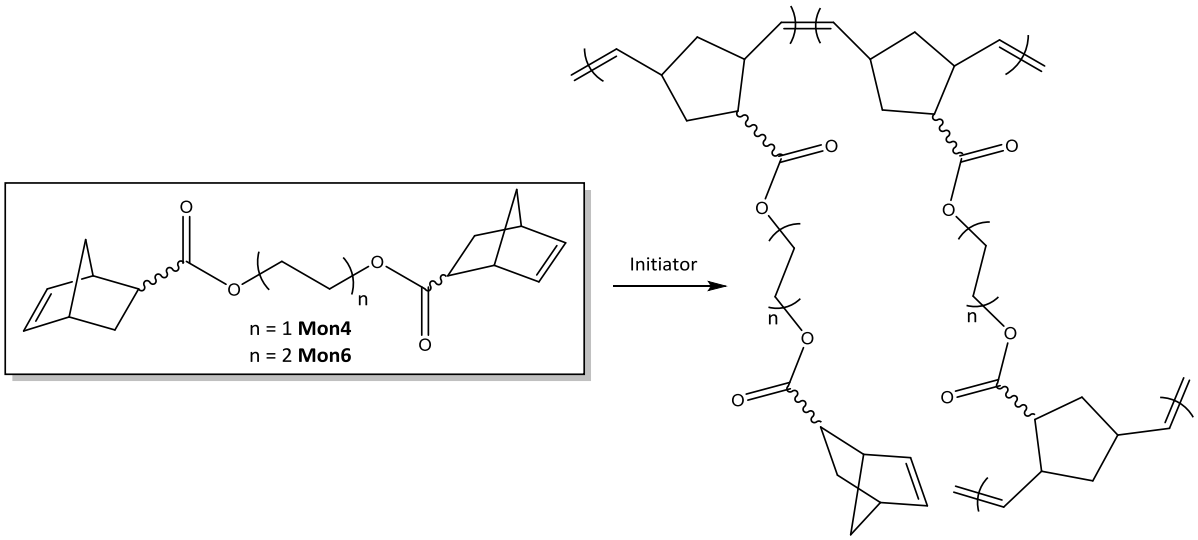

Scheme 4. Polymerisation of *Mon4* and *Mon6*.

First, the heat generation upon mixing ***Mon4*** with 150 ppm ***M2*** was investigated to evaluate the reactivity of this new class of monomers compared with that of ***Mon1*** – ***Mon3***. After 45 min, the temperature had not changed. The formulation was heated up to 40 °C. Another 45 min later the sample was solid and very elastic (category 50). The sample was stored at 80 °C overnight to complete curing and reached a hardness of category 90-100 on the next day. The absence of an exotherm and rather slow curing was caused by the chemical nature of the particular monomer and initiator. In ROMP the norbornene double bond coordinates to central Ru-atom. In the propagation step a second free coordination site is occupied by norbornene double bond from a second monomer-molecule. In the instance of ***Mon4***, the intramolecular carbonyl group can competitively coordinate at the second free coordination site (Figure 55). This interfering mechanism decelerates the polymerisation and hence lowers the rate of released heat. This effect has a significant influence on processing window and curing duration.

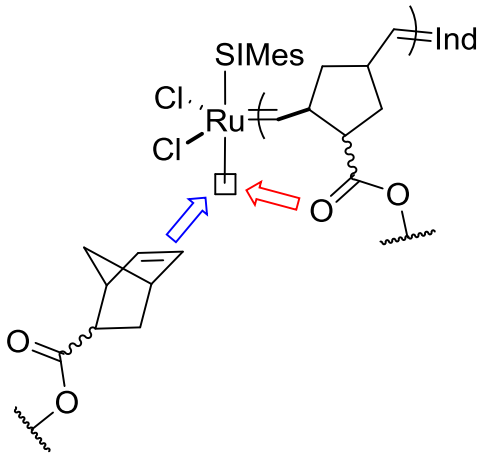

Figure 55. Competitive coordination of one monomer molecule and intramolecular carbonyl group.

For further measurements, the more reactive initiator ***M20*** was used because a detectable temperature rise and appealing (short) curing duration are preferable. The heat generation upon mixing ***Mon4*** with ***M20*** (150 and 100 ppm) at 25 °C was investigated. Again, no significant exotherm was detectable. However, polymerisation took place. Therefore, the measurements were repeated but instead of heat, the curing progress was evaluated according to Table 1 (*cf.* chapter 3.1.2.1). Gelation occurred within 1.5 min at both 150 and 100 ppm ***M20*** (Figure 56, dashed red and orange line). Category 70 and 60 were reached after less than 13 min, respectively. Curing overnight resulted in solid and hardly elastic materials (category 90).

Repeating the curing tests with ***Mon6*** instead of ***Mon4*** showed higher reactivity compared with ***Mon4*** (Figure 56, black, green, blue and purple plain line). Similar to the ***Mon4***/***M20*** formulation, heat generation did not occur at any loading (50-150 ppm); hence the curing progress was again evaluated according to Table 1 (cf. chapter 3.1.2.1). Compared with ***Mon4***, gelation point was reached within the same time frame. Further, the curing progress was faster, also at 50 ppm. At 150 ppm ***M20***, the sample was solid but still elastic (category 70) after 2 min, hardly elastic (category 90) and after 8 min and fully cured (category 100) after 24 h in total. Lower loadings yielded solid, slightly elastic materials (category 80) within 10-15 min which were hardly elastic (category 90) after 24 h.

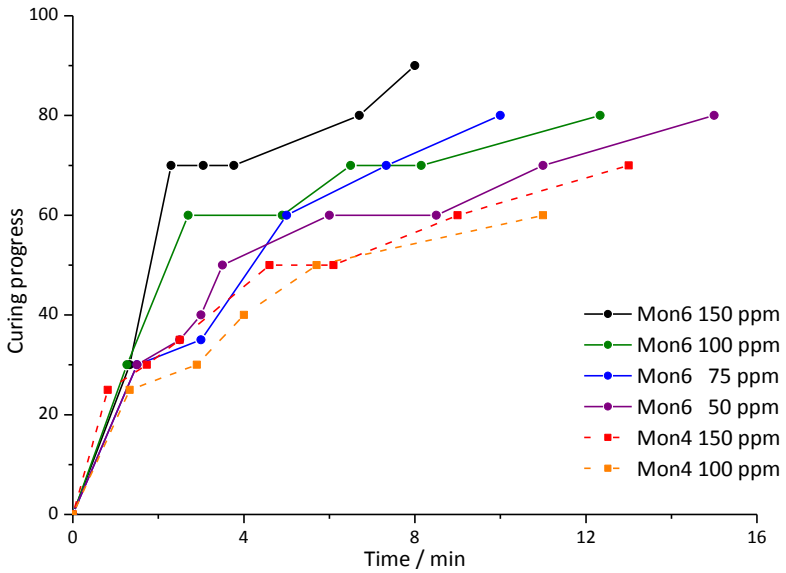

Figure 56. Curing progress according to Table 1 of *Mon4* and *Mon6* with various *M20*-loadings at 25 °C.

Due to the increased reactivity of ***Mon6*** compared with ***Mon4*** (probably caused by the longer linker moiety and hence enhanced flexibility) curing tests were conducted with ***M2*** as initiator. Heat generation was not observed. Still, polymerisation took place leading to a solid and very elastic material (category 50) after 1 h which was hardly elastic (category 80) after 24 h. Based on this measurement, ***M20*** proved to be the more suitable initiator in this context.

Shoulder test bars were produced at various curing conditions to determine the mechanical properties of ***Poly4*** and ***Poly6*** (Table 20). The colour of the formulations changed from red to colourless after quite a short time indicating fast initiation. Unlike the hydrocarbon-based test bars, the samples were highly brittle and broke when taken out of the mold after 1.5 h. The samples were left in the mold for 24 h to gain defect free samples. But also with this procedure, no suitable test bars (cured at room temperature, 100 ppm ***M20***) could be obtained.

Table 20. Loadings and curing temperatures for the preparation of shoulder test bars based on *Mon4* and *Mon6*.

Monomer	Loading	Curing temperature
Mon4	50 ppm	24 h at 40 °C
	50 ppm	5 min at rt, 24 h at 80 °C
Mon6	100 ppm	24 h at rt
	50 ppm	24 h at 40 °C
	50 ppm	5 min at rt, 24 h at 80 °C

The mechanical properties of ***Poly4*** and ***Poly6*** were compared to ***pDCPD*** cured with 20 ppm ***M2*** (Table 21 and Figure 57). Comparing the samples cured at 80 °C, both ***Poly4*** and ***Poly6*** could not reach the E-modulus of ***pDCPD***. In particular, the E-modulus and $Stress_{max}$ of ***Poly6*** were approximately half of that of ***pDCPD.*** The E-modulus and $Stress_{max}$ of ***Poly4*** were even lower than that. Further, curing at 40 °C was insufficient to obtain similar mechanical properties. The values for both E-modulus und $Stress_{max}$ were several folds lower than those of the samples cured at 80 °C. The decreased E-modulus was likely caused by a lower degree of cross-links and the larger linker between the individual polymer chains. This in turn causes enhanced flexibility of the network compared with ***pDCPD***.

Table 21. Mechanical properties of *Poly4* and *Poly6* cured with 20 ppm *M20* at either 40 or 80 °C compared with *pDCPD*.

Polymer	Curing temp. / °C	E- modulus / GPa	$Stress_{max}$ / MPa	$Strain_{max}$ / %
pDCPD (20 ppm ***M2***)	40	1.56	37.6	12.70
	80	1.80	55	4.00
Poly6	40	0.30	6.81	9.25
	80	0.97	24.05	5.95
Poly4	40	0.03	1.30	8.05
	80	0.80	17.39	6.85

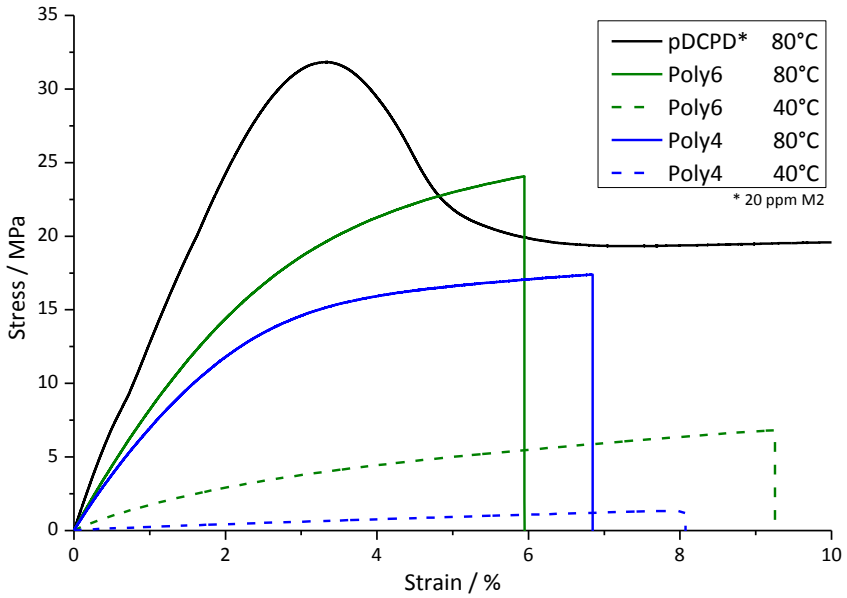

Figure 57. Tensile test of *Poly4* and *Poly6* with 50 ppm *M20* at 40 or 80 °C compared with *pDCPD* (20 ppm *M2*).

Poly6 was chosen as representative for the class of di-norbornene-ester over ***Poly4*** in further experiments due to higher E-modulus and $Stress_{max}$.

*3.3.1.2. Trimethylolpropane-tri-(norbornene-carboxylate) (**Mon8**)*

Mon8 was designed aiming at a polymer with a higher degree of cross-links. It is an analogue to ***Mon4*** and ***Mon6*** but contains three polymerisable sites linked by a trimethylolpropane-ester unit. The synthesis followed the protocol used to derive ***Mon4*** and ***Mon6*** but with trimethylolpropane triacrylate as dienophile (cf. chapter Synthesis).

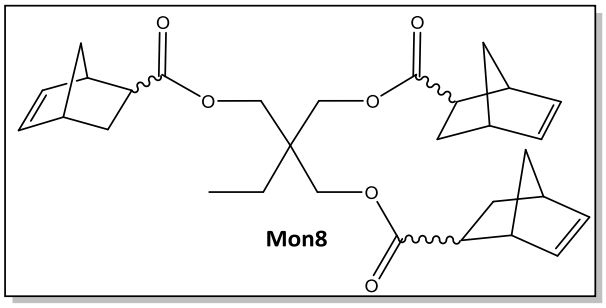

Figure 58. Chemical structure of *Mon8*.

The polymerisation of ***Mon8*** with 150 ppm ***M20*** was investigated at 25 °C analogue to the experiments with ***Mon4*** and ***Mon6***. Heat generation was not observed. However, a gel-like solid was obtained after 4 min. After 16 h the material was fully cured (category 100). In this experiment, the viscosity was by far higher compared with the two other monomers. Still, homogenous distribution of the initiator was achieved. Test bars were produced with 50 ppm ***M20*** at both 40 and 80 °C. Theoretically, the amount of cross-links in ***Poly8*** is higher compared with ***Poly4*** and ***Poly6***. However, decreased E-modulus and $Stress_{max}$ indicated

decreased degree of cross-linkages in ***Poly8*** (Figure 59). In particular, the E-modulus of ***Poly8*** (E = 0.43 GPa, red plain line) was about half of those of ***Poly4*** (E = 0.80 GPa, blue plain line) and ***Poly6*** (E = 0.97 GPa, green plain line). It seemed likely that the viscosity of the monomers influences the degree of polymerisation as well as the formation of a cross-linked network. Therefore, the highly viscous monomer ***Mon8*** was copolymerised with equal amounts of ***Mon6*** and 50 ppm ***M20***. Thereby, the advantages of an enhanced theoretical degree of cross-links and a lowered viscosity compared with ***Poly6*** and ***Mon8*** were combined, respectively. The E-modulus of ***Poly8-co-6*** (E = 0.67 GPa, purple plain line) was still lower than that of ***Poly6*** after 24 h. ***Poly8-co-6*** was also cured for 120 h in total (E = 1.10 GPa, purple dashed-dotted line) to obtain a higher E-modulus as polymerisation continued at low rates. Further, it seemed likely that curing at 40 °C for 24 h was insufficient to tap the full potential in terms of degree of polymerisation and cross-links.

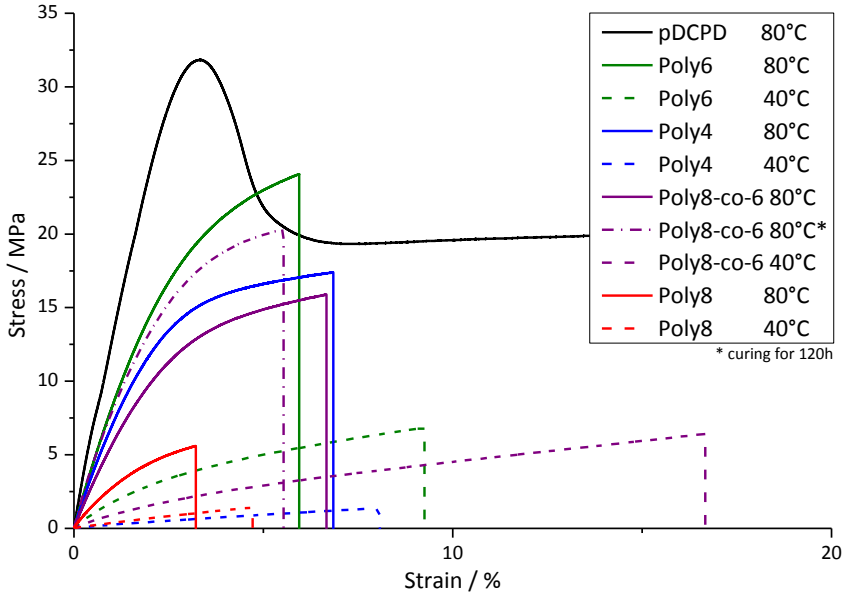

Figure 59. Tensile test of *Poly4*, *Poly6*, *Poly8-co-6* and *Poly8* cured with 50 ppm *M20* at 40 or 80 °C compared with *pDCPD* cured with 20 ppm *M2*.

Next, the influence of the viscosity of the monomers ***Mon4***, ***Mon6***, ***Mon8*** and the mixture ***Mon8+Mon6*** on the mechanical properties of the respective polymers were closely investigated. The viscosity was determined using a cone-plate rheometer (cf. chapter 3.1.1.1). The data from this experiment and from tensile testing was summarized in Table 22.

Table 22. Mechanical properties of *pDCPD* cured with 50 ppm *M2* and *Poly4*, *Poly6*, *Poly8-co-6* and *Poly8* cured with 50 ppm *M20* cured both at 40 and 80 °C compared with the viscosity of the respective monomers; E-modulus of polymers cured at 80 °C for 24 h are highlighted.

Polymer	Curing temp. / °C	E-modulus / GPa	$Stress_{max}$ / MPa	$Strain_{max}$ / %	$Viscosity_{Mon}$ / Pa*s
pDCPD	40 °C	1.56	37.6	12.70	-
	80 °C	1.80	55	4.00	
Poly6	40 °C	0.30	6.81	9.25	0.1
	80 °C	0.97	24.05	5.95	
Poly4	40 °C	0.03	1.30	8.05	0.1
	80 °C	0.80	17.39	6.85	
Poly8-co-6	40 °C (120 h)	0.11	6.41	16.62	0.5
	80 °C	0.67	15.90	6.67	
	80 °C (120 h)	1.10	20.30	5.50	
Poly8	40 °C	0.04	1.39	4.72	10.10
	80 °C	0.43	5.57	3.21	

Two trends emerged from this data set. On the one hand, viscosity increased with increasing size of the monomer (***Mon4***, ***Mon6*** < ***Mon8+Mon6*** << ***Mon8***). On the other hand, the E-modulus of polymer cured at 80 °C (*cf.* Table 22 and Figure 60) decreased with increasing viscosity (***Poly6*** > ***Poly4*** > ***Poly8-co-6*** > ***Poly8***).

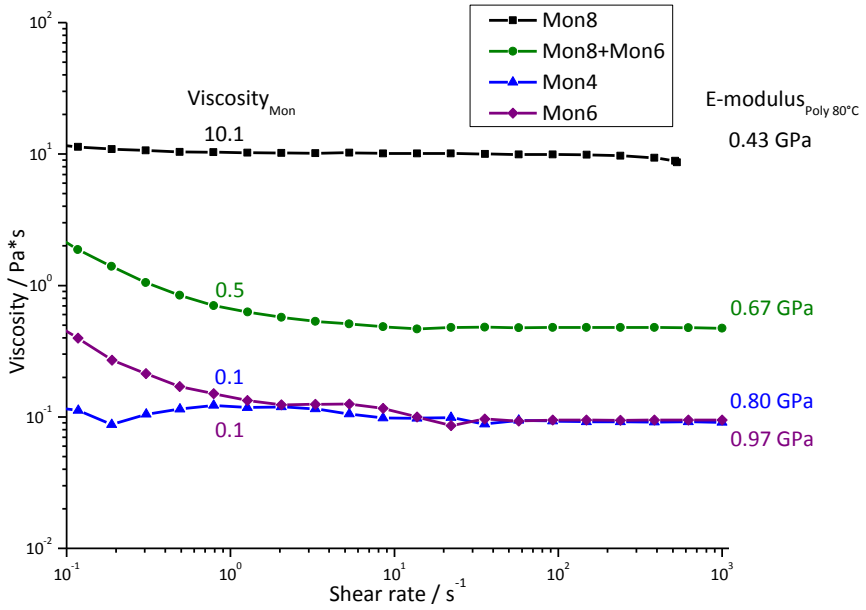

Figure 60. Viscosity of *Mon8*, *Mon8+Mon6*, *Mon4* and *Mon6* vs. E-modulus of *Poly8*, *Poly8-co-6*, *Poly4* and *Poly6*.

3.3.1.3. Rheokinetic measurements

So far, the polymerisation progress was analysed referring to the heat generation or the change in viscosity/hardness after mixing monomer and initiator. Another way to characterise the curing progress and the gelation time are rheokinetic measurements, cf. chapter 3.1.2.3. The curing process was monitored by the shear storage and shear loss modulus G' and G'' is. The gel point (=cross-point of G' and G'') of the ***DCPD*/*M2*** formulation was reached after 7.5 minutes (Table 23 and Figure 61). Due to the bad signal-to-noise ratio, the gelation time of the ***Mon6*/*M2*** and the ***Mon8+Mon6*/*M2*** formulation could only be determined within several minutes (Figure 62 and Figure 63). The obtained gelation time is much longer than that determined in the respective preliminary tests (gelation/ category 30). This was caused by the plates of the rheometer which were cooled at 23 °C. Hence, the cooling system removed any heat released by the opening of the norbornene ring and slowed down the polymerisation. Further, the end of the curing process was observed in the polymerisation of ***DCPD*** after 250 min. The values for G'_{end} and G''_{end} correspond to the moduli of ***pDCPD*** cured and measured at 23 °C. In case of ***Mon6*** and ***Mon8+Mon6,*** an undefined problem occurred during the measurement resulting in random noise. The polymerisation of ***Mon8*** was also investigated but the gel point was not reached after 16 h.

Table 23. Rheokinetic parameters from the polymerisation of *DCPD*, *Mon6*, *Mon6+Mon8* and *Mon8 with 50 ppm M20*.

Monomer	$\eta_{(25\,°C)}$ / mPa*s	Gelation time / min	G'_{end} / Pa	G''_{end} / Pa
DCPD	-	7.5	$6.6*10^6$	$6.1*10^5$
Mon6	97	13.3-16.6	*	*
Mon8+Mon6	485	40.0-43.3	*	*
Mon8	10140	not reached after 16 h	-	-

* not determinable

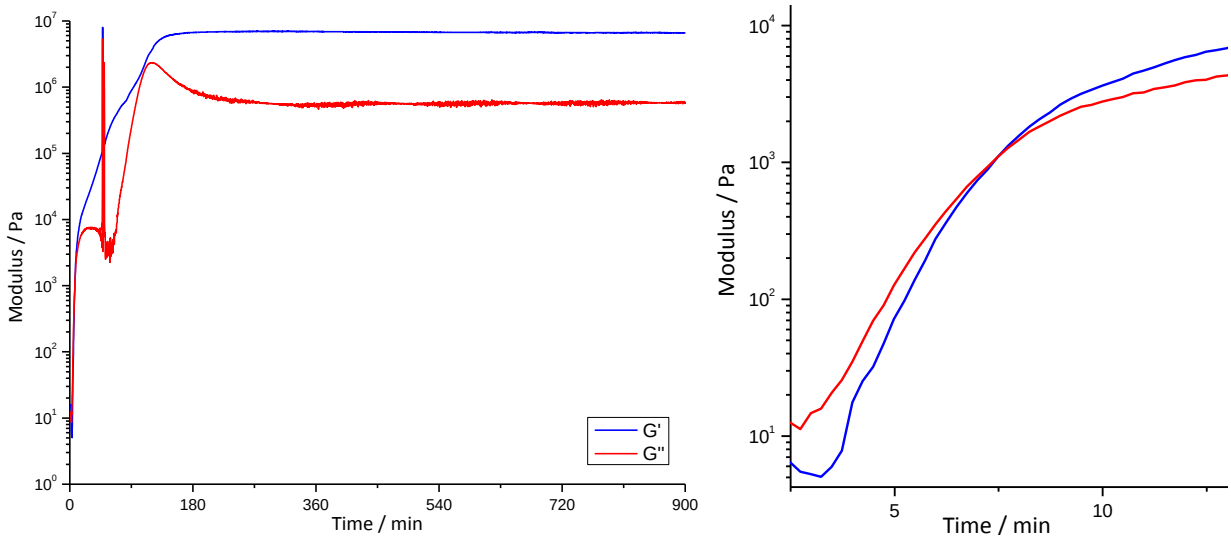

Figure 61. Rheokinetic measurement of polymerisation of *DCPD* with 50 ppm *M20* (left); close-up view (right).

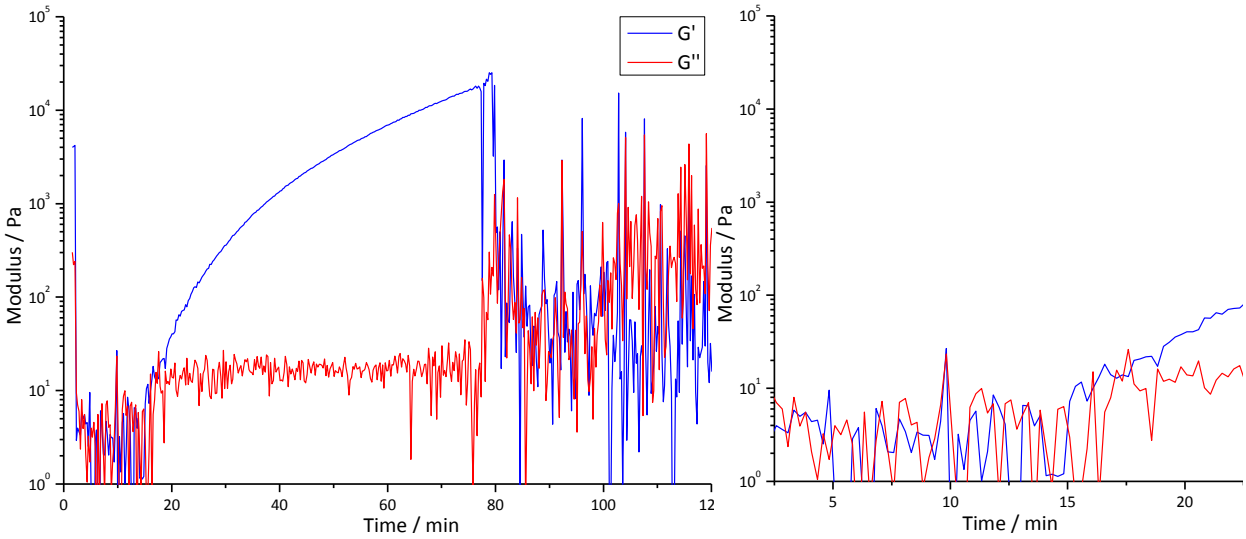

Figure 62. Rheokinetic measurement of polymerisation of *Mon6* with 50 ppm *M20* (left); close-up view (right).

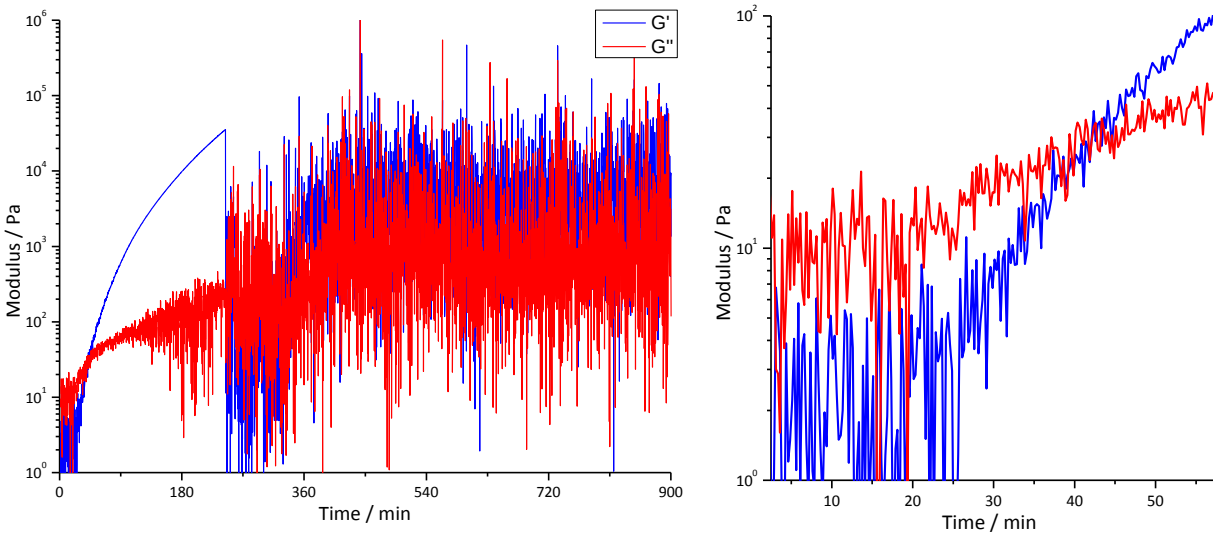

Figure 63. Rheokinetic measurement of polymerisation of *Mon8+Mon6* with 50 ppm *M20* (left); close-up view (right).

*3.3.1.4. Long term alkali resistance of **Poly6***

The resistance towards alkaline media of ***Poly-norbornene-esters*** was investigated because this is an essential feature of chemical anchors in concrete walls, *cf.* chapter 3.1.3.3. ***Poly6*** was chosen as representative of the ***Poly-norbornene-esters*** because it reached the higher E-modulus and $Stress_{max}$ than ***Poly4***, ***Poly8-co-6*** and ***Poly8*** (*cf.* Table 22 and Figure 59). Five discoidal samples were produced and exposed to an alkaline medium as described in chapter 3.1.3.3. The appearance of the samples (colour, …), weight and Shore-D hardness were determined after 1, 5 and 7 days as well as 2, 4 and 12 weeks (Table 24 and Figure 64). Surprisingly, the Shore-D hardness decreased rapidly between 15 and 30% within one week (highlighted in Table 24 and Figure 64) which would be critical in the target application. However, these results were caused by problems in calibration of the test equipment. Once located, this problem was eliminated easily. Over a period of 12 weeks Shore-D hardness increased more than 30%. This was related to hardening process at the surface of the sample. Meanwhile the sample changed from colourless to orange and lost about 3-4% weight which is considered negligible.

Table 24. Long term alkali resistance of *Poly6*; change in Shore D – hardness and weight; inaccurate values of Shore D-hardness of the first week are highlighted.

Storage Time	Shore D – hardness					Weight				
	1	2	3	4	5	1	2	3	4	5
0 d	58.0	57.9	56.9	59.2	56.6	10.21	10.24	10.08	9.96	10.49
1 d	52.1	53.1	51.2	51.7	46.9	10.22	10.25	10.09	9.97	10.48
5 d	50.3	48.3	53.8	51.9	48.2	10.19	10.22	10.05	9.93	10.41
7 d	48.8	48.3	48.1	46.0	37.4	10.17	10.20	10.04	9.92	10.38
2 weeks	74.9	75.4	74.7	74.6	70.7	10.13	10.16	9.99	9.87	10.32
4 weeks	77.7	78.3	78.4	78.1	74.0	10.07	10.10	9.94	9.81	10.22
12 weeks	78.4	79.1	79.4	79.7	76.6	9.86	9.92	9.79	9.59	10.07
Δ(0d/12 weeks)	35.2%	36.6%	39.5%	34.6%	35.3%	-3.5%	-3.2%	-2.8%	-3.7%	-4.0%

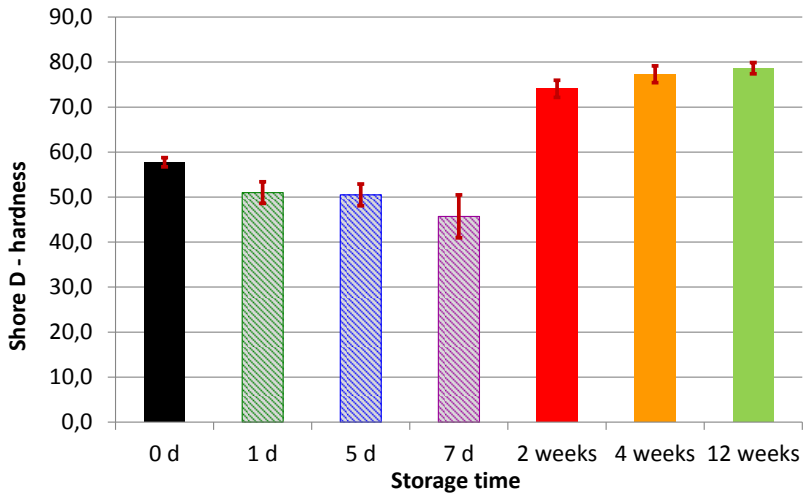

Figure 64. Alkali resistance of *Poly6*; change in Shore D – hardness; inaccurate values of Shore D-hardness of the first week are hatched.

3.3.2. Hydroxy-functionalised norbornene-ester Mon9

Mon9 (2- hydroxyethyl- *endo*- norbornene- carboxylate, Figure 65) is a mono-norbornene-ester (synthesis *cf.* chapter Synthesis). Due to the lack of a second ROM-polymerisable group only a linear polymer chain and hence lower E-modulus can be achieved. Nevertheless, this monomer might prove useful as a reactive diluent also because it exhibits a rather low viscosity (η = 51.5 mPa*s).

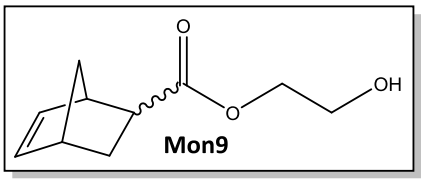

Figure 65. Chemical structure of *Mon9*.

First, the homopolymerisation of ***Mon9*** was investigated (Table 25 und Figure 67). Different to the other norbornene-esters a distinct temperature rise (θ_{max} = 42 and 70 °C) was detected upon mixing the monomer with 100 and 150 ppm ***M20***. Compared with the polymerisation of ***DCPD*** with the same ***M20***-loadings, t_{max} was about four times longer. At t_{end} the materials were solid and (rather) elastic (category 60-70). However, ***Poly9*** was still not fully cured after 24 h even at the highest loading. In contrast to this, curing of ***Poly6*** did not result in a temperature rise but fully cured materials after 24 h at 150 ppm ***M20***. At 75 ppm the temperature rise was rather low. However, the sample was a solid and very elastic material at t_{end}. 50 and 25 ppm ***M20*** led to gel-like materials after t_{end} and 24 h, respectively.

Table 25. Polymerisation of *Mon9* with various *M20*-loadings at 25 °C.

$n_{Initiator}$ / ppm	θ_{max} /°C	t_{max} /min	t_{end} /min	$category_{end}$	$category_{24h}$
25	25	0.00	10.00	15	30
50	26	3.20	15.00	35	35
75	28	5.42	11.00	50	60
100	42	4.43	8.05	60	80
150	70	2.28	5.43	70	90

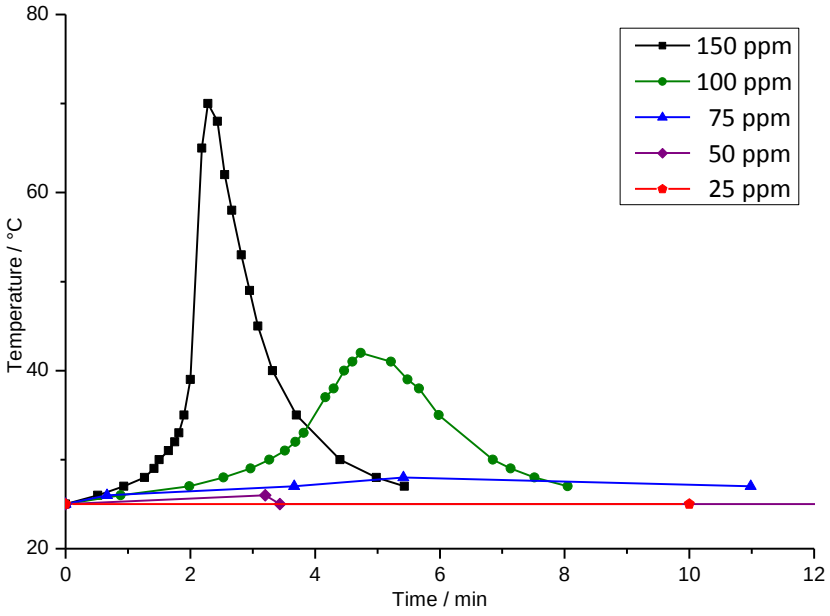

Figure 66. Heat generation upon mixing *Mon9* with various loadings of *M20* at 25 °C.

Furthermore, ***Mon9*** was mixed with 150 ppm ***M2.*** Gelation occurred within 24 h but the initial red colour remained indicating a very low initiation rate (Figure 67, left sample). In case of ***M20*** the initial red colour disappeared at t_{max}. The higher the loading the less orange the samples appeared at t_{end} (Figure 67, 4 samples to the right, 50-150 ppm ***M20***).

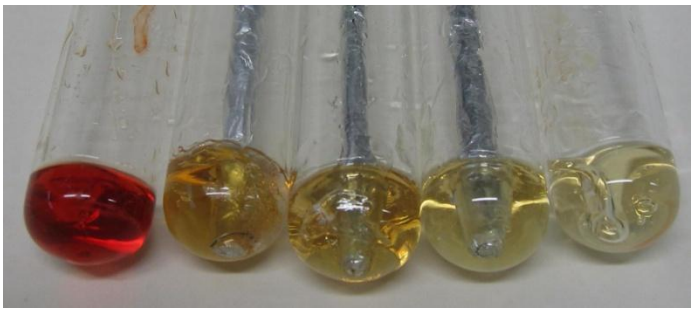

Figure 67. *Poly9* polymerised with 25 ppm M2 and 50, 75, 100 and 150 ppm *M20* (l.t.r.) at 25 °C.

For the preparation of shoulder test bars 50 ppm ***M20*** and 100µL DCM per 1.8 g monomer were used. Curing at 40 °C resulted in colourless, very elastic and sticky test bars. Further, they still smelled of ***Mon9*** indicating incomplete consumption of the monomer. The mechanical properties could not be determined as usual due to its very high elasticity. The test bars cured at 80 °C for 24 h were yellowish, twisted and smelled of monomer. These test bars were also not applicable in tensile testing.

Copolymerisation of ***Mon9*** and ***Mon6*** was investigated to show whether the addition of ***Mon9*** would enhance the E-modulus compared with that of the homopolymer ***Poly6***. Equal amounts of the monomers were mixed and polymerised with 50 ppm ***M20*** at 80 °C. The gelation occurred within 1 min while the formulation was still held at room temperature. The final test bars were rather brittle and sticky. The E-modulus of ***Poly6-co-9*** was by far lower than that of ***Poly6*** (E = 0.2 GPa and 0.97 GPa, respectively). Further, the ***Poly9-co-6***-

test bars broke at $Stress_{max}$ of approx. 4.5 MPa. It seemed that addition of ***Mon9*** did not result in a higher degree of cross-links in the copolymer compared with the ***Poly6***-homopolymer. Polymerisations with different ratios of ***Mon6*** and ***Mon9*** were therefore not investigated.

3.3.3. Carbamate-linked norbornene ester Mon10

Mon10 (bis(ethyl-norbornene-carboxylate)-(4,4'-methylene-diphenyl-dicarbamte)) is a di-norbornene-ester based on 2 molecules ***Mon9*** and an aromatic dicarbamate – linker (Figure 68, *cf.* chapter Synthesis). The aromatic rings introduce more rigidity to the linker moiety compared with the alkyl-linked monomers which might result in a higher E-modulus.

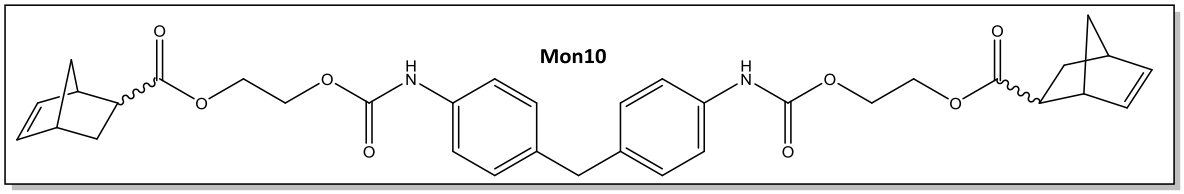

Figure 68. Chemical structure of *Mon10*.

Mon10 is solid at room temperature, hygroscopic but pulverulent when stored under N_2-atmosphere. The melting point of the monomer was not determinable at ambient conditions. ***Mon10*** was diluted with ***Mon9*** (ratio: 1:1, w/w) resulting in a yellowish, cloudy liquid and then copolymerised with 50 ppm ***M20***. The obtained shoulder test bars were gel-like, sticky and not suitable for tensile testing. Further characterisation was not conducted.

3.3.4. Bis-(methyl-norbornene) ether Mon11

Mon11 (1,1'-biphenyl-4-bis(methoxy-norbornene)) is the only di- norbornene- ether investigated in this work (Figure 69). This monomer lacks of a propagation-interfering carbonyl group next to the norbornene-moiety, *cf.* chapter 3.3.1.1 and Figure 55. Hence, a faster propagation is expected. However, due to side-reactions and purifications problems in the preparation (cf. Synthesis) the monomer was not obtained in pure form, and no further characterisation was done.

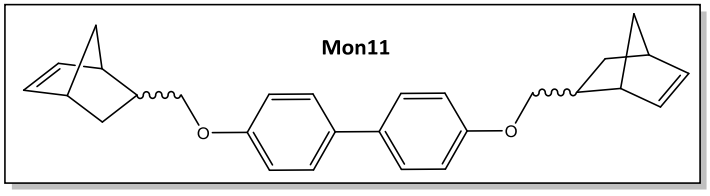

Figure 69. Chemical structure of *Mon11*.

3.3.5. Ester-linked bis-methylnorbornene Mon12

Mon12 (bis(norbornene-2-methyl)succinate) is a constitutional isomer to the alkyl-linked norbornene-ester ***Mon6*** (Figure 70).

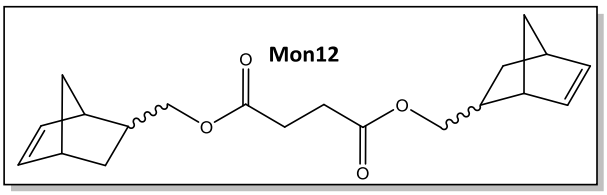

Figure 70. Chemical structure of *Mon12.*

The distance between the initiator and the carbonyl group is increased. Therefore, the carbonyl group in ***Mon12*** is expected to interfere less in propagation than ***Mon6*** (*cf.* chapter 3.3.1.1 and Figure 55). Hence, faster polymerisation speed and earlier gelation in processing is expected. Both ***Mon12*** and ***Mon6*** have a viscosity of approx. 0.1 Pa*s (114 and 97 mPa*s, respectively). Therefore, any difference in reactivity between those two monomers is based on differences in the chemical structure. The less active initiator ***M2*** was chosen to facilitate processing of the test bar formulation. Homogenous distribution of initiator (50 ppm) in the formulation was not achieved due to enhanced reactivity leading to test bars with uneven mechanical properties after curing at 80 °C for 24 h. For the next test bars, 25 ppm ***M2*** was used. Additionally, the whole amount of solvent (100 µL DCM) added to the formulation was used to dissolve the initiator. Thereby, homogenous distribution was ensured. Tensile testing revealed E-moduli of 0.36 and 0.07 GPa for samples cured with 50 and 25 ppm ***M2*** at 80 °C, respectively.

3.3.6. Comparative study of polymers by dynamic mechanical analysis (DMA)

Dynamic mechanical analysis (*cf.* chapter 3.1.3.2) was conducted to investigate the T_g and post-curing of samples cured at 40 and 80 °C. In respect of the target application, T_g higher than 70 °C is favourable. Post-curing which occurs as the sample is heated up to 180 °C indicates previous incomplete curing. The cylindric samples were cured at 40 and 80 °C to reveal whether these two curing temperatures are sufficient to obtain fully cured polymers within 24 h. Additionally, ***Mon6*** was polymerised with both ***M2*** and ***M20*** to analyse the impact of the activity of the initiator on the final properties of the polymer. The sample preparation and the measurements were conducted according to the general procedure in chapter Experimental and 3.1.3.2.

*3.3.6.1. **pDCPD** cured with 50 ppm **M2** at 40 and 80 °C*

pDCPD cured for 24 h at 40 °C exhibited two distinct zones coloured red and yellow within the sample. This phenomenon was already observed in shoulder test bars (cf. Figure 36) indicating uneven initiation. The two zones were then analysed separately (Figure 71).

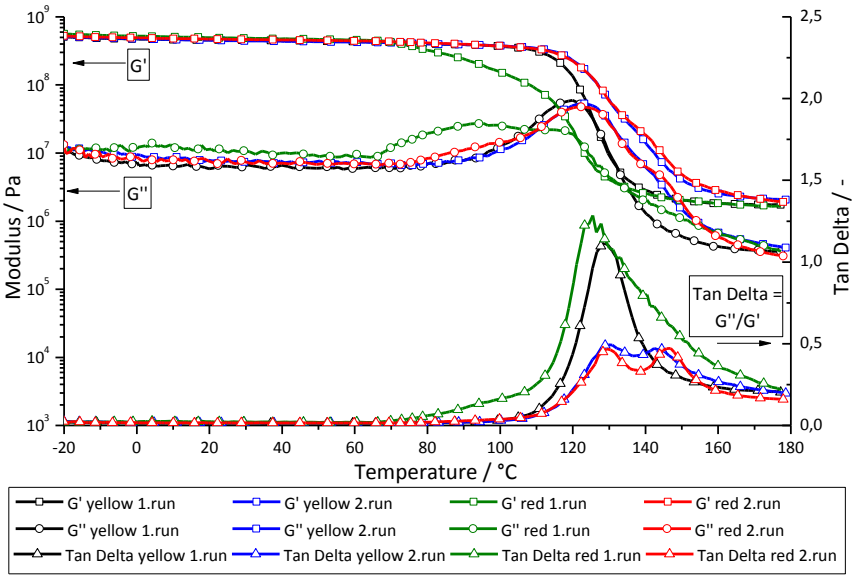

Figure 71. DMA measurement of *pDCPD* cured with 50 ppm *M2* at 40 °C, yellow (1.run) and red sample (1./2.run).

In the first run (black and green lines) the curve progress of G' and G'' of both samples looked rather similar differing only in the temperature at which G' decreased and G'' increased (in the red sample 40 °C earlier). The T_g was detected at approx. 129 °C ±3 °C for both samples. From -20 to 110 °C, the G' curves proceed constantly at about $5.0*10^8$ Pa, then decreased and reached a plateau again at $1.8*10^6$ Pa at 170 °C. The G'' curve started at $\approx 10^7$ Pa, a magnitude of 10^2 Pa lower than G'. In addition, a fast increase of G''

approximating G' curves with a maximum close to the T_g was observed at 70 and 90 °C in red and yellow sample, respectively, followed by a decrease down to $3.5*10^5$ Pa.

In the second run (blue and red lines) rather similar curves of G', G'' and tanδ were obtained for both samples. However, the obtained curves differed significantly from those of the first run. This altered curve progress was based on a post-curing effect as both samples were heated up to 180 °C before the second run. Further, the red sample turned yellow after the first run. Interestingly, two distinct T_gs were observed at 130 and 145 °C.

Curing of ***DPCD*** at 80 °C led to homogenous ***pDCPD*** samples. Both first and second run (red lines) looked similar to the second run (green lines) of the samples cured at 40 °C (Figure 72) and showed the same two T_gs. In contrast to 40 °C, curing for 24 h at 80 °C was sufficient to obtain the maximum performance in terms of dynamic mechanical properties and material characteristics of ***pDCPD***.

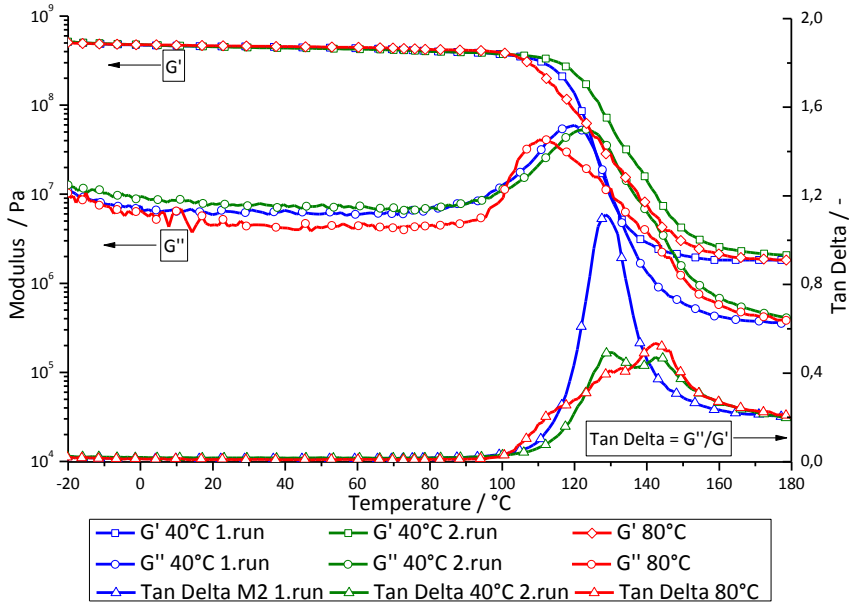

Figure 72. DMA measurement of *pDCPD* cured with 50 ppm *M2* at 40 (1./2.run) and 80 °C (1.run).

*3.3.6.2. **Poly6** cured with 50 ppm **M20** at 40 and 80 °C*

Like ***DCPD***, ***Mon6*** was cured with 50 ppm ***M20*** at both 40 and 80 °C. The G' curve of samples cured at 40 °C (blue line) showed a constant decrease till and less steep increase after 70 °C, respectively (Figure 73). The T_g was detected at 56 °C. The increase in G' after 70 °C was related to post-curing. The G'' curve decreased also after 70 °C because the viscous component in the post-curing sample decreases. Unfortunately, the samples broke during cooling to -20 °C after the first run, so no second run could not be performed. The samples expanded during heating which led to a larger gap between the clamps. However, the gap was not adapted to the contracting sample during cooling. The gap between the two pieces

was the same distance as the gap at the end of the heating program. Hence, elongation of these samples is a completely reversible process.

The G' of samples cured at 80 °C (green lines) resulted in a plateau after 70 °C indicating a fully cured samples during preparation (Figure 73). Furthermore, the T_g was detected at 75 °C which is a significant increase (approx. 20 °C) compared with the samples cured at 40 °C. This is another indication of incomplete curing of ***Poly6*** at 40 °C (Figure 74). A second run of the sample cured at 80 °C showed the same curve progress

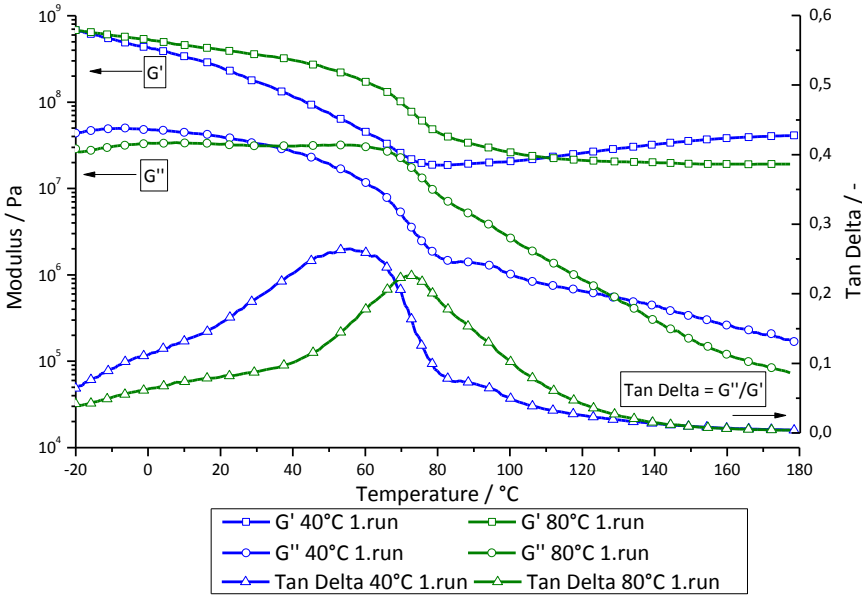

Figure 73. DMA measurement (1.run) of *Poly6* cured with 50 ppm *M20* at 40 and 80 °C.

*3.3.6.3. **Poly6** cured with 50 ppm **M20** and **M2** at 40 °C*

Curing of ***Mon6*** with ***M2*** at 40 °C led to a lower T_g (18 °C) and a different curve progress in the first run (blue line) compared with ***Mon6*** cured with ***M20*** (Figure 74). Obviously, the reactivity of the initiator has a significant effect on the properties of ***Poly6*** cured at 40 °C which is supported by the observations made in preliminary curing tests, *cf.* chapter 3.3.1.1. Increasing G' after 70 °C indicated post-curing as already discussed for ***M20***-samples. Further, this caused an increasing G'' between 100 and 150 °C. In the second run of the M2-sample, no post-curing (indicated by an increasing G' in the rubber region) occurred as the sample is fully cured. However, an increased T_g compared with the first run was detected at 92 °C, another indication of post-curing in the first run. This T_g is apparently higher than that of the ***M20***-sample. But there is actually a second though small peak in the tanδ curve of the ***M20***-samples. This is likely caused by the post-curing in the first run of this sample leading immediately to a higher T_g.

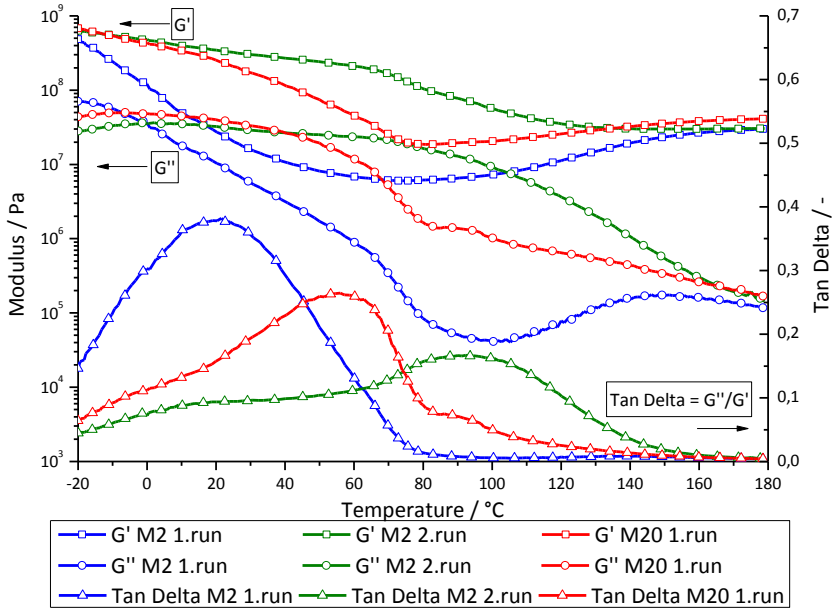

Figure 74. DMA measurement of *Poly6* cured with 50 ppm *M2* (1./2.run) and *M20* (1.run) at 40 °C.

*3.3.6.4. **Poly8-co-6** with 50 ppm **M2** cured at 40 and 80 °C*

Copolymerisation of ***Mon6*** and ***Mon8*** (1:1, w/w) aimed to increase the amount of cross-links and hence increased E-modulus and $Stress_{max}$ compared with the homopolymer ***Poly6***. Different to preparation of shoulder test bars, ***M2*** was chosen as initiator to facilitate processing. Tensile testing already showed that the theoretical higher degree of cross-links was not achievable due to the enhanced viscosity of ***Mon8***, cf. chapter 3.3.1.2 (Table 22 and Figure 60). The E-modulus of ***Poly6*** was even higher than that of ***Poly8-co-6*** (0.97 and 0.67 GPa, respectively).

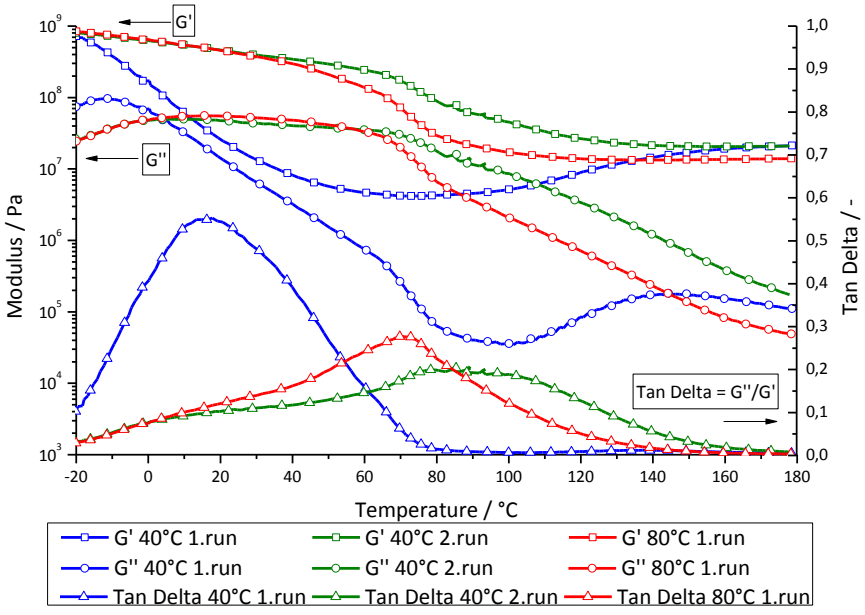

Figure 75. DMA measurement of *Poly8-co-6* cured with 50 ppm *M2* at 40 (1./2.run) and 80 °C (1.run).

However, the DMA measurements did not follow these trends (Figure 75). The T_g in the first and second run detected at 17 and 89 °C were rather similar to those of ***Poly6*** cured with ***M2*** at 40 °C. A broad maximum in tanδ was observed in the second run which made precise detection of the T_g difficult. Further, the T_g of ***Poly8-co-6*** cured at 80 °C at 72 °C was even higher than that of ***Poly6***. Similar to ***Poly6***, post-curing effects were observed in the first run of the sample cured at 40 °C (blue line) but neither in the second run (green line) nor in the first run (red line) of the sample cured at 80 °C.

*3.3.6.5. **Poly8** and **Poly9** cured with 50 ppm **M2** at 80 °C*

The samples of the ***Poly8*** and ***Poly9*** were prepared with 50 ppm ***M2*** at 80 °C. Unfortunately, both polymers were rather elastic and slightly sticky indicating a T_g below room temperature. Therefore, DMA measurements could not be performed with these samples.

*3.3.6.6. **Poly12** cured with 50 ppm **M2** at 80 °C*

The preparation of DMA samples with a loading of 50 ppm ***M2*** was achieved by using the whole amount of solvent used for the formulations (100 µL DCM) to dissolve the initiator. Three samples were cured at 80 °C which had the same G' and G'' curves in the first run (Figure 76). The T_g was detected at 70 °C. Unfortunately, each sample broke during the first run between 120 and 140 °C. Hence, no further information about post-curing and the T_g in the second run was obtained.

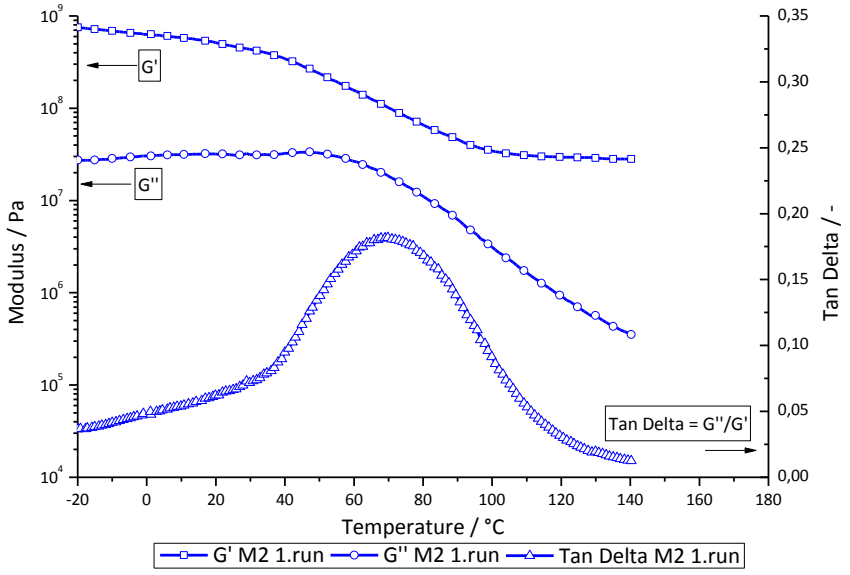

Figure 76. DMA measurement (1.run) of *Poly12* cured with 50 ppm *M2* at 80 °C.

*3.3.6.7. **pDCPD**, **Poly6**, **Poly8-co-6** and **Poly12** cured at 80 °C*

Based on the DMA results the performance of ***pDCPD*** and the ***Poly-norbornene-esters*** cured at 80 °C was discussed (Table 26 and Figure 77). As mentioned before, 80 °C was sufficient to produce fully cured materials in 24 h.

The most significant parameter in this comparative study is the T_g. ***pDCPD*** showed two distinct T_gs at 130 and 145 °C (black lines). The reason for this result is not confirmed by this method but two distinct domains within the ***pDCPD*** network were suggested. The T_gs of ***Poly6***, ***Poly8-co-6*** and ***Poly12*** were lower than those of ***pDCPD*** (blue, green and red line). This corresponds to the fact that the T_g is increased in polymers with a more rigid backbone and a higher degree of cross-links.[39] Surprisingly, each ***Poly-norbornene-ester*** reached a T_g in the same range between 70 and 75 °C. This was quite interesting because the mechanical properties of these polymers showed a different trend. It was assumed that the chemical structure and the viscosity of the monomers have a bigger influence on the mechanical properties determined by uniaxial, isothermal measurement. In dynamic tests the interaction between the polymers (e.g. between the ester-groups) might have a larger impact.

Table 26. Thermal-mechanical properties of *pDCPD*, *Poly6*, *Poly8-co-6* and *Poly12* cured at 80 °C.

Polymers	Initiator	T_g / °C	$G'_{-20\,°C}$ / Pa	$G'_{180\,°C}$ / Pa	$G'_{-20\,°C}$ / Pa	$G''_{180\,°C}$ / Pa
pDCPD	***M2***	130/145	$5.0*10^8$	$1.8*10^6$	$1.0*10^7$	$3.8*10^5$
Poly6	***M20***	75	$6.8*10^8$	$1.9*10^7$	$2.9*10^7$	$7.4*10^4$
Poly8-co-6	***M2***	72	$8.5*10^8$	$1.4*10^7$	$2.4*10^7$	$5.0*10^4$
Poly12	***M2***	70	$7.5*10^8$	$2.8*10^{7\#}$	$2.7*10^7$	$3.5*10^{5\#}$

value at 140 °C

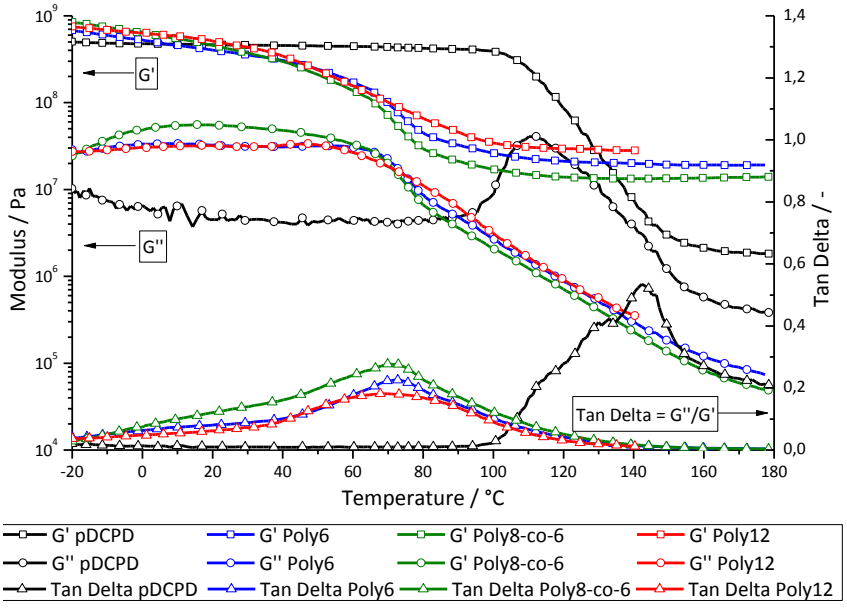

Figure 77. DMA measurement (1.run) of *pDCPD*, *Poly6*, *Poly8-co-6* and *Poly12* cured at 80 °C.

[39] H. Ren, J. Sun, B. Wu, Q. Zhou, Polymer **2006**, 47, 8309-8316.

Another interesting aspect is the development of the G' and G'' moduli throughout the measurement. The level of G' and G'' of ***pDCPD*** stayed rather constant until its T_g. At the T_g G'' passed through a maximum, while G' started to decrease directly from its constant level. Afterwards, both G' and G'' decreased to a level of $2*10^6$ and $4*10^5$ Pa, respectively. In case of the ***Poly-norbornene-esters***, the curve of G' and G'' exhibited the same shape for each polymer. Interestingly, G' decreased whereas G'' stayed constant and vice versa in the glassy and the rubber region, respectively. Further, the G' of the ***Poly-norbornene-esters*** and ***pDCPD*** was at the same level between -20 °C and room temperature. However, the ***Poly-norbornene-***esters exhibited a G' higher by a factor of 10 at 180 °C. In contrast to this, the viscous component (G'') was higher for the ***Poly-norbornene-esters*** than ***pDCPD*** in the glassy region but the situation reversed in the rubber region of the polymers.

3.4. Synthesis

In the following chapter the synthetic routes to the monomer mentioned in the chapters 3.2 and 3.3 are described.

3.4.1. Cyclic hydrocarbon-based monomers Mon1, Mon2, Mon3

Mon1, ***Mon2*** and ***Mon3*** are di-, tri- and tetracyclic Diels – Alder adducts based on cyclopentadiene (Cp) and the according dienophile, respectively (Scheme 5).

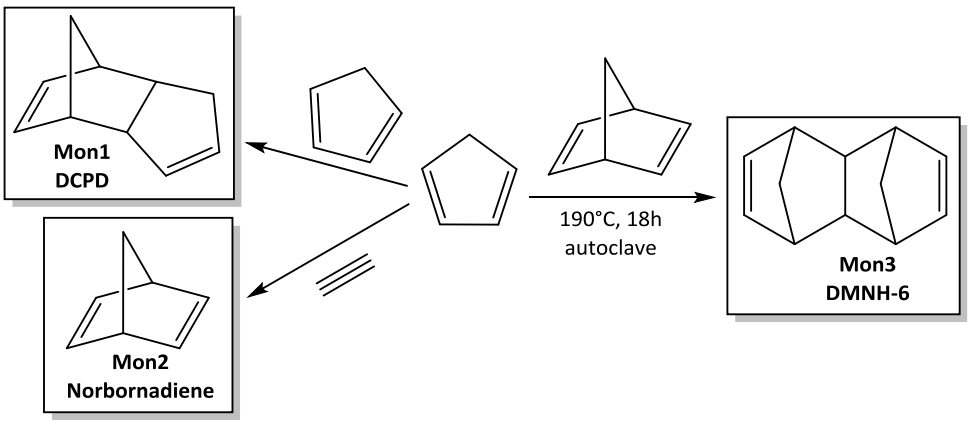

Scheme 5. Diels – Alder adducts *Mon1*, *Mon2*, *Mon3* based on Cp and according dienophile.

The tricyclic dicyclopentadiene (***DCPD***) is the stable dimer of Cp and a cheap by-product from the C5 stream of naphtha crackers.[25] ***Norbornadiene*** is a dicyclic adduct of Cp and acetylene. Both monomers were purchased (ABCR and Aldrich, respectively) and used without further purification unless specified otherwise.

The preparation of the naphthalene – derivative ***Mon3***, 1,4,4a,5,8,8a-Hexahydro- 1,4,5,8-*endo*-*exo*- dimethano- naphthalene (***DMNH-6***), also referred to as tetracyclo[6,2,$1^{3,6}$,$0^{2,7}$]-dodeca-4,9-diene (BVD)[38], was carried out according to the procedure established by Stille *et. al*.[36] ***Norbornadiene*** and Cp, both freshly distilled, were mixed with hydroquinone as catalyst in an autoclave and stirred at 190 °C for 18 h. The crude product was purified by vacuum distillation (107-111 °C at 40 mbar) yielding 91%. The isomeric mixture of *endo*-*endo*, *exo*-*exo* and *exo*-*endo* (Figure 78 a-c) and impurities (3-10%). from residual ***norbornadiene*** were identified in ^{1}H-NMR spectroscopic analysis.

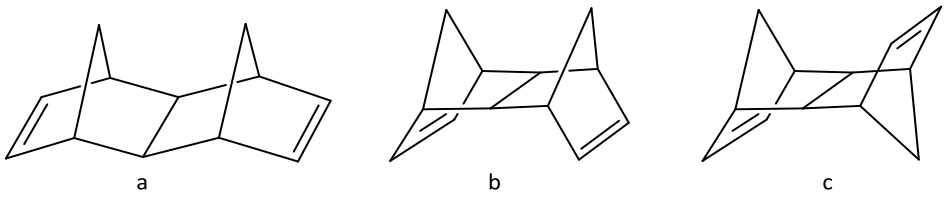

Figure 78. Isomers of *Mon3*, *endo-endo* (a), *exo-exo* (b), *exo-endo* (c).

The isomeric ratio of 83:17 in terms of *exo-endo* to *endo-endo* or *exo-exo* was determined by relating the integral of signal at 6.21 ppm (corresponding to 2H) with that of the signal at 5.31 ppm (corresponding to 4H) as shown in Figure 79.

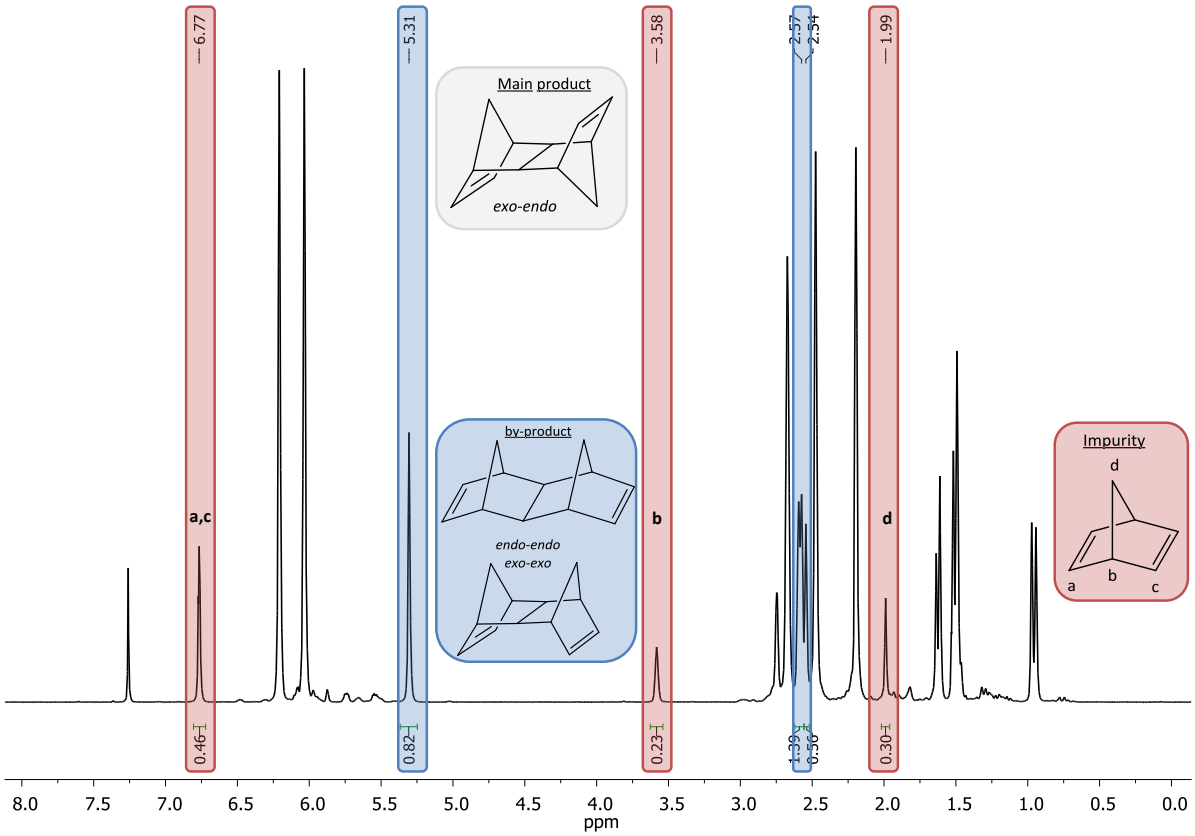

Figure 79. ^{1}H-NMR spectrum (300 Hz, $CDCl_3$) of *Mon3*.

3.4.2. Alkyl-linked bi- and tri-norbornene-esters Mon4, Mon6, Mon8

The preparation of ***Mon4***, ***Mon6*** and ***Mon8*** is based on a Diels – Alder reaction of Cp with the corresponding alkyl mono-, di- and tri-acrylate (Scheme 6).

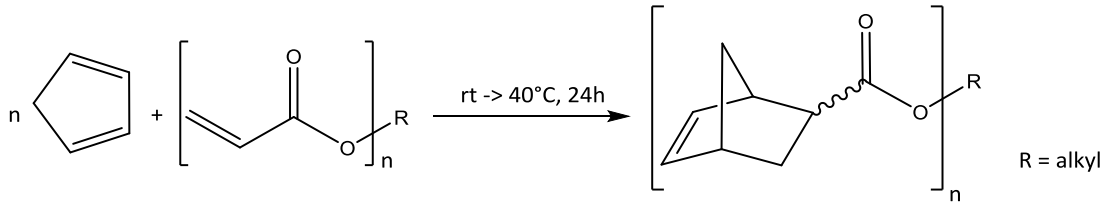

Scheme 6. Diels – Alder reaction to *Mon4*, *Mon6*, *Mon8*, *Mon9*.

Mon4 and ***Mon6*** are symmetric bis-norbornene esters linked by ethane- and butane-moieties, respectively (Scheme 7).

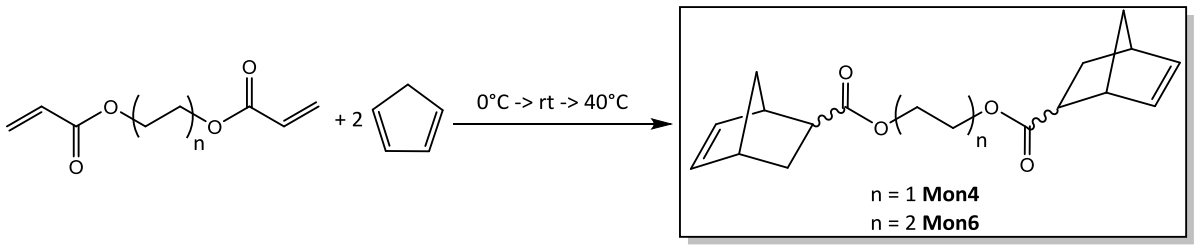

Scheme 7. Synthesis of *Mon4* and *Mon6*.

Mon4 was synthesized from an excess of freshly distilled Cp and ethylene diacrylate via a solvent-free Diels-Alder reaction in 24 h. Mixing of the components required ice cooling, while the reaction was first stirred at rt for 7 h and further at 40 °C. Purification by column chromatography was required in order to remove residual Cp. This procedure yielded a colourless, low viscous liquid (91%). The *endo-endo* isomer was identified as main product analysed via ^{1}H-NMR spectroscopy (Figure 80). The *endo*/*exo* - ratio was determined as 8:2 by comparing the integrals of the signals at 5.94 ppm (corresponding 2H, *endo*) and 6.14 ppm (corresponding 4H, *exo*) as shown in Figure 80.

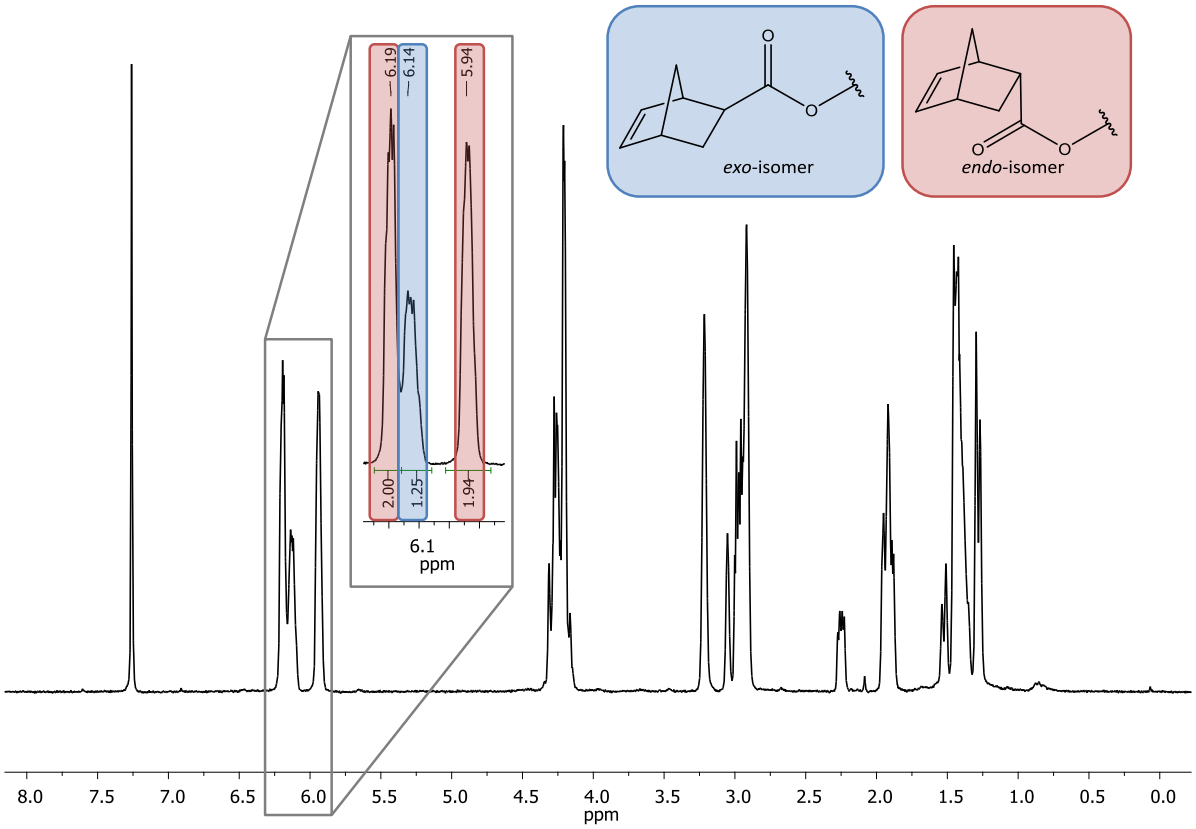

Figure 80. ^{1}H-NMR spectrum (300 Hz, $CDCl_3$) of *Mon4*.

Mon6 was purchased from Orgentis Chemicals though additional purification was required because impurities were detected and identified as unconverted acrylate by ^{1}H-NMR spectroscopy. The amount of impurity (approximately 10%) was determined by comparing the integrals of the acrylate at 6.37 and 5.84 ppm (corresponding acrylate double bond H_{cis} and H_{trans}) with those of the *endo*-norbornene double bond at 6.18 and 5.92 ppm (Figure 81).

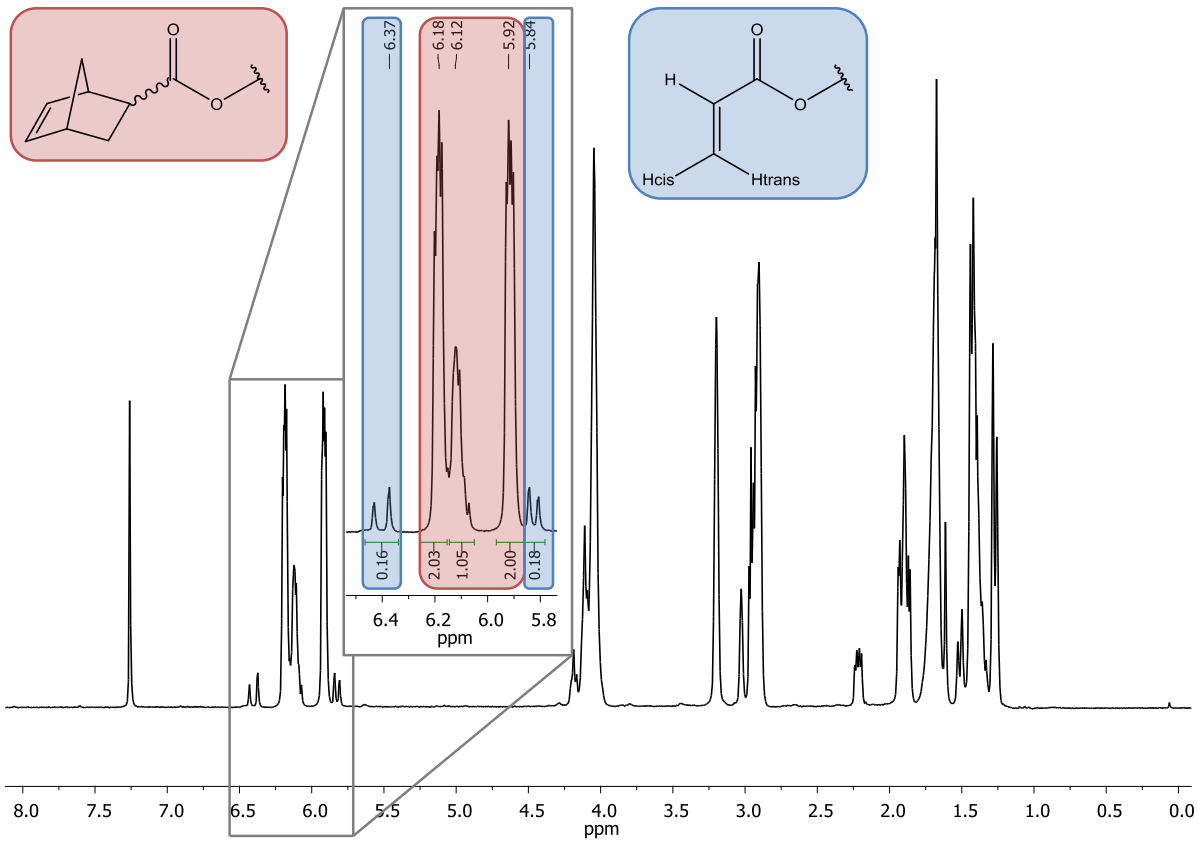

Figure 81. ^{1}H-NMR-spectrum (300 Hz, $CDCl_3$) of *Mon6* purchased from Orgentis with unconverted acrylate.

The residual acrylate double bond was converted according to the synthesis of ***Mon4*** yielding full conversion to the norbornene-derivative after 18 h. Residual Cp was again removed by column chromatography. The main product was the *endo*-*endo*-derivative and an *endo*/*exo* – ratio of 8:2 was determined by ^{1}H-NMR spectroscopy (*cf.* Figure 80).

Mon8 is a tri-norbornene ester analogue to ***Mon4*** and ***Mon6*** but linked by a trimethylolpropane moiety (Scheme 8).

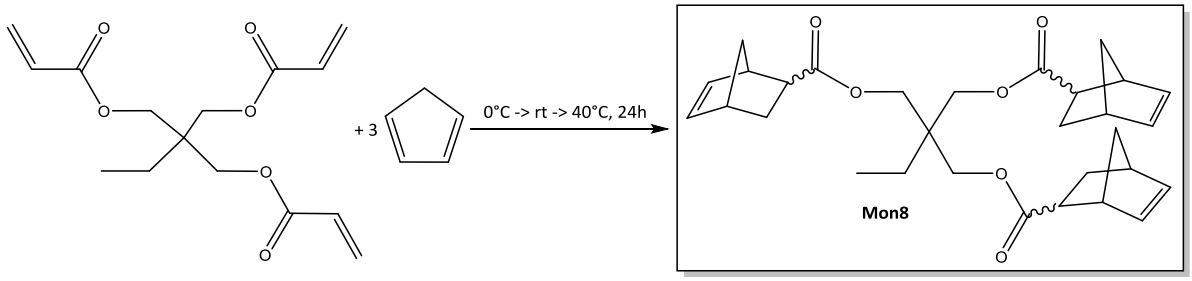

Scheme 8. Synthesis of Mon8.

The synthesis followed the protocol of the ***Mon4*** - preparation. Due to increased viscosity of the reaction mixture DCM was added to ensure stirring. Pure product (Yield = 81%) was achieved after 23 h at 40 °C and purification via column chromatography as described for ***Mon4***. The *endo*/*exo* – ratio of 82:18 was determined by ^{1}H-NMR spectroscopy (cf. Figure 80).

3.4.3. Hydroxy-functionalised norbornene-ester Mon9

Mon9 is a mono-norbornene ester functionalized with a terminal hydroxyl – group (Scheme 9). The synthesis followed the protocol of the ***Mon4*** – preparation yielding 96% after 21.5 h and purification by column chromatography. The *endo*/*exo* – ratio of 8:2 was determined by ^{1}H-NMR spectroscopy as described in Figure 80.

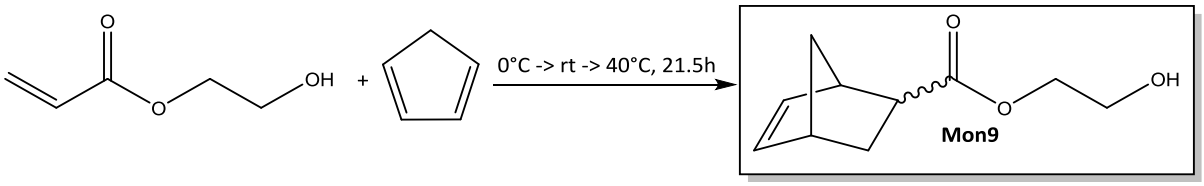

Scheme 9. Synthesis of Mon9.

3.4.4. Carbamate-linked norbornene ester Mon10

Mon10 is a bis-norbornene ester derivative based on two molecules of ***Mon9*** but with a methylene diphenyl dicarbamate – linker (Scheme 10).

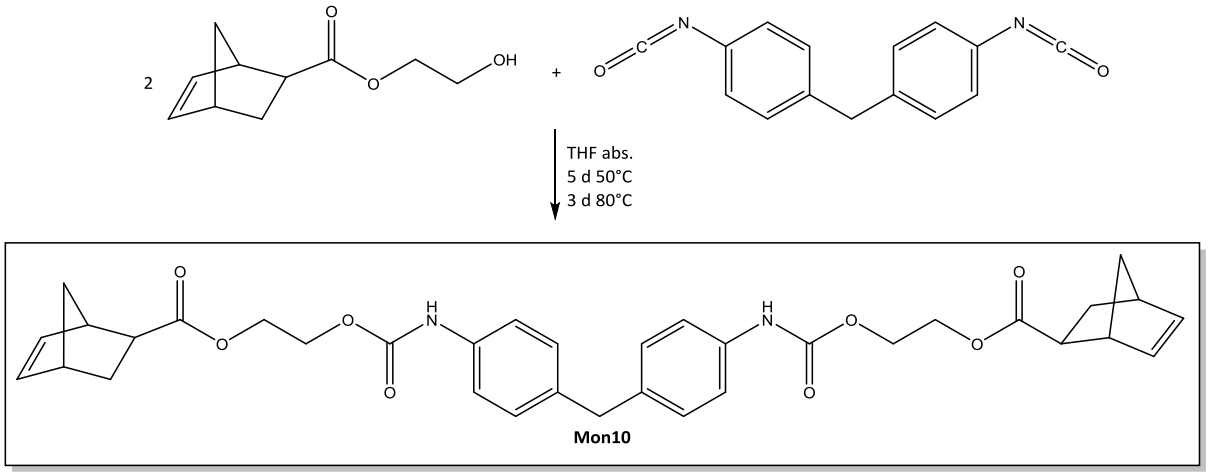

Scheme 10. Synthesis of *Mon10*.

Mon10 was synthesized according to the procedure published by Sui *et. al*.[40] Methylene diphenyl diisocyanate (MDI, 1.0 eq) was mixed with a slightly deficient amount of ***Mon9*** (1.95 eq) in order to avoid separation from excess of ***Mon9*** in the purification step. The reaction was performed under inert conditions with THF *abs.* as solvent. The reaction mixture was first stirred at 50 °C for 5 days and further at 80 °C for 3 days to yield full conversion of ***Mon9***. The reaction mixture was subsequently quenched with ethanol in order to convert the unreacted isocyanate into a carbamate moiety. This side product was not separated from the crude product yielding a colourless solid (94%) with 90% of the desired product and 10% mono-norbornene ester ethyl-carbamate. The melting point of the solid

[40] X.C. Sui, *Chinese Chem. Lett.* **2011**, *22*, 374 - 377.

product was not determinable due to its hygroscopic nature. The product was stored under N_2 atmosphere to maintain its pulverulent appearance.

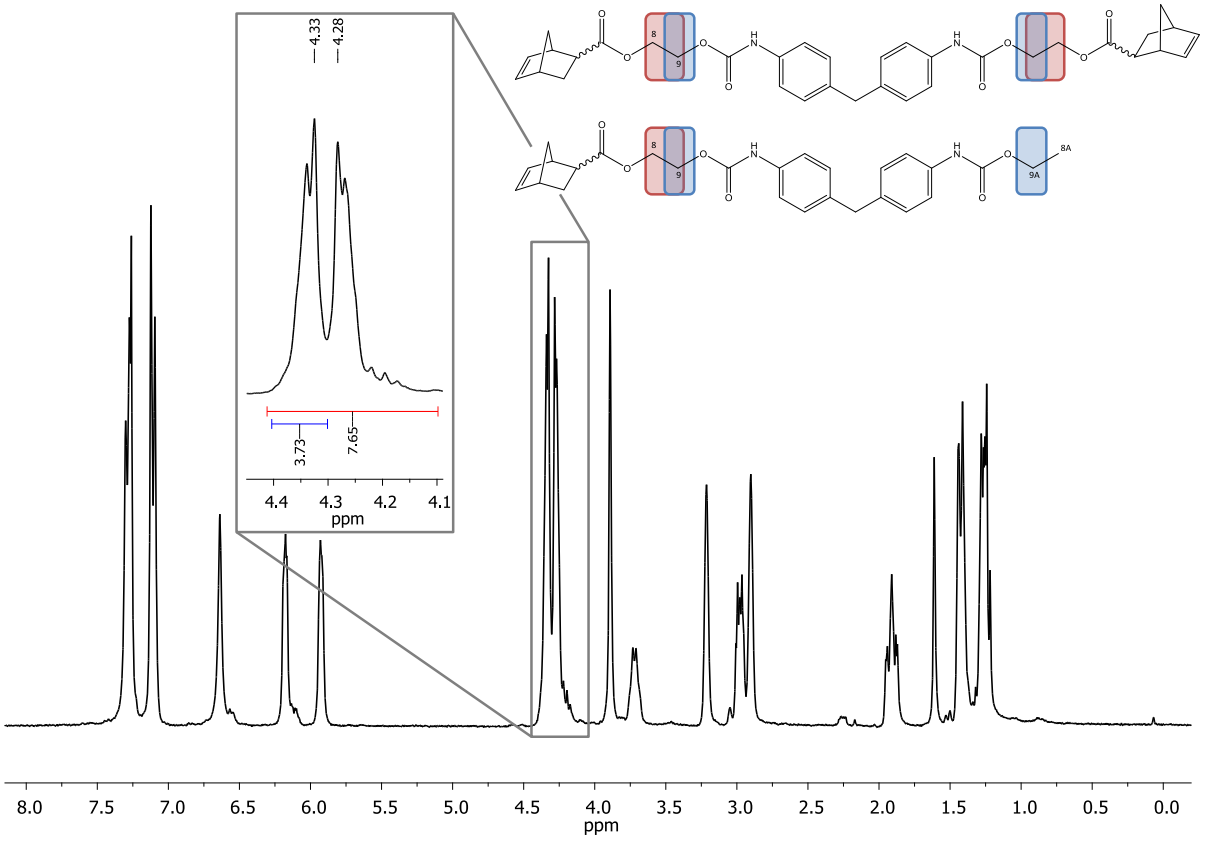

Figure 82. ^{1}H-NMR spectrum (300 Hz, $CDCl_3$) of *Mon10*.

The product ratio was determined by analysing the contribution signal 9 of the main product and signal 9A of the side product to the integrals at 4.33 ppm and comparing it with the integral of signal 8 of the main product at 4.28 ppm in the ^{1}H-NMR spectrum (Figure 82). Additionally, the *endo*/*exo* – ratio of 86:16 was determined by ^{1}H-NMR spectroscopy according to Figure 80.

3.4.5. Bis-(methyl-norbornene) ether Mon11

Mon11 is a symmetric bis-(methyl-norbornene) ether linked by a biphenyl-group (Scheme 11). The preparation includes basically two steps: Diels-Alder reaction (A) and ether synthesis (*O*-allylation, (B)).

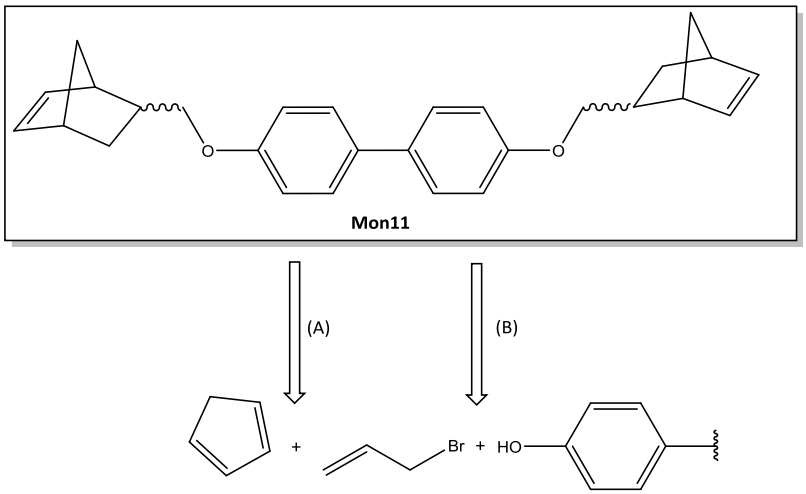

Scheme 11. Retro-synthesis of *Mon11*, (A) Diels-Alder reaction, (B) *O*-allylation.

Two pathways were investigated using either 2-(bromomethyl)-5-norbornene (a) or allyl bromide (b) as bromide species in the *O*-allylation step (Scheme 12). This synthesis step followed the protocol published by Chang *et. al*.[41]

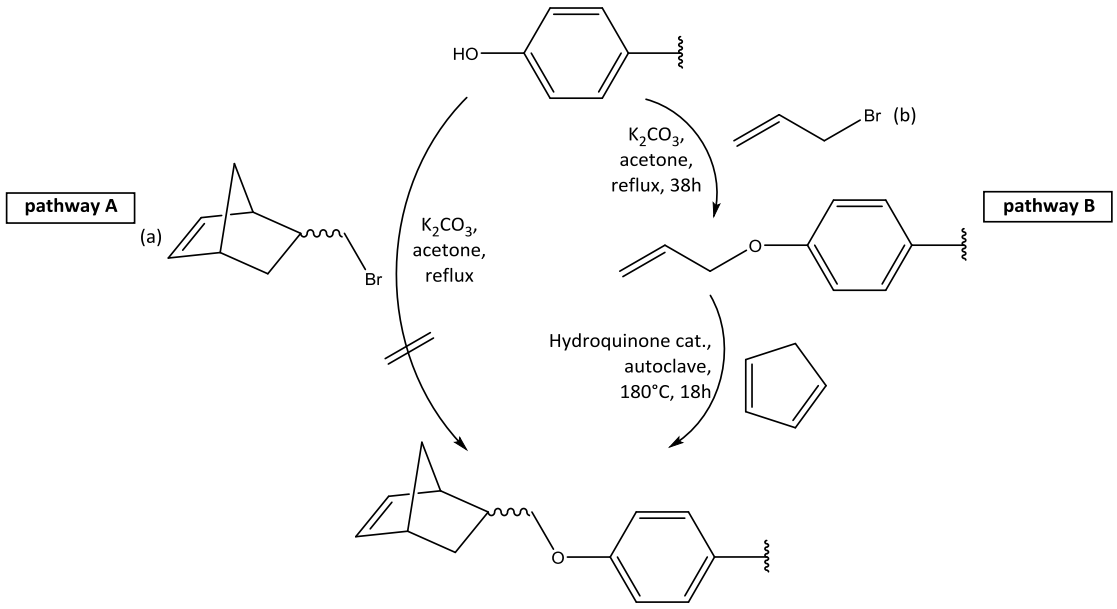

Scheme 12. Pathways A and B for the synthesis of *Mon11*.

2-(Bromomethyl)-5-norbornene was added to a solution of dihydroxybiphenyl in acetone with dispersed K_2CO_3 and stirred at 50 °C for 19 h (pathway A). Conversion was detected by TLC analysis. However, the yellow solid could not be identified as desired product by ^{1}H-NMR

[41] M.-Y. Chang, T.-W. Lee, M.-H. Wu, *Org. Lett* **2012**, *14* (9), 2198 – 2201.

spectroscopy. In particular, no characteristic norbornene signals were observed in the spectrum.

Allyl bromide as starting material led under the same reaction conditions to a pure, cream-coloured, solid product with a yield of 91% after 18 h (pathway B). In the second step, the norbornene moiety was introduced in a Diels-Alder reaction. Due to the +M effect of the ether group in the dienophile species which is unfavourable for Diels-Alder reactions, elevated temperatures were required. Cp was formed *in-situ* by cracking of ***DCPD*** in the autoclave. The reaction was stirred at 180 °C for 19 h. Analysis with ^{1}H-NMR spectroscopy and TLC indicated full conversion of the allyl species to a number of different products. After separation by column chromatography with Cy/EtOAc 3:1 (v:v) as eluent several product were identified including the desired and mono-substituted product (Figure 83, (a) and (b)). Moreover, by-products were formed by Claisen rearrangement of the *O*-allylated product to a phenol – derivative substituted with a propenyl – group at one of the aromatic carbon atoms (Figure 83, products (c) and (d)). Additional column chromatography of the fractions containing product (a) and (b) with Cy/EtOAc 500:1 (v:v) as eluent yielded in no further purification. Therefore, yield could not be quantified.

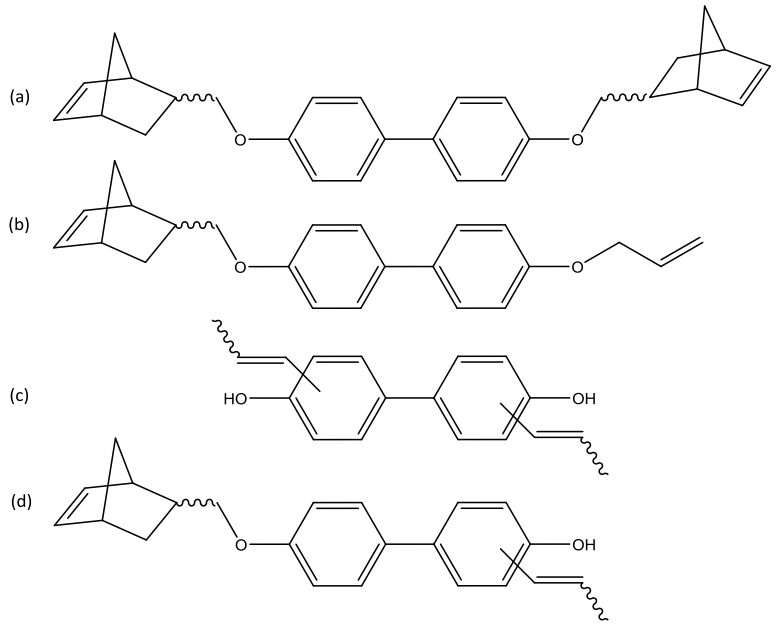

Figure 83. (a), (b) Mono- and di-norbornene ether by Diels-Alder reaction; (c) product by Claisen rearrangement; (d) mixed product.

Generally, both pathways lacked of the possibility to yield the desired product with both high purity and yield. Although the first step in pathway B is a satisfying method to generate the allyl species, the required elevated temperatures caused Claisen rearrangement leading to the discussed by-products in the second step. Pathway A might require better reaction progress monitoring and evaluation of the reaction conditions.

3.4.6. *Ester-linked bis-methylnorbornene Mon12*

Mon12 is a symmetric bis(2-methyl-5-norbornene)- derivative linked by a succinyl group and a constitutional isomer to ***Mon6*** differing in the position of the carbonyl group (Scheme 13).

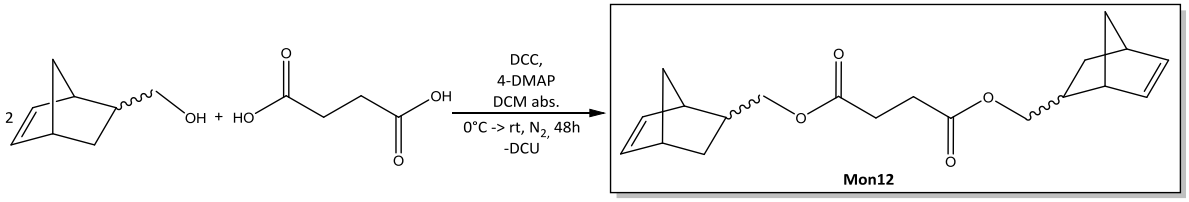

Scheme 13. Synthesis of Mon12.

Following the protocol published by Crivello *et. al.*[42], the monomer was derived in a Steglich esterification reaction under inert conditions in presence of dicyclohexylcarbodiimide (DCC) and 4-(dimethyl amino)-pyridine (4-DMAP) as coupling reagent and catalyst, respectively. Full conversion was yield by stirring at room temperature for 48 h. Dicyclohexylurea (DCU), a side-product which was partially soluble in the monomer, was removed by precipitation with pentane. Further purification by column chromatography with Cy/EtOAc 500:1 (v:v) as eluent was required to remove mono-substituted by-product and excess of norbornene-methanol resulting in a yellowish liquid. The *endo*/*exo* - ratio was determined as 3:1 by comparing the integrals of the CH_2-group next to the carbonyl group at 3.87 – 3.67 ppm (*endo*) and 4.16 - 3-99 ppm (*exo*) (Figure 84).

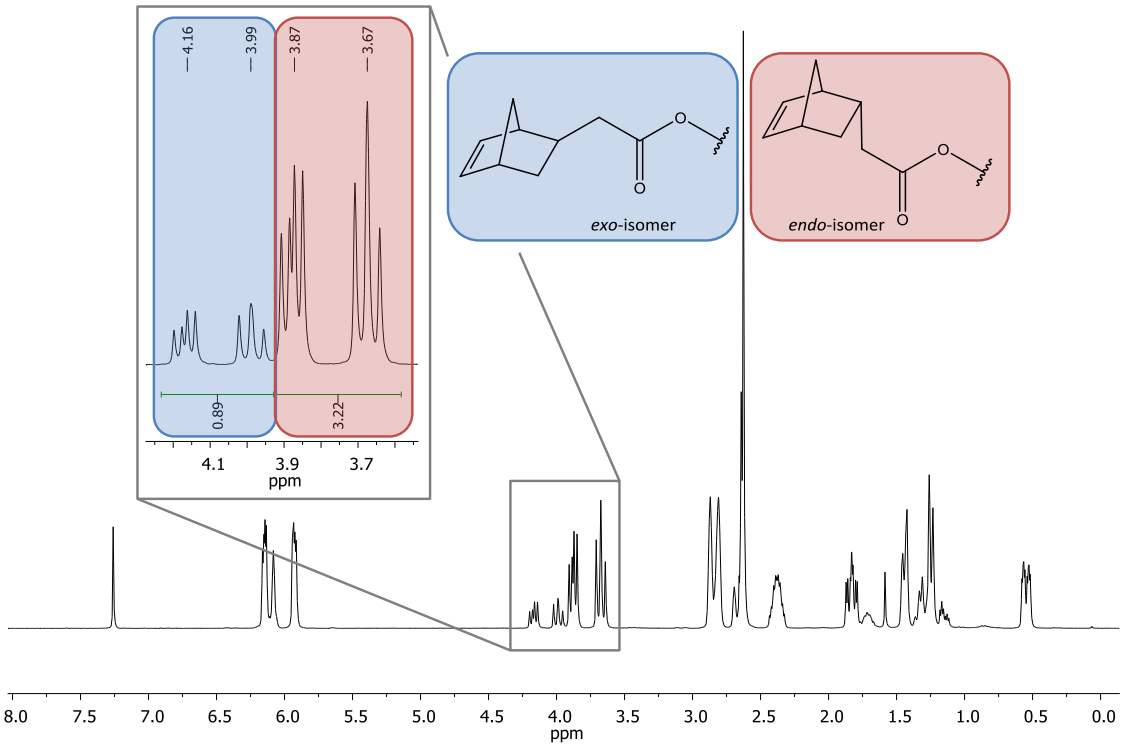

Figure 84. ^{1}H-NMR spectrum (300 Hz, $CDCl_3$) of *Mon12*.

[42] J.V. Crivello, R. Narayan, *Macromolecules* **1996**, *26*, 433 – 438.

4. Conclusion and Outlook

The current work discloses the investigations on Ring Opening Metathesis Polymerisation-based thermosets for the purpose of introducing this polymerisation in chemical anchor systems at lower and moderate curing temperatures (4-40 °C). The ROMP-based formulations were designed in a manner to fulfil the respective performance specifications, namely appealing working window and processing duration (15 min and 24h, respectively), outstanding mechanical and thermal properties (E-modulus > 1.8 GPa, $Stress_{max}$ > 20 MPa, T_g > 70 °C) and chemical resistance.

In a first comparative study of ROMP with a number of indenylidene bearing Grubbs-type 1st and 2nd generation initiators and the commercially available dicyclopentadiene revealed the possibility of adjusting the reactivity of the system and hence, working window and processing duration by varying the type and loading of the initiator and the curing temperature. In this study, ***pDCPD*** cured at 80 °C protruded with 20 ppm ***M2*** as its mechanical properties which were equal or even higher compared to the required. However, curing at lower temperatures led to rather elastic materials. To obtain better results, the more reactive hydrocarbon monomers, norbornadiene and 1,4,4a,5,8,8a-hexahydro-1,4,5,8-*endo*-*exo*-dimethanonaphtalene were employed. Unfortunately, foaming of these samples occurred during polymerisation as the exothermic process initiates *retro*-Diels-Alder reaction to a great extent.

Novel multifunctional norbornene monomers with various architectures were successfully synthesised as alternative to the hydrocarbon monomers. Multiple polymerisation sites and linkers based on different functional groups and rigidity should result in cross-linked networks with the hoped-for properties even at low curing temperatures. The opposite was the case due to two distinct inherent effects. On the one hand, carbonyl groups in the linker moiety coordinate competitively to the vacant site and thus, decelerate the polymerisation speed. On the other hand, increasing viscosity of the monomers led to decreasing mechanical properties of the respective. This outcome was reflected in partially poor mechanical properties of these poly-norbornenes cured at 80 °C.

Summarizing, thermosetting materials based on Ring Opening Metathesis Polymerisation fulfilling the requirements for processing and the materials properties have been gained albeit only at high curing temperatures around 80 °C. Even so, the systems investigated in this work are far from applicable as chemical anchors. However, both potential and drawbacks of the hydrocarbon and norbornene-systems have been pointed out in various experiments. Further work on this topic will includes the improvement of the performance by combining highly reactive monomers with low viscosity with more active initiators. This promising approach suggests further ambition towards ROMP-based chemical anchors.

5. Experimental

5.1. Instruments and Materials

All chemicals for the synthesis of monomers were purchased from commercial sources (Sigma Aldrich, Fluka, ABCR, Orgentis Chemicals, Alfa Aesar or Sohena) and used without further purification unless specified otherwise. Complexes ***M1*** [dichloro (3-phenyl-1H-inden-1-ylidene) bis (tricyclohexylphosphine) ruthenium(II)], ***M10*** [dichloro (3-phenyl-1H-inden-1-ylidene) bis (tricyclohexylphosphine) ruthenium(II)] ***M11*** [dichloro- bis(isobutylphobane) (3-phenyl-1H-inden-1-ylidene) ruthenium(II), ***M2*** [1,3-bis (2,4,6-trimethylphenyl)- 2-imidazolidinylidene] dichloro (3-phenyl-1H-inden-1-ylidene) (tricyclohexylphosphine) ruthenium(II) and ***M20*** [1,3-bis(2,4,6-trimethylphenyl)- 2-imidazolidinylidene] dichloro (3-phenyl-1H-inden-1-ylidene) (triphenylphosphine) ruthenium(II) for ring opening metathesis polymerisation (ROMP) was obtained from UMICORE AG & Co. KG. Complex ***EP06.3*** was prepared by Eva Pump and used as received. Unless specified otherwise, solvents and auxiliary materials were used as purchased.

For TLC silica gel 60 F254 on aluminium sheets (Merck) was used. Visualization was done by exposure with UV light and / or dipping into an aqueous solution of $KMnO_4$ (0.1 %) or sulphuric solution of cerium sulphate /ammonium molybdate.

Silica gel 60 (220-440 mesh ASTM) was used for column chromatography.

NMR spectroscopy (^{1}H, ^{13}C) was done on a Bruker Avanze 300 MHz spectrometer. Deuterated solvents were obtained from Cambridge Isotope Laboratories Inc. and remaining peaks were referenced according to literature.[43] Peak shapes are specified as follows: s (singlet), bs (broad singlet), d (doublet), dd (doublet of doublets), t (triplet), q (quadruplet), m (multiplet).

FT-IR spectra were recorded on a Bruker Alpha-P infrared spectrometer, equipped with an attenuated total reflection (ATR) accessory using a diamond crystal.

Determination of viscosity was performed on a Paar-Physica UDS 200 Universal Dynamic Spectrometer by Helga Reischl, Institute of Chemistry, University of Graz and on a Malvern "Kinexus Ultra" rheometer by Klaus Gebauer at Hilti Entwicklungsgesellschaft mbH, Kaufering. The latter was also used for rheokinetic measurements with disposable plates. DMA measurements were done on a Malvern "Bohlin C-VOR 120"

[43] H.E. Gottlieb, A. Kotlyar, A. Nudelman, *J. Org. Chem.* **1997**, *62*, 7512.

5.2. Syntheses

5.2.1. Naphthalene – derivative via Diels-Alder reaction

Naphthalene-derivatives can be synthesized via Diels-Alder reaction according to Scheme 14. The synthesis-procedure was published in: J.K. Stille, D.A. Frey, *J. Am. Chem. Soc.* **1959**, *81*, 4273-4275.

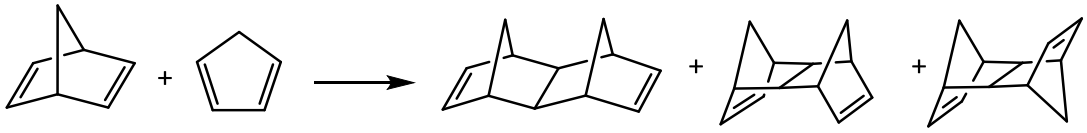

Scheme 14. Reaction scheme for the Diels-Alder reaction of norbornadiene and cyclopentadiene.

*5.2.1.1. 1,4,4a,5,8,8a-Hexahydro-1,4,5,8-*endo-exo-*dimethanonaphtalene (*Mon3*)*

Freshly distilled norbornadiene (27.6 g, 300 mmol, 1.0 eq) was added to freshly distilled cyclopentadiene (19.8 g, 300 mmol, 1 eq, Cp) and hydroquinone (0.04 g, 0.36 mmol, 0.0012 eq) in an autoclave under nitrogen atmosphere. The reaction mixture was stirred at 190 °C for 8 hours. The crude product was purified via distillation under reduced pressure. Yield: 10.43 g (22 %, impurity: norbornadiene 3%), colourless liquid

Analytical data in accordance with published values[36]

bp: 107 - 111 °C (at 40 mbar)

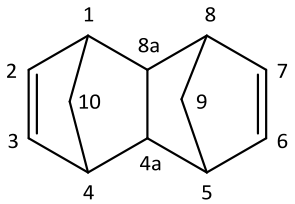

*..*exo-endo,* '..*exo-exo* or *endo-endo*

^{1}H-NMR (300 Hz, $CDCl_3$): δ = 6.20 (s, 2H, 2*, 3*), 6.03 (s, 2H, 6*, 7*), 5.30 (s, 4H, 1', 2', 6', 7'), 2.75 (s, 2H, 4a', 8a'), 2.67 (s, 2H, 5*, 8*), 2.59 (s, 4H, 1', 4', 5', 8'), 2.56 (d, 1H, , $^3J_{H,H}$ = 8.8 Hz, 10*), 2.49 (s, 2H, 1*, 4*), 2.19 (s, 2H, 4a*, 8a*), 1.62 (d, 1H, $^3J_{H,H}$ = 7.8 Hz, 9*), 1.54 (d, 1H, $^3J_{H,H}$ = 7.8 Hz, 9*),1.49 (t, 4H, 9', 10'), 0.96 (d, 1H, $^3J_{H,H}$ = 8.8 Hz, 10*)

exo-endo/*endo-endo* or *exo-exo* - ratio: 84/16

^{13}C-NMR (75 Hz, $CDCl_3$): δ = 141.2 (2C, 2*, 3*); 136.1 (2C, 6*, 7*), 131.5 (4C, 2', 3', 6', 7'), 55.5 (2C, 9', 10'), 55.7 (1C, 9*), 48.07 (2C, C_q, 4a*, 8a*), 44.5 (4C, C_q, 1', 4', 5', 8'), 44.4 (2C, C_q, 5*, 8*), 43.0 (2C, C_q, 4a', 8a'), 42.6 (1C, C_q, 1*, 4*), 40.4 (1C, 10*)

ATR-IR: $\tilde{\nu}$ = 3057 cm-1 (=C-H str.), 2958 cm-1 (-C-H str.), 1572 cm-1 (C=C), 711 cm-1 (cis-CH=CH)

5.2.2. Norbornene esters via Diels-Alder reaction

Norbornene esters ***Mon4***, ***Mon6***, ***Mon*** and ***Mon9*** and norbornene ether ***Mon11*** were synthesized via a solvent-free Diels-Alder reaction with Cp and the according alkyl acrylate and vinyl ether as starting materials, respectively (Scheme 15).

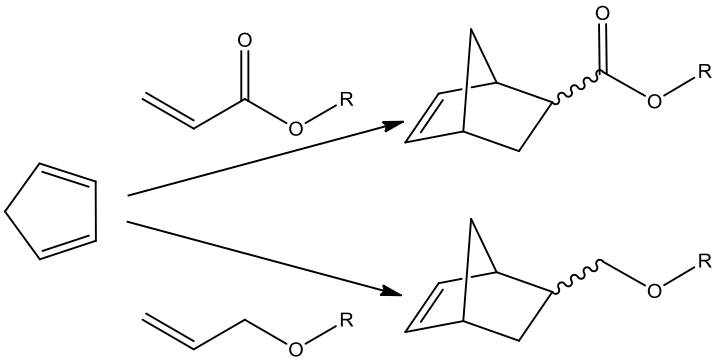

Scheme 15. Diels-Alder reaction of Cp with alkyl acrylate and vinyl ether.

*5.2.2.1. endo-endo-Ethane-1,4-diyl-bis-(norbornene-carboxylate) (**Mon4**)*

Freshly distilled Cp (8.06 g, 0.122 mol, 2.2 eq) was added dropwise under ice cooling to ethylene diacrylate (9.43 g, 0.055 mol, 1.0 eq). After 30 min the ice cooling was removed and the mixture was stirred at room temperature. As the reaction exhibited exothermic behaviour, ice cooling was applied for 5 min. Afterwards no further exothermic behaviour was observed. The progressing reaction was monitored via TLC (R_f (product) = 0.62, Cy/EtOAc, 3:1 (v:v), detection: $KMnO_4$,) and ^{1}H-NMR spectroscopy (disappearing signal of acrylate-double bond). Due to incomplete conversion, 2 mL (1.6 g) CP were slowly added to the mixture. After 6 h another 0.5 mL (0.4 g) Cp were added and the mixture stirred over night at 40 °C. Full conversion was monitored via ^{1}H-NMR. Excessive Cp was removed via flash column chromatography using cyclohexane as eluent. The pure product was eluted with Cy/EtOAc (3:1 (v:v)) as eluent and dried under reduced pressure. Yield: 15.06 g (91 %), colourless liquid.

TLC: R_f = 0.62 (Cy/EtOAc, 3:1 (v:v), detection: $KMnO_4$)

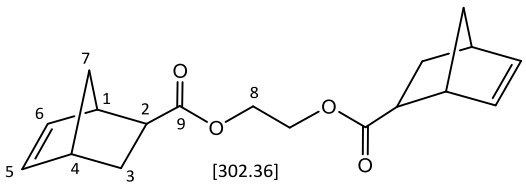

^{1}H-NMR (300 Hz, CDCl3): δ = 6.19 (m, 2H, $5a_{endo}$, $6a_{endo}$), 6.14 (m, 4H, 5_{exo}, 6_{exo}) 5.94 (m, 2H, $5b_{endo}$, $6b_{endo}$), 4.21 (s, 4H, 8_{endo}), 3.21 (s, 2H, 1_{endo}), 2.96 (m, 2H, 2_{endo}), 2.92 (m, 2H, 4_{endo}), 1.92(m, 2H, $3a_{endo}$), 1.42 (m, 4H, $3b_{endo}$, 7_{endo}),1.28 (d, 2H, $^{3}J_{H,H}$ = 8.0 Hz, 7_{endo})

endo/*exo*-ratio: 8/2

^{13}C-NMR (75 Hz, $CDCl_3$): δ = 176.3 (2C, C_q, 9); 138.2 (2C, 5a, 6a), 132.7 (2C, 5b, 6b), 62.4 (2C, 8) 49.9 (2C, 7), 46.9 (2C, 1), 43.6 (2C, 2), 42.9 (2C, 4), 30.7 (2C, 3)

*5.2.2.2. endo-endo-Butane-1,4-diyl-bis-(norbornene-carboxylate) (**Mon6**)*

endo-endo-Butane-1,4-diyl-bis-(norbornene-carboxylate) was purchased from Orgentis Chemicals containing impurities identified as unconverted acrylate. Hence, the product was purified by converting acrylate with Cp analogously to the procedure in 3.3.1.1 to the desired product.

Freshly distilled Cp (4.0 g, 0.06 mol, 2.9 eq) was added dropwise under ice cooling to *endo-endo*-butane-1,4-diyl-bis-(norbornene-carboxylate) (70 g, 0.21 mol) with 10 % unconverted butane diacrylate (0,021 mol, 1.0 eq). After 30 min ice cooling was removed and the reaction stirred at room temperature over night. Analysis via ^{1}H-NMR spectroscopy revealed incomplete conversion. Full conversion was obtained after adding 6.4 g CP and heating at 40 °C over night. Excessive Cp was removed via flash column chromatography using cyclohexane as eluent. The pure product was eluted with Cy/EtOAc (3:1 (v:v)) as eluent and dried under reduced pressure. Yield: 15.06 g (91 %), colourless liquid.

TLC: R_f = 0.64 (Cy/EtOAc, 3:1 (v:v), detection: $KMnO_4$)

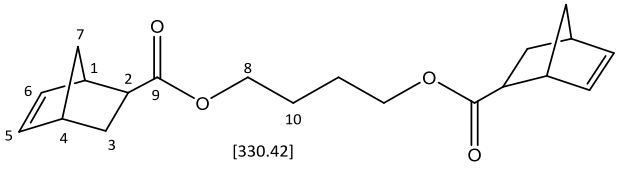

^{1}H-NMR (300 Hz, $CDCl_3$): δ = 6.19 (m, 2H, $5a_{endo}$, $6a_{endo}$), 6,12 (m, 2H, 5_{exo}, 6_{exo}), 5.92 (m, 2H, $5b_{endo}$, $6b_{endo}$), 4.11 (m, 2H, 8_{exo}), 4.05 (s, 4H, 8_{endo}), 3.20 (s, 2H, 1_{endo}), 2.96 (m, 2H, 2_{endo}), 2,91 (m, 2H, 4_{endo}), 1.90 (m, 2H, $3a_{endo}$), 1.68 (m, 4H, 9_{endo}), 1.42 (m, 4H, $3b_{endo}$, $7a_{endo}$),1.28 (d, 2H, $^{3}J_{H,H}$ = 8.13 Hz, $7b_{endo}$)

endo/*exo*-ratio: 8/2

^{13}C-NMR (75 Hz, $CDCl_3$): δ = 174.9 (2C, C_q 10); 137.9 (2C, 5a, 6a), 132.4 (2C, 5b, 6b), 63.8 (2C, 8) 49.8 (2C, 7), 45.9 (2C, 1), 43.5 (2C, 2), 42.7 (2C, 4), 29.3 (2C, 3), 25.6 (2C, 9)

*5.2.2.3. Trimethylolpropane-tri-(norbornene-carboxylate) (**Mon8**)*

Freshly distilled Cp (44.1 g, 0.67 mol, 3.3 eq) was added dropwise to ice cooled trimethylolpropane triacrylate (60 g, 0.20 mol, 1.0 eq). The colourless mixture was stirred for 1.5 h before the ice cooling was removed. After another 30 min exothermic behaviour was observed, hence ice cooling was applied again for 10 min. The colour of the mixture had changed to light yellow and the viscosity was increased causing hindered stirring. Due to incomplete conversion monitored via ^{1}H-NMR spectroscopy 5 mL (4 g) Cp was added. Additionally, 20 mL DCM was added as solvent in order to decrease the viscosity ensuring stirring. After 8 h in total, the reaction was still incomplete. Therefore 2 mL (1.6 g) Cp was added and the mixture was stirred at 40 °C over night. Full conversion was monitored via ^{1}H-NMR after 24h in total. The solvent was removed under reduced pressure. Excessive Cp was removed via flash column chromatography using cyclohexane as eluent. The pure product was eluted with Cy/EtOAc (3:1 (v:v)) as eluent and dried under reduced pressure. Yield: 80.2412 g (81 %), colourless, highly viscous liquid with residual traces of solvent

TLC: R_f = 0.69 (Cy/EtOAc, 3:1, (v:v), detection: $KMnO_4$)

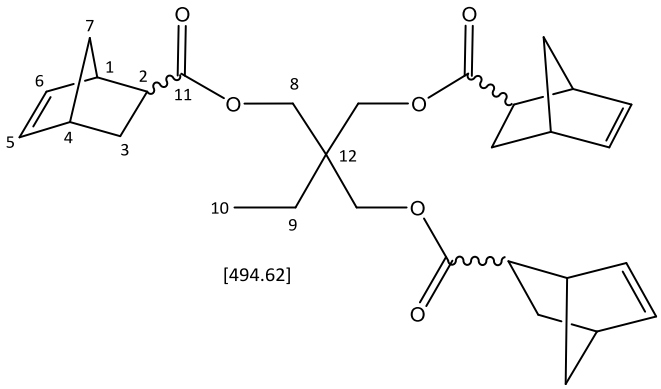

[494.62]

^{1}H-NMR (300 Hz, $CDCl_3$): δ = 6.19 (m, 3H, $5a_{endo}$, $6a_{endo}$), 6.12 (m, 2H, 5_{exo}, 6_{exo}), 5. 88 (m, 3H, $5b_{endo}$, $6b_{endo}$), 4.04 (m, 6H, 8_{exo}), 3.95 (s, 6H, 8_{endo}), 3.19 (s, 3H, 1_{endo}), 2.97 (m, 3H, 2_{endo}), 2.90 (m, 3H, 4_{endo}), 1.90 (m, 3H, $3a_{endo}$), 1,49 (m, 2H, 9_{endo}), 1.42 (m, 6H, $3b_{endo}$,$7a_{endo}$), 1.28 (d, 3H, $7b_{endo}$), 0.87 (m, 3H, 10_{endo})

endo/*exo*-ratio: 82/18

^{13}C-NMR (75 Hz, $CDCl_3$): δ = 174.5 (3C, C_q, 11), 138.1 (3C, 5a, 6a), 132.4 (3C, 5b, 6b), 63.7 (3C, 8) 49.8 (3C, 7), 45.9 (3C, 1), 43.5 (3C, 2), 42.6 (3C, 4), 29.3 (3C, 3), 27.1 (C, C_q, 12), 23.1 (C, 9), 7.5 (C, 10)

*5.2.2.4. 2-Hydroxyethyl-endo-norbornene-carboxylate (**Mon9**)*

Freshly distilled Cp (27.7 g, 0.419 mol, 1.1 eq) was added dropwise to ice cooled trimethylolpropane triacrylate (60 g, 0.20 mol, 1.0 eq). After 1.5 h the ice cooling was removed and the reaction stirred at room temperature. As the reaction developed heat, it was cooled again for 10 min. 5 mL (4 g) CP were added one hour later and the mixture stirred at 40 °C. After 18 h the conversion, monitored via ^{1}H-NMR spectroscopy, was still incomplete, so 5 mL (4 g) CP was added. After 21 h in total the conversion was complete. The crude product was purified via flash chromatography. Excessive Cp was removed using cyclohexane as eluent. The pure product was eluted with Cy/EtOAc (1:1 (v:v)) as eluent and dried under reduced pressure. Yield: 66.78 g (96 %), yellowish liquid

TLC: R_f = 0.62 (Cy/EtOAc, 1:1, (v:v), detection: $KMnO_4$)

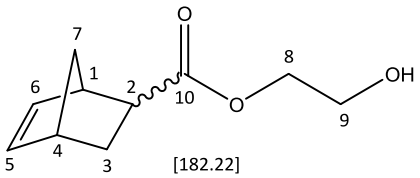

[182.22]

^{1}H-NMR (300 Hz, $CDCl_3$): δ= 6.19 (m, 1H, $5a_{endo}$, $6a_{endo}$), 6.13 (m, 2H, 5_{exo}, 6_{exo}) 5.94 (m, 1H, $5b_{endo}$, $6b_{endo}$), 4.22 (t, 2H, 8_{exo}), 4.16 (t, 2H, 8_{endo}), 3.79 (t, 2H, 9_{endo}), 3.22 (m, 1H, 4_{endo}), 2.98 (m, 1H, 2_{endo}), 2.91 (s, 1H, 1_{endo}), 2.08 (s, b, OH), 1.91 (m, 1H, $3a_{endo}$), 1.43 (m, 2H, $3b_{endo}$, $7a_{endo}$), 1.28 (d, 1H, $^3J^{H,H}$ = 8.3 Hz, $7b_{endo}$)

endo/*exo*-ratio: 8/2

^{13}C-NMR (75 Hz, $CDCl_3$): δ = 176.7 (1C, C_q, 10_{exo}), 175.2 (1C, C_q, 10_{endo}), 138.2 (1C, $5a_{exo}$, $6a_{exo}$), 137.9 (1C, $5a_{endo}$, $6a_{endo}$), 135.7 (1C, $5b_{exo}$, $6b_{exo}$), 132.2 (1C, $5b_{endo}$, $6b_{endo}$), 66.1 (1C, 8_{exo}), 65.9 (1C, 8_{endo}), 61.4 (1C, 9_{endo}), 61.4 (1C, 9_{exo}), 49.7 (1C, 7_{endo}), 46.7 (1C, 7_{exo}), 46.4 (1C, 1_{exo}), 45.8 (1C, 1_{endo}), 43.3 (1C, 2_{endo}), 43.1 (1C, 2_{exo}), 42.6 (1C, 4_{endo}), 41.7 (1C, 4_{exo}), 30.3 (1C, 3_{exo}), 29.3 (1C, 3_{endo})

*5.2.2.5. 1,1'-Biphenyl-4-bis(methoxy-norbornene) (**Mon11**)*

4,4'-Bis(alllyloxy)-biphenyl (0.5630 g, 2.1 mmol, 1.0 eq, see 5.2.3.1) was added to dicyclopentadiene (0.2832 g, 2.1 mmol, 1.0 eq, DCPD) and hydroquinone (0.90 mg, 0.008 mmol, 0.0039 eq) in an autoclave. The reaction mixture was stirred at 180 °C for 18 h yielding to a dark brown, liquid crude product. TLC-analysis revealed full conversion of the 4,4'-bis(alllyloxy)-biphenyl into several products (R_f = 0.91, 0.85, 0.58, 0.53, 0.37, Cy/EtOAc 3:1 (v:v), detection: UV light, $KMnO_4$). Purification by column chromatography with Cy/EtOAc 3:1 (v:v) as eluent resulted in the detection of the desired product and identification of several by-products discussed chapter 3.4.5. An additional purification step by column chromatography with Cy/EtOAc 500:1 (v:v) did not yield into separation of the product (di-substituted) from its by-product (mono-substituted). Therefore, yield could not be quantified.

TLC: R_f = 0.82 (Cy/EtOAc 10:1 (v:v), detection: $KMnO_4$)

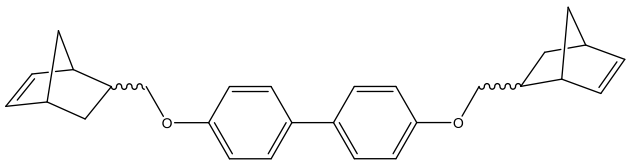

[398.55]

5.2.1. Carbamate formation

The carbamate-linked bis-norbornene ester (***Mon10***) was synthesized from two equivalents ***Mon9*** and a diisocyanate (Scheme 16) according to the procedure published in: Sui X.C., *Chinese Chem. Lett.* **2011**, *22*, 374 – 377.

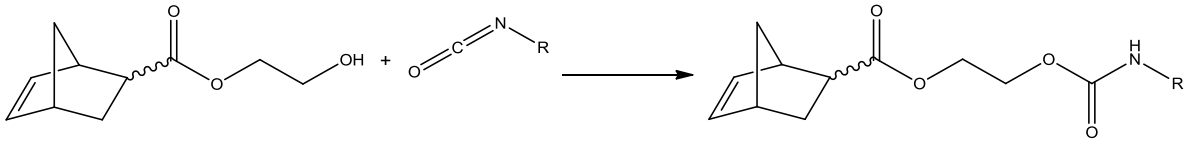

Scheme 16. Carbamate formation.

*5.2.1.1. Bis(ethyl-norbornene-carboxylate)-(4,4'-methylene-diphenyl-dicarbamte) (**Mon10**)*

Methylene diphenyl diisocyanate (3.96 g, 16 mmol, 1.0 eq) and 2-hydroxyethyl-*endo*-norbornene-carboxylate (5.62 g, 31 mmol, 1.95 eq) were dissolved in 30 mL THF abs. under

inert conditions. The reaction was stirred at 50 °C for 5 days. As conversion was not complete monitored via ^{1}H-NMR spectroscopy, the reaction was stirred at 80 °C for 3 days yielding full conversion of 2-hydroxy-*endo*-norbornene carboxylate. The reaction was quenched with ethanol. Solvents were removed under reduced pressure. The dried product was analysed by ^{1}H-NMR spectroscopy detecting the desired diester (84 %) and monoester-ethyl-carbamate as by-product (16 %). Yield: 9.26 g (94 %, purity: 90 %), colourless – yellowish solid, hygroscopic

Analytical data in accordance with published values[40]

TLC: R_f = 0.83 (Cy/EtOAc, 2:3, (v:v), + Et_3N, detection: $KMnO_4$)

Main product:

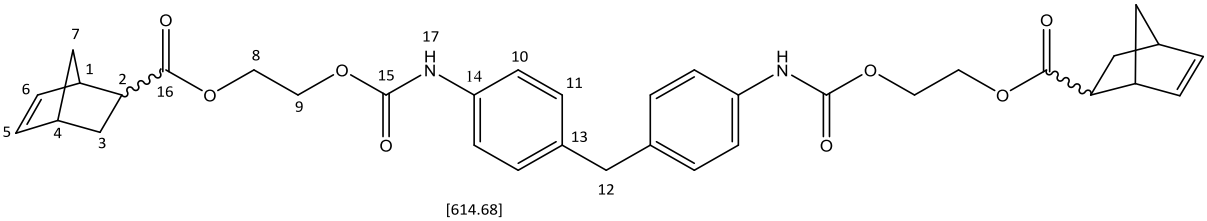

[614.68]

By-product:

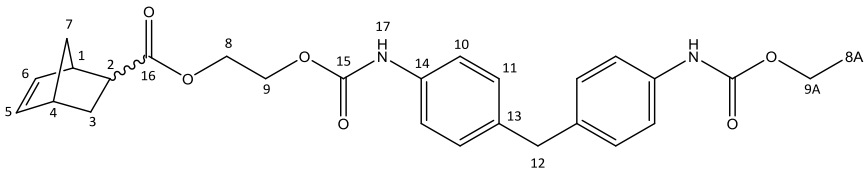

[478.54]

^{1}H-NMR (300 Hz, $CDCl_3$): δ = 7.29 (d, 4H, $10a_{endo}$, $11a_{endo}$), 7.10 (d, 4H, $10b_{endo}$, $11b_{endo}$), 6.63 (s, 1H, N-H), 6.17 (m, 2H, $5a_{endo}$, $6a_{endo}$), 6.11 (m, 2H, $5a_{exo}$, $6a_{exo}$), 5,93 (m, 2H, $5b_{endo}$, $6b_{endo}$), 4,31 (m, 4H, 8_{endo}), 4.20 (m, 4H, 9_{endo}, 2H, 9A), 3.88 (s, 2 H, 12_{endo}), 3.21 (s, 2H, 1_{endo}), 2.96 (m,2H, 2_{endo}), 2.90 (s, 2H, 4_{endo}), 1.91 (m, 1H,$3a_{endo}$), 1.43 (m, 2H, $3b_{endo}$), 1.37 (t, 2H, $8A^{b}$), 1.28 (m, 2H, 7_{endo})

endo/*exo*-ratio: 84/16

^{13}C-NMR (75 Hz, $CDCl_3$): δ = 174.7 (2C, C_q, 16); 138.0 (2C, 5a, 6a), 136.7 (2C, C_q, 14), 135.9 (2C, C_q, 15) 132.4 (2C, 5b, 6b), 63.2 (2C, 8) 62.3 (2C, 9), 49.8 (2C, 7) 46.5 (2C, 2), 45.9 (2C, 1), 43.2 (2C, 4), 40.7 (1C, 12), 29.4 (2C, 3)

5.2.2. Esterification

For the synthesis of bis-norbornene ester - derivative ***Mon12*** succinic acid and 5-norbornene-2-methanol were used as starting materials following the protocol published in: Crivello J.V., Narayan R., *Macromolecules* **1996**, *26*, 433 – 438.

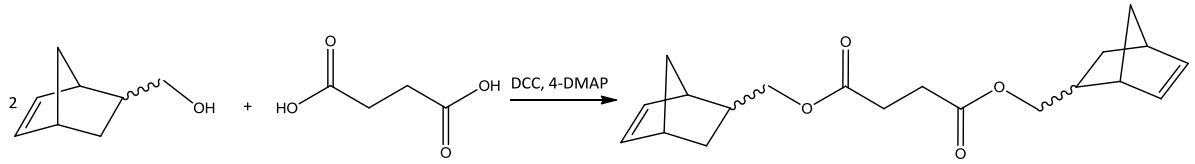

Scheme 17. Esterification of succinic acid with norbornene-methanol.

*5.2.2.1. Bis(norbornene-2-methyl)succinate (**Mon12**)*

5-Norbornene-2-methanol (10.30 g, 82.9 mmol, 2.47 eq), succinic acid (3.98 g, 33.7 mmol, 1.0 eq) and 4-dimethylamino-pyridine (0.167 g, 1.4 mmol, 0.04 eq, 4-DMAP) were dissolved in 150 mL DCM abs. under inert conditions and ice cooling. To this solution dicyclohexylcarbodiimide (16.62 g, 80.6 mmol, 2.39 eq, DCC) dissolved in 50 mL DCM abs. was added. After 10 min the ice cooling was removed and a colourless precipitate was observed considered to be the urea-derivative of the DCC-catalyst. The reaction mixture was stirred at room temperature for 24 h. Due to incomplete conversion monitored via TLC 1.68 g DCC (8.14 mmol, 0.24 eq) was added and the reaction was stirred for further 24 h yielding full conversion. The colourless precipitate was then removed by filtration over celite. 4-DMAP and unreacted acid were removed by extraction with hydrochloric acid- and saturated bicarbonate solution, respectively. TLC analysis of the crude product revealed incomplete removal of urea by-product (R_f = 0.04, Cy/EtOAc, 5:1 (v:v), detection: CAM) which seemed to be soluble in the desired product. Pentane was added in order to precipitate the by-product which subsequently was filtrated over anhydrous sodium sulphate. This procedure was repeated once. However, the by-product could not be completely removed. The product was further purified by column chromatography with cyclohexane: ethyl acetate 50:1 (v:v) as eluent. Thereby, mono-substituted by-product (R_f=0.24, Cy/EtOAc, 5:1(v:v), detection: KMnO4), the excess of norbornene-methanol (R_f=0.18, Cy/EtOAc, 5:1(v:v), detection: KMnO4) as well as the urea by-product could be removed completely. Yield: light yellow liquid, low viscosity (46 %)

Analytical data in accordance with published values[42]

TLC: R_f = 0.70 (Cy/EtOAc, 5:1 (v:v), detection: CAM)

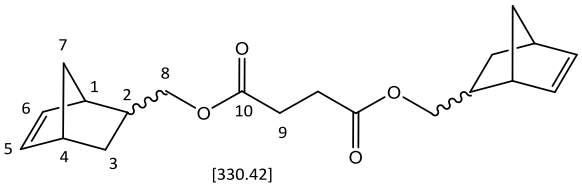

[330.42]

^{1}H-NMR (300 Hz, $CDCl_3$): δ = 6.14 (m, 2H, $5a_{endo}$, $6a_{endo}$), 6.08 (m, 5_{exo}, 6_{exo}), 5.93 (m, 2H, $5b_{endo}$, $6b_{endo}$), 4.16 - 3.99 (m, 8_{exo}), 3.87 – 3,68 (t, 4H, 8_{endo}), 2.87 (s, 2H, 1_{endo}), 2.81 (s, 2H, 4_{endo}), 2.65 (m, 4H, 9_{endo}), 2.37 (m, 2H, 2_{endo}), 1.83 (m, 2H, $3a_{endo}$), 1.43 (m, 2H, $7a_{endo}$), 1.25 (m, 2H, $7b_{endo}$), 0.54 (m, 2H, $3b_{endo}$)

endo/*exo*-ratio: 3/1

^{13}C-NMR (75 Hz, $CDCl_3$): δ = 172.5 (2C, C_q, 10_{exo}), 172.4 (2C, C_q, 10_{endo}); 137.7 (2C, $5a_{endo}$, $6a_{endo}$), 137.1 (2C, $5a_{exo}$, $6a_{exo}$), 136.3 (2C, $5b_{exo}$, $6b_{exo}$), 132.3 (2C, $5b_{endo}$, $6b_{endo}$), 68.9 (2C, 8_{exo}), 68.3 (2C, 8_{endo}) 49.5 (2C, 7_{endo}), 45.1 (2C, 7_{exo}), 43.9 (2C, 1_{endo}), 43.8 (2C, 1_{exo}), 42.3 (2C, 2_{endo}), 41.7 (2C, 2_{exo}), 39.1 (2C, 4_{exo}), 37.9 (2C, 4_{endo}), 29.4 (2C, 3_{endo}), 29.7 (2C, 3_{exo}), 29.1 (2C, 9_{endo})

5.2.3. O-Allylation

The vinyl ether precursor for the synthesis of ***Mon11*** was derived by *O*-allylation of a diol-compound with two equivalents allyl bromide (Scheme 18) according to the procedure published in: M.-Y. Chang, T.-W. Lee, M.-H. Wu, *Org. Lett* **2012**, *14* (9), 2198 – 2201.

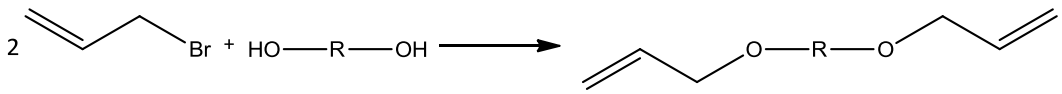

Scheme 18. O-allylation with allyl bromide.

5.2.3.1. 4,4'-Bis(alllyloxy)-biphenyl

K_2CO_3 (1.32 g, 9.5 mmol, 4.0 eq) was added to a colourless solution of 4,4'-dihydroxybiphenyl (0.44 g, 2.4 mmol, 1.0 eq) in pure acetone. The colourless suspension was stirred at room temperature for 10 min before allyl bromide (0.60 g, 5.0 mmol, 2.1 eq) was added. The reaction mixture was stirred 50 °C over night. Analysis via ^{1}H-NMR-spectroscopy and TLC after 20 h showed conversion to the desired product (R_f = 0.75, Cy/EtOAc, 3:1 (v:v), detection: $KMnO_4$) and mono-substituted by-product ((R_f = 0.43, Cy/EE 3+1, detection: $KMnO_4$) as well as unconverted diol (R_f = 0.21, Cy/EE 3+1, detection: $KMnO_4$). Allyl bromide (50.3 mg, 0.42 mmol, 0.2 eq) was added leading to full conversion (detected via TLC) after

further 18 h. The solvent was removed under reduced pressure and the reaction mixture taken up in 250 mL ethyl acetate. The organic phase was washed twice with distilled water, once with saturated sodium chloride solution and dried over anhydrous sodium sulphate. The solvent was removed under reduced pressure. Yield: 0.60 g (94 %), pulverulent, cream-coloured, glittering solid.

Analytical data in accordance with published values[41]

TLC: R_f = 0.75 (Cy/EtOAc, 3:1 (v:v), detection: $KMnO_4$)

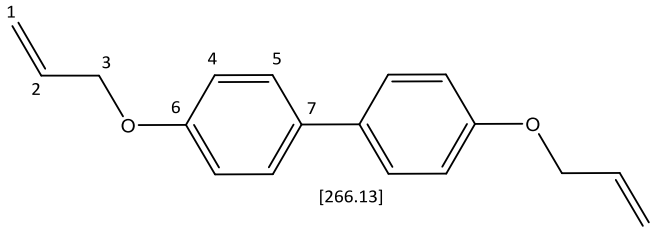

^{1}H-NMR (300 Hz, $CDCl_3$): δ = 7.47 (d, 4H, $^3J_{HH}$ = 8.7 Hz, 5), 6.98 (d, 4H, $^3J_{HH}$ = 8.7 Hz, 5), 6.16 – 6.03 (m, 2H, 2), 5.48 - 5.42 (dd, 2H, $^3J_{HH\textit{cis}}$ = 17.22 Hz, $^2J_{HH}$ = 1.44 Hz, 1*cis*), 5.33 - 5.29 (dd, 2H, $^3J_{HH\textit{trans}}$ = 10.47 Hz, $^2J_{H,H}$ = 1.2 Hz, 1*trans*), 4.58 (d, 4H, $^3J_{H,H}$ = 5.25 Hz, 7)

^{13}C-NMR (75 Hz, $CDCl_3$): δ = 157.9 (2C, C_q, 6); 133.7 (2C, C_q, 7), 133.5 (2C, 2), 127.8 (4C, C_{arom}, 5), 117.8 (2C, 1), 115.2 (4C, C_{arom}, 4), 69.1 (2C, 3)

5.2.4. Ring opening metathesis polymerisation (ROMP)

5.2.4.1. Homopolymerisation in bulk – General procedure

For the typical bulk-polymerisation, the monomer was filled into a test tube and 50 µL DCM were added. 2 g monomer was used in case of DCPD (15.1 mmol) and norbornadiene (21.7 mmol), 1 g monomer in case of DMNH-6 (6.3 mmol), Mon4 (3.3 mmol), Mon6 (3.0 mmol), Mon8 (2.0 mmol), Mon9 (5.5 mmol). A stock solution of initiator in dichloromethane was prepared for each loading. 50µL initiator-solution was added to the monomer. Loadings reached from 25 to 150 ppm and polymerisations were carried out at 4, 25 and 40 °C. By measuring the heat generation and noting the change in viscosity (cf. Table 1) the polymerisation progress was monitored. The weighed portions of monomers and initiators and the reactions conditions are summarized in Table 27.

Table 27. Homopolymerisation of *DCPD* (2 g, 15.1 mmol) at 4, 25 and 40 °C and of norbornadiene (2 g, 21.7 mmol), *DMNH-6* (1 g, 6.3 mmol), *Mon4* (1g , 3.3 mmol), *Mon6* (1 g, 3.0 mmol), *Mon8* (2.0 mmol) and *Mon9* (5.5 mmol) at 25 °C.

Monomer	Initiator loading		*M1*	*M2*	*M20*
	ppm	mol	mg	mg	mg
DCPD	25	$3.8*10^{-7}$	0.35	0.36	0.35
	50	$7.6*10^{-7}$	0.70	0.72	0.70
	75	$1.1*10^{-6}$	1.05	1.08	1.06
	100	$1.5*10^{-6}$	1.40	1.44	1.41
	150	$2.3*10^{-6}$	2.10	2.16	2.11
Norbornadiene	50	$1.1*10^{-6}$	-	1.03	-
	75	$1.6*10^{-6}$	-	1.55	-
	100	$2.2*10^{-6}$	-	2.06	-
	150	$3.2*10^{-6}$	-	3.09	-
DMNH-6	25	1.6*10-7	-	0.15	-
	50	$3.2*10^{-7}$	-	0.30	-
	75	$4.7*10^{-7}$	-	0.45	-
	100	$6.5*10^{-7}$	-	0.60	-
	150	$9.5*10^{-7}$	-	0.90	-
Mon4	100	$3.3*10^{-7}$	-	-	0.31
	150	$5.0*10^{-7}$	-	0.48	0.46
Mon6	50	$1.5*10^{-7}$	-	-	0.14
	75	$2.3*10^{-7}$	-	-	0.21
	100	$3.0*10^{-7}$	-	-	0.28
	150	$4.5*10^{-7}$	-	0.43	0.42
Mon8	150	$3.0*10^{-7}$	-	-	2.80
Mon9	25	$1.4*10^{-7}$	-	-	0.13
	50	$2.8*10^{-7}$	-	-	0.26
	75	$4.1*10^{-7}$	-	-	0.38
	100	$5.6*10^{-7}$	-	-	0.51
	150	$8.3*10^{-7}$	-	0.78	0.76

*5.2.4.2. Co-Polymerisation of DCPD (**Mon1**) and norbornadiene (**Mon2**) in bulk*

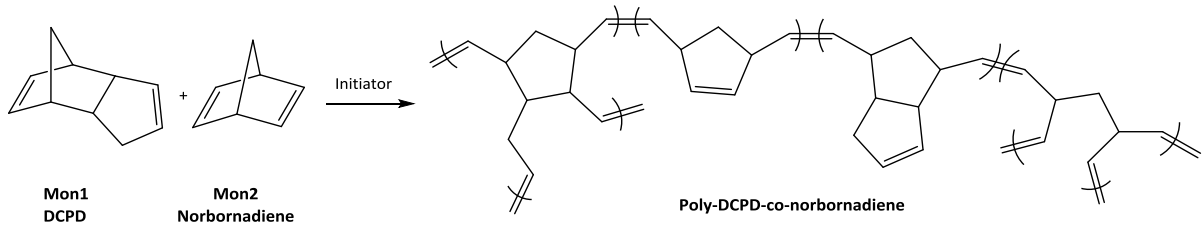

Scheme 19. Copolymerisation of *DCPD* (*Mon1*) and Norbornadiene (*Mon2*)

DCPD (***Mon1***) and norbornadiene (***Mon2***) were mixed in various ratios (1:0, 2:1, 1:1, 1:2) in a test tube and dissolved in 50 µL DCM. A loading of 150 ppm ***M2*** (in 50 µL DCM) was used and the polymerisation was carried out at 25 °C. Polymerisation progress was monitored by measuring the heat generation. The weighed portions of monomers and initiators and the reactions conditions are summarized in Table 28.

Table 28 Copolymerisation of DCPD and norbornadiene (2 g) with 150 ppm initiator and 25 °C.

Ratio	***M2*-loading**	
DCPD*:*Norbornadiene	**mol**	**mg**
1:0	$2.3*10^{-6}$	2,15
2:1	$2.6*10^{-6}$	2,47
1:1	$2.8*10^{-6}$	2,63
1:2	$2.9*10^{-6}$	2,78

5.2.5. Sample preparation

5.2.5.1. Simultaneous Thermal Analysis (STA)

Sample preparation for a monomer: 1.0 mL ***DCPD*** (0.98 g, 7.4 mmol) was molten in a 40 °C water bath and mixed with 60 µL DCM to keep it at liquid state. About 15 mg of the sample was transferred into a DSC pan, which was subsequently closed, but supplied with a small opening and then subjected to the STA run.

Sample preparation for a monomer/initiator formulation: For the analysis of monomer-initiator-formulations mixing was performed shortly before measurements were started. 1 mL ***DCPD*** (0.98 g, 7.4 mmol) was molten in a 40 °C water bath and mixed with DCM and added to the initiator (various loading, from stock solutions) added with a syringe ensuring homogenous distribution in a glass vial. A total amount of 60 µL DCM was used in order to keep DCPD at liquid state and for the stock solution. The formulation was shock-frozen by

placing the vial into liquid nitrogen and stored in a Styrofoam container till measurement. Immediately before the measurement, about 15 mg formulation was transferred into a DSC pan, which was subsequently closed, but supplied with a small opening and then subjected to the STA run.

5.2.5.2. Rheokinetics measurements

2 g monomer (***DCPD***, ***Mon6***, ***Mon8***, ***Mon6+Mon8*** (1:1)) were mixed with 50 µL DCM and 50 µL of a ***M2***-solution (50 ppm, from stock solution of initiator in DCM) in a vial and subsequently poured on the lower plate of the rheometer. The upper plate is lowered down to a distance of 1 mm between the two plates and the rheokinetic measurement was started. The measurement was conducted at 23 °C. The time between the mixing of the monomer and ***M2*** and the first data point must be added to the obtained data set. For the measurement disposable plate-plate-items made of aluminium were used to facilitate removal of the sample after measurement. The weighed portions of monomers and initiators and the reactions conditions are summarized in Table 28.

Table 29. Rheokinetic measurement of *DCPD*, *Mon6*, *Mon8* and a mixture of *Mon8* and *Mon6* with 50 ppm *M2*.

Monomer	***M2*-loading**		
	mmol	**mol**	**mg**
DCPD	15.1	$7.6*10^{-7}$	0.72
Mon6	6.0	$3.0*10^{-7}$	0.28
Mon8	4.0	$6.0*10^{-7}$	0.56
Mon8+Mon6 (1:1)		$2.5*10^{-7}$	0.24

5.2.5.3. Tensile Testing

The monomer (1.5 g and 28 g for small and large molds, respectively) was dissolved in DCM or toluene (50 µL or 1680 µL for small and large molds, respectively) at room temperature in a vial and mixed with dissolved initiator (same amount of solvent as for monomer). The still liquid monomer / initiator formulation was immediately filled into the steel mold. Subsequently, curing was performed at 4 °C (in refrigerator), room temperature (23 - 25 °C), 40, 60 or 80 °C with preceding 5 min at room temperature (in the oven) for total 24 h. When the material reached solid state, it was removed from the mold and stored at the adjusted temperature. The parameters used in the preparation are summarized in Table 30 (DCPD, large mold) and Table 31 (small mold).

Table 30. Preparation of a 14.0 mL test bar (large mold) of *DCPD* (13.7 g, 0.1 mol) for tensile testing.

Initiatior loading		M1	M10	M11	M2	EP06.3	Curing Temp.
/ ppm	/ mol	/ mg	/ mg	/ mg	/ mg	/ mg	/ °C
5	$5.2*10^{-7}$	0.46	-	-	0.68	-	60, 80
10	$1.4*10^{-6}$	0.92	-	-	1.35	-	60, 80
20	$2.8*10^{-6}$	1.85	2.49	2.12	2.70	1.83	60, 80
35	$3.6*10^{-6}$	3.23	-	-	-	-	60, 80
50	$5.2*10^{-6}$	4.61	-	-	6.75	-	4, 25, 40, 60, 80
100	$1.4*10^{-6}$	9.22	-	-	-	-	4, 25, 40

Table 31. Preparation of a 1.5 g test bar (small mold) of *DMNH-6*, *Mon4*, *Mon6*, *Mon8*, *Mon9*, *Mon12* and the mixture *Mon8+Mon6*, *Mon6+Mon9*, *Mon9+Mon10* for tensile testing.

Monomer	Initiatior loading		M2	M20	Curing Temp.
	/ ppm	/ mol	/ mg	/ mg	/ °C
DMNH-6	10	$9.5*10^{-8}$	0.09	-	25, 80
	50	$4.7*10^{-7}$	0.45	-	80
Mon4	50	$2.5*10^{-7}$	-	0.23	40, 80
Mon6	50	$2.3*10^{-7}$	-	0.21	40, 80
	100	$4.6*10^{-7}$	-	0.43	40, 80
Mon8	50	$1.5*10^{-7}$	-	0.14	40, 80
Mon8+Mon6 (1:1)	50	$2.3*10^{-7}$*	-	0.21	40, 80
Mon9	50	$4.1*10^{-7}$	-	0.38	40,80
Mon6+Mon9 (1:1)	50	$3.8*10^{-7}$*	-	0.35	80
Mon9+Mon10 (1:1)	50	$3.2*10^{-7}$*	-	0.30	80
Mon12	25	$1.4*10^{-7}$*	0.13	-	80

*1.8 g monomer

5.2.5.4. Dynamic mechanical analysis (DMA)

For the preparation of cylindric samples for DMA measurements, 2 g monomer (***DCPD*** molten (0.015 mol), ***Mon6*** (6.1 mmol), ***Mon8*** (4.0 mmol), ***Mon8+Mon6*** (1:1), ***Mon9*** (0.011 mol), ***Mon12*** (6.1 mmol)) were mixed with 50 µL DCM and 50 µL of an initiator-solution (50 ppm ***M2*** or ***M20***, from a stock solution in DCM). In case of ***Mon12*** the whole amount of solvent was used to dissolve the initiator to ensure a homogenous distribution in the monomer - initiator – formulation. The formulations were subsequently filled into a PE-tube (5 mm diameter, 45 mm length). The samples were cured in upright position for 24 h

either at 40 °C or 80 °C with preceding 5 min at room temperature. The parameters used in the preparation are summarized in Table 32.

Table 32. Preparation of 2 g cylindric samples of *DCPD*, *Mon6*, *Mon8*, *Mon8+Mon6* (1:1), *Mon9* and *Mon12* for dynamic mechanical analysis.

Monomer	Initiatior loading		M2	M20	Curing Temp.
	/ ppm	/ mol	/ mg	/ mg	/ °C
DCPD	50	$7.6*10^{-7}$	0.72	-	40, 80
Mon6	50	$3.0*10^{-7}$	-	0.28	40, 80
	50	$3.0*10^{-7}$	0.29	-	40
Mon8	50	$2.0*10^{-7}$	0.19	-	80
Mon8+Mon6 (1:1)	50	$2.5*10^{-7}$	0.24	-	40,80
Mon9	50	$5.5*10^{-7}$	0.52	-	80
Mon12	50	$3.0*10^{-7}$	0.29	-	80

.

5.2.5.5. Alkali resistance test

For the preparation of discodial samples for alkali resistance test, 10.5 g monomer (***DCPD*** molten (0.08 mol), ***Mon6*** (0.03 mol)) were mixed with 315 µL DCM and 315 µL of an initiator-solution (50 ppm ***M2*** or ***M20***, from a stock solution in DCM). The still liquid formulation was filled into the mold and subsequently cured at 40 °C in the oven for 24 h. When the material reached solid state, it was removed from the mold and further cured at the adjusted temperature. Afterwards, the samples were stored for another 24 h at ambient conditions.

Appendix

List of Figures

List of Schemes

List of Tables